İZMİR KÂTİP ÇELEBİ ÜNİVERSİTESİ
2010
GRADUATE SCHOOL OF NATURAL AND APPLIED SCIENCES

Influence of Lignocellulosic Fillers and Interfaces on Thermal and Mechanical Properties of Biocomposites

Submitted to the Graduate School of Natural and Applied Sciences in partial fulfillment of the requirements for the degree of

Doctor of Philosophy

in Mechanical Engineering

by

Mustafa Öncül

ORCID 0000-0002-4441-6353

July, 2023

This is to certify that we have read the thesis **Influence of Lignocellulosic Fillers and Interfaces on Thermal and Mechanical Properties of Biocomposites** submitted by **Mustafa Öncül**, and it has been judged to be successful, in scope and in quality, at the defense exam and accepted by our jury as a DOCTORAL THESIS.

APPROVED BY:

Advisor: **Prof. Dr. Kutlay Sever**
İzmir Kâtip Çelebi University

Committee Members:

Assist. Prof. Dr. Ebubekir Atan
İzmir Kâtip Çelebi University

Prof. Dr. Mücahit Sütçü
Manisa Celal Bayar University

Assoc. Prof. Dr. Ebru Bozacı
Ege University

Assoc. Prof. Dr. Seçkin Erden
Ege University

Date of Defense: June 19, 2023

Declaration of Authorship

I, **Mustafa Öncül**, declare that this thesis titled **Influence of Lignocellulosic Fillers and Interfaces on Thermal and Mechanical Properties of Biocomposites** and the work presented in it are my own. I confirm that:

- This work was done wholly or mainly while in candidature for the Doctoral degree at this university.
- Where any part of this thesis has previously been submitted for a degree or any other qualification at this university or any other institution, this has been clearly stated.
- Where I have consulted the published work of others, this is always clearly attributed.
- Where I have quoted from the work of others, the source is always given. This thesis is entirely my own work, with the exception of such quotations.
- I have acknowledged all major sources of assistance.
- Where the thesis is based on work done by myself jointly with others, I have made clear exactly what was done by others and what I have contributed myself.

Date: 19.06.2023

Influence of Lignocellulosic Fillers and Interfaces on Thermal and Mechanical Properties of Biocomposites

Abstract

This thesis consists of five main parts. In the first part, the properties of novel lignocellulosic fillers were investigated. The cellulose, hemicellulose, and lignin ratios of fillers were determined by chemical composition analysis, the chemical bonds in the molecular structure were defined by Fourier transform infrared (FTIR) spectroscopy, the crystallographic properties of fillers were determined by X-ray diffraction (XRD) analysis, thermal stabilities were stated by thermogravimetric analysis (TGA), and morphological properties were analyzed by scanning electron microscopy (SEM). Hence, the results obtained for the alternate lignocellulosic fillers were brought to the literature.

In the second part, biocomposite production was performed by adding untreated fillers to polypropylene (PP) with particle sizes under 100 microns and 100-250 microns at the rates of 5%, 10%, 15%, and 20% by weight. The effects of the particle size of fillers and filler types on the mechanical and viscoelastic properties of biocomposites were investigated by performing tensile tests, three-point bending tests, and dynamic mechanical analyses (DMA). When the mechanical properties of biocomposites were compared with the neat PP; it was determined that the biocomposite, which contains 10% of wood filler with under 100 microns particle size, provided the optimum values among all other fillers with a tensile strength of

21.2 MPa, a tensile modulus of 1150 MPa, a flexural strength of 34 MPa, and a flexural modulus of 1334 MPa.

In the third step, wood filler under 100 microns was treated with sodium hydroxide (NaOH) at 3%, 5%, and 10% ratios in order to determine the ideal ratio for surface modification. According to the results of the FTIR analysis, 5% NaOH was determined as the most effective modification parameter. In the fourth part of the study, maleic anhydride-grafted polypropylene (MAPP) was added to the PP at 1%, 3%, and 5% by weight. Tensile and three-point bending tests were applied to the samples to determine the ideal additive ratio. As a result of these tests, with 29 MPa tensile strength, 1075 MPa tensile modulus, 47 MPa flexural strength, and 1864 MPa flexural modulus values, the best results were obtained in the 3 wt. % MAPP added sample.

In the fifth and last step, the final biocomposite with improved thermal and mechanical properties was produced by using the most ideal ratios obtained until this stage of the thesis study. The content of this biocomposite consists of 5% alkali-treated wood (<100μ) 10 wt. %, and 3 wt. % MAPP-filled polypropylene. According to the mechanical analysis results, this biocomposite provided an increase of 10% in tensile strength and 60% in tensile modulus when compared to PP. Nevertheless, when the thermal properties of the 5AT10W-3MAPP biocomposite were compared with pure PP, the thermal stability and crystallization rates of the biocomposites improved by 21.5 °C and 5.6%, respectively.

Keywords: Biocomposites, lignocellulosic fillers, surface treatments, thermal and mechanical properties

Lignoselülozik Dolgu Malzemelerinin ve Arayüzeylerin Biyokompozitlerin Termal ve Mekanik Özelliklerine Etkisi

Öz

Bu tez çalışması temel olarak beş ana bölümden oluşmaktadır. Çalışmanın birinci bölümünde daha önce çalışılmamış alternatif lignoselülozik dolgu malzemelerinin özellikleri araştırılmıştır. Bu malzemelerin selüloz, hemiselüloz ve lignin oranları kimyasal kompozisyon analiziyle, molekül yapısındaki bağların tanımlanması Fourier dönüşümlü kızılötesi (FTIR) spektroskopisiyle, kristallografik özellikleri X-ışını kırınım (XRD) analiziyle, termal kararlılıkları termogravimetik analiz (TGA) ile ve morfolojik özellikleri taramalı elektron mikroskobu (SEM) kullanılarak incelenmiştir. Böylece budama atığı kiraz ağacı dallarının odun ve kabuk kısımları için elde edilen sonuçlar literatüre kazandırılmıştır.

İkinci kısımda, odun ve kabuk dolgu malzemeleri 100 mikron altı ve 100-250 mikron arası parçacık boyutlarında polipropilenin (PP) içerisine ağırlıkça %5, %10, %15 ve %20 oranlarında katılarak biyokompozit malzeme üretimi gerçekleştirilmiştir. Üretilen bu numunelere çekme, üç nokta eğme ve dinamik mekanik analiz (DMA) testleri yapılarak odun ve kabuk dolgu malzemelerinin ve farklı dolgu malzemelerinin parçacık boyutunun biyokompozitlerin mekanik ve viskoelastik özelliklerine etkisi incelenmiştir. Saf PP referans alınarak üretilen biyokompozitlerin mekanik özellikleri karşılaştırıldığında; 21.2 MPa çekme dayanımı, 1150 MPa çekme

modülü, 34 MPa eğilme dayanımı ve 1334 MPa eğilme modülü değerlerine sahip olan ağırlıkça %10 oranda 100 mikron altı odun dolgu malzemesi içeren biyokompozitin diğer tüm dolgu malzemeleri ve oranları içerisinde optimum değerleri verdiği belirlenmiştir.

Çalışmanın üçüncü adımında, 100 mikron altı odun dolgu malzemesine, yüzey modifikasyonu için ideal oranının belirlenmesi amacıyla, 60 dakika sabit sürede, %3, %5 ve %10 oranlarında sodyum hidroksit (NaOH) ile yüzey işlemine tabi tutulmuştur. FTIR analiz sonuçlarına göre en etkili modifikasyon parametresi olarak %5 NaOH oranı tespit edilmiştir. Çalışmanın dördüncü bölümünde, saf PP'nin içerisine ağırlıkça %1, %3 ve %5 oranlarında maleik anhidrit aşılı polipropilen (MAPP) ilave edilmiştir. İdeal katkı oranının belirlenmesi için numunelere çekme ve üç nokta eğme testleri uygulanmıştır. Bu testler sonucunda, 29 MPa çekme dayanımı, 1075 MPa çekme modülü, 47 MPa eğilme dayanımı ve 1864 MPa eğilme modülü değerleri ile en iyi sonuç ağırlıkça %3 MAPP katkılanmış numunede elde edilmiştir.

Çalışmanın beşinci ve son adımında ise, tez çalışmasının bu aşamasına kadar elde edilen en ideal oranlar kullanılarak termal ve mekanik özellikleri iyileştirilmiş nihai biyokompozit malzeme üretilmiştir. Bu malzemenin içeriği ağırlıkça %10 oranında %5 NaOH ile modifiye edilmiş 100 mikron altı odun dolgusu ve ağırlıkça %3 MAPP'tan oluşmaktadır (5AT10W-3MAPP). Elde edilen mekanik analiz sonuçlarına göre, bu kompozisyon saf PP ile karşılaştırıldığıda çekme dayanımında yaklaşık %10, çekme modülünde ise yaklaşık %60 oranında bir artış göstermiştir. Benzer şekilde, 5AT10W-3MAPP numunesinin termal özellikleri saf PP ile karşılaştırıldığında biyokompozitlerin termal kararlılığı ve kristalleşme hızlarında sırasıyla 21.5 ℃ ve %5.6 oranlarında iyileşme gözlemlenmiştir.

Anahtar Kelimeler: Biyokompozitler, lignoselülozik dolgular, yüzey işlemleri, termal ve mekanik özellikler

In the Name of Allah, the Entirely Merciful, the Especially Merciful

Acknowledgment

I thank my advisor Professor Kutlay Sever for his supervision and mentoring during my thesis study. I benefited from his experience and his approach towards the knowledge in general. I thank to my committee members, Dr. Ebubekir Atan and Professor Mücahit Sütçü for their time and feedback on the thesis. I also thank to Assoc.Prof.Dr. Ebru Bozacı and Assoc.Prof.Dr. Seçkin Erden for their partipication in my thesis defence. I additionally thank Dr. Metehan Atagür for his collaboration and mentoring me in my thesis study.

Besides, it is my pleasure to thank all of the people that helped me to get to this point. I would also thank Professor Refik Polat, Professor Mehmet Çevik, Scientist Dr. Mehmet Hakan Özdener, Assoc.Prof.Dr. Muhammet Hüseyin Çetin, and Mehmet Baki Öztürk for their encouragement. Their support will guide me in the rest of my life as being until now. Also, my special thanks and prays go to Professor Necmettin Erbakan.

This work partially supported by Scientific Research Projects, İzmir Kâtip Çelebi University under grant number 2021-TDR-FEBE-0011.

My endless thanks go to my dear parents Ayşe and İlyas for their unflappable support, understanding and care in my life. I also thank my siblings Sıdıka, Abdullah, Esma, Fatih, Zehra and all my nephews and nieces for their invaluable care and bond.

Last but not least, my special gratitude goes to my wife Fatma for her understanding and patience. Her and our children's, Saliha and Ahmet Emre, presence has been a blessed haven for me.

Table of Contents

List of Figures

List of Tables

List of Abbreviations

a.u.	Arbitrary Unit
ASTM	American Society for Testing and Materials
DMA	Dynamic Mechanical Analysis
DSC	Differential Scanning Calorimetry
FTIR	Fourier Transformed Infrared Spectroscopy
H_2SO_4	Sulfuric Acid
HCl	Hydrochloric Acid
KBr	Potassium Bromide
MAPP	Maleic anhydride grafted polypropylene
MFI	Melt Flow Index
$NaClO_2$	Sodium Chloride
NaOH	Sodium Hydroxide
NH_3	Ammonia
PMCs	Polymer Matrix Composites
PP	Polypropylene
PSD	Particle Size Distribution
SEM	Scanning Electron Microscopy
TGA	Thermogravimetric Analysis
XRD	X-Ray Diffraction

Chapter 1

Introduction

In this section, a general definition and classification of composite materials were given. Within this classification, polymer matrix composites, which were also the subject of this study, were discussed in detail. Polypropylene, a thermoplastic material, has been studied, too. Secondly, general information about lignocellulosic materials used as fillers in polymer composites was specified. Afterward, some of the methods used to increase the bonding of hydrophilic lignocellulosic fibers and hydrophobic polymers were summarized.

1.1. Composites

Composites are materials prepared by combining them in a certain order at the macro level in order to obtain superior properties by improving the weaknesses of different materials that do not have chemical interactions between them. In the 1950s, composite materials began to be used in the automotive industry for vehicle bodies. After the 1960s, composites started to become widespread as engineering materials, together with polymer matrix composites. Composites have shown rapid growth as they generally perform better when used as a substitute for steel and aluminum in structural applications [1].

Composite materials consist of matrix and reinforcing materials. In composites, there is a reinforcement used as a core and a matrix material forming the majority in volume around the reinforcement. While reinforcement provides strength properties such as strength and load bearing to the composite material, the purpose of the matrix is to delay the rupture of the composite, to keep the fibers together under load, and to distribute the load homogeneously among the fibers.

The popularity of composite materials lies in the fact that, when prepared in a well-planned manner, they tend to exhibit the best properties of their components and even exhibit some new desirable properties that none of their components show. Some of the properties that can be improved by creating a composite material are strength, hardness, corrosion resistance, fatigue life, attractiveness, temperature-dependent behavior, and thermal insulation or thermal/electrical conductivity [2].

1.2. Polymer Matrix Composites

Polymer matrix composites (PMCs) are materials consisting of a polymer matrix combined with a reinforcing dispersed phase, also called a filler. PMCs are very popular due to their low cost and simple fabrication methods. The use of pure polymers for structural purposes is limited by the low mechanical properties of the polymers. PMCs offer improvements over pure polymers in properties such as tensile strength, hardness, corrosion resistance, temperature resistance, thermal conductivity, coefficient of thermal expansion, and flammability. The properties of PMCs are determined by factors such as the properties of the filler, the orientation of the filler in the polymer matrix, the concentration of the filler in the polymer matrix, and the properties of the polymer matrix [3].

1.2.1 Matrix Materials

A polymer is a large molecule made up of repeating structural units, monomers, made up of carbon, hydrogen, and other non-metallic elements. The two main classes of polymers are thermoset and thermoplastic. Both types of polymers are used in composites. Thermoplastic polymers are polymers that melt when heated and reversibly melt and become solid when cooled. Thermoset polymers are polymers that solidify irreversibly when exposed to certain conditions such as heating, cooling, or irradiation [4].

Polymers are widely used materials due to their ease of processing, lightness, and high toughness. On the other hand, polymers have lower hardness and strength compared to ceramics and metals. Polymers are often strengthened by incorporating reinforcements or fillers into the matrix to improve their mechanical, thermal, or

electrical properties. These reinforcements or fillers can be in the form of fibers, platelets, whiskers, or particles [3,5].

Strengthening polymers with reinforcements or fillers to obtain composites with new properties has been an active branch of research in recent decades. Real interest in polymer-based composite materials as an industrial commodity began in the 1960s. Since then, polymeric composites have become widely used engineering materials and are widely used in automotive, electronics, construction, household appliances, etc. It has been produced in large quantities to be used in numerous applications in industries.

Two different approaches are used for the classification of polymer matrix composites. The first approach is based on the physical structure of the filling, such as whether it is fibrous or laminated. The second a.pproach is based on the type of matrix, which is the matrix phase of a composite. The classification of polymer matrices is illustrated in Table 1.1 [6,7].

Table 1.1: The classification of polymer matrices

Polymer Matrix	Petrol-based non-degradable	PP, PE, PVC etc.
	Petrol-based bio-degradable	PBS, PCL etc.
	Bio-based non-degradable	Bio-PE, Bio-PET etc.
	Bio-based bio-degradable	PLA, Bio-PBS etc.

1.2.2 Filler Materials

Additives for polymer matrix composites can be categorized as reinforcements and fillers. Reinforcements usually increase polymer modulus and strength. The reason for this increase may be that reinforcements are much stiffer and stronger than polymers. Therefore, they also have a significant impact on thermal expansion,

thermal stability, transparency, etc. The term reinforcement is mostly used for long or continuous fibers, while the term filler is mostly used for short fibers, flakes, and particulates [3,8]. Most fillers do not provide the desired performance to improve composite properties. It can be said that reducing the cost of composites is the most important advantage of fillers. The filler source can be either natural or artificial. Examples of natural ones obtained from nature are summarized in Table 1.2 [3]. Clay and talc are samples for inorganic filler, and wood fiber, leaf, seed, and stem fibers are samples for organic filler.

Table 1.2: Chemical family classification

Chemical family	Fillers
Organics	
Natural	Cellulose fibers, wood flour and wood fibers
Synthetic	Polyamide, polyester and aramid fibers
Carbon, graphite	Carbon fibers, carbon nanotubes and graphite fibers
Inorganics	
Oxides	Glass fibers, MgO, SiO2 and Al2O3
Salts	CaCO3, CaSO4 and phosphates
Silicates	Talc, mica, wollastonite and kaolin
Metals	Boron and steel

In nature, the hierarchical structure of lignocellulosic fibers, as shown in Figure 1.1 [9], is based on their elementary components, leading to their unique strength and high-performance properties. A characteristic wood fiber wall contains four main layers, cell wall structure part, the primary wall and three layers of secondary wall; the outer (S1), middle (S2) and inner (S3) layers. The thickness of the layers, other than the S2 layer, remains relatively constant from one fiber to another.

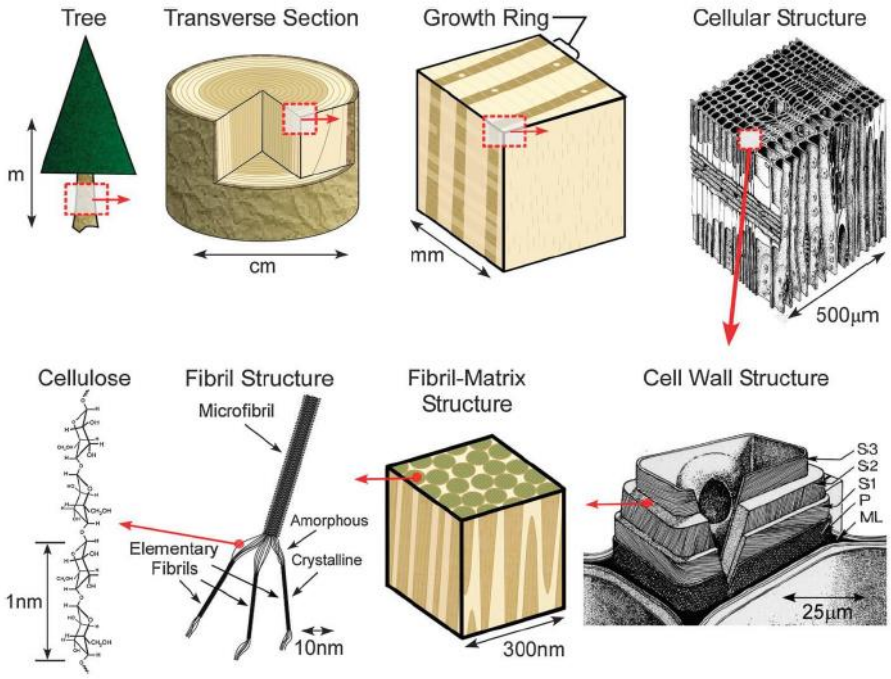

Figure 1.1: Hierarchial structure of wood from macro to nano scale

In this study, bing cherry tree (Prunus avium L.) pruning branches were used as filler material. According to the Food and Agricultural Organization data between 2014 and 2018, it is seen that Turkey ranks first in cherry fields, followed by the United States, Chile, Syria, Italy, Spain, and Iran, respectively. Turkey maintains its global leadership by creating 20% of the total cherry field with 85 hectares and 25% of the total cherry production with 640 tons in 2018. Also, the number of bing cherry trees in Turkey is approximately 27 million, according to the Türkiye Statistical Institute [10].

The importance of pruning in cherry cultivation is high in terms of yield and plant health. Furthermore, pruning is necessary in order to perform other agricultural tasks in aquaculture and to keep the tools and equipment operational [11]. The significance of pruning in cherry cultivation is very considerable and mandatory in terms of yield and development, too. Pruning residues exposed to existing habits are usually destroyed by burning on-site. This both creates carbon dioxide in the atmosphere and leads to potential energy loss. In this study, bing cherry tree pruning branch residues were used as filler materials in thermoplastics. Alkali treatment and maleic

anhydride-grafted polypropylene coupling agents have been successfully applied for interface improvement between filler and matrix material.

1.3. Biocomposites

Biocomposites are applicable for many areas in industry, from biodegradable to durable. However, there are some problems that delay their adaptation to some areas, in conjunction with water, using at high-temperatures, and very high-strength applications. These limitations are in many cases linked to the fiber-polymer matrix interface, polymer properties, or temperature limitation of the lignocellulosic fibers. To achieve the optimum performance of biocomposites, an adequate degree of adhesion is usually required between the surface of the hydrophilic lignocellulosic fibers and the typically hydrophobic polymer matrix. Due to the presence of hydroxyl and other polar groups in various components of lignocellulosic fibers, moisture absorption in biocomposites tends to be high, leading to poor interfacial bonding between fibers and matrix polymer [12]. Temperature stress on fibers during processing also has an effect on the strength properties of the biocomposite and limits its maximum service temperatures [13].

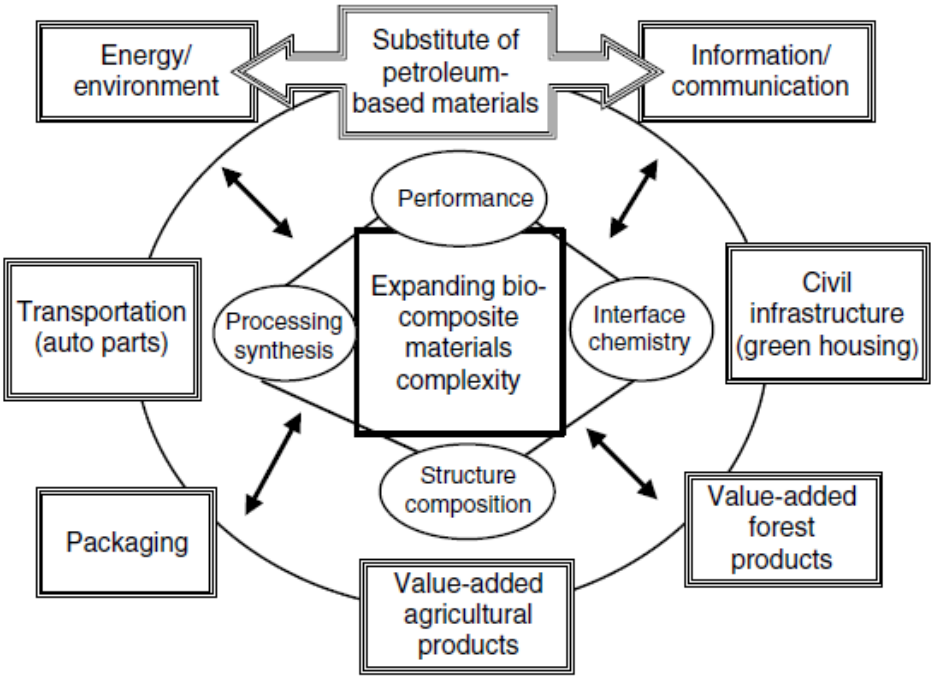

Figure 1.2: The relationship between the development of biocomposite materials and their uses

The relationship between the development of biocomposite materials and their uses is shown schematically in Figure 1.2 [7]. The challenge in replacing traditional composites with biocomposites is to design materials that show structural-functional stability during both storage and use but are susceptible to microbial and environmental degradation [7]. The limits of biocomposites may be managed through their use and industrial interactions through value-added products for a variety of applications from energy and environmentally beneficial perspectives, thereby establishing effective communication that will enable the real-world use of biocomposite materials.

Chapter 2

Background and Literature Survey

Controlling fiber-polymer interfaces, or interfacial interaction between fiber and matrix, is a critical component in the production of high-strength biocomposites. Stress transfer between matrix and filler is enabled by good interfacial bonding. Inherently hydrophilic lignocellulosic fibers are incompatible with a normally hydrophobic, polar polymeric substrate, resulting in poor bonding [14]. This can be seen in particle-filled biocomposites as poor fiber dispersion, agglomerates, and porosity, which results in low strength qualities, substantially impact strength properties, and high water absorption [15,16].

The interfacial adhesion between fiber and polymer matrix can be formed by mechanical interlocking, electrostatic bonding, chemical bonding, or inter-diffusion bonding. Mechanical interlocking occurs when a fiber surface is rough and increases interfacial shear strength but has less effect on transverse tensile strength. Electrostatic bonding can occur only via close interaction between fiber and other components in a composite and requires different electrostatic charges in fiber, matrix, or additives. Chemical bonding occurs when chemical groups on fiber surfaces react with matrix or other additives, creating bonds between fiber and polymer matrix. In inter-diffusion bonding, the atoms and molecules of the fiber and matrix interact at the interface by, for example, chain entanglement, and the strength is dependent on the length of the chains entangled [14,17].

One important factor in creating good interfaces between fiber and polymer is the sufficient wetting of fibers when mixed with the polymer melt. In many cases, the wetting is a compound of sufficient polymer melt viscosity to enable proper wetting of fibers and temperature in the process [17]. With polymers having high melt viscosity at temperatures preferred for lignocellulosic fibers, proper fiber dispersion

and wetting may not be sufficient. The poor fiber - matrix interaction in final products has an effect on durability and abrasion properties, creep performance, and wetting performance. To tackle this challenge, fiber and polymer modification methods, as well as additive systems, are being developed. The main methods are different physical and chemical modifications of fibers, modifications of polymers, and the use of coupling agents.

Lignocellulosic fibers are compatible with chemical modification due to the presence of hydroxyl groups. Hydroxyl groups may be involved in hydrogen bonding within cellulose molecules, thus reducing their activity towards the matrix. Chemical modifications can activate these groups or introduce new compounds that can be effectively coupled with the matrix. One of the most common chemical modification methods in the literature is alkali treatment using sodium hydroxide (NaOH). The alkali treatment improves the fiber surface adhesive properties by removing natural and artificial impurities from the surface. As a result, the surface tension and thus the wettability of the lignocellulosic fibers are improved, resulting in better bonding between the fibers and the matrix [18].

Alkali treatment is defined as exposing the fibers to a highly concentrated aqueous solution containing a strong base so that they swell well. As a result, the structure, dimensions, morphology, and mechanical properties of the fiber change. NaOH is the most common chemical used to clean the surface of lignocellulosic fibers and changes the structure of natural cellulose I and cellulose III by depolymerization and producing short-length crystals. Basic fiber properties such as strength and elongation at break can be changed by selecting the appropriate treatment parameters [19].

Maleic coupling agents are commonly used in reinforcing composites containing fillers and fibers. Maleic anhydride is used to modify the fiber surface as it is used in the polymer matrix to improve the mechanical properties and interfacial bonds of composites. The PP chain ensures the adhesion of maleic anhydride and the formation of maleic anhydride-grafted polypropylene (MAPP). It provides covalent bonds between the MAPP copolymer and the processed cellulose fiber interface. Used as a coating agent for surface modification of natural fibers, MAPP significantly improves the mechanical properties of lignocellulosic fiber-filled

biocomposites such as tensile strength, modulus of elasticity, flexural strength, stiffness, and impact strength [20]. Through the reaction of the hydroxyl groups on the cellulose surface with maleic anhydride, there is a decrease in the intramolecular hydrogen bonds between the fibers. This results in better dispersion of the fibers within the matrix.

Vijaya et al. (2022) studied the extraction and characterization of cellulose fibers obtained from the bark of Ziziphus nummularia. The water retting method was used to extract Ziziphus nummularia fibers from its bark. The extracted fibers were analyzed for their chemical, crystalline, thermal, mechanical, and physical properties. The surface characteristics of the fiber surfaces were examined using a scanning electron microscope and an atomic force microscope. The chemical analysis results showed that the cellulose content was 52%. The crystalline index was 46%, and the crystallite size was 2 nm. The maximum degradation temperature is 348 °C, obtained from thermogravimetric analysis. The researchers reported that the morphological properties of Ziziphus nummularia fibers had a good surface roughness that helped form interlocks with the polymer matrix [21].

Hossain et al. (2022) studied a cellulosic fiber extracted from the bark of jack tree branches. They reported that the chemical composition of the fiber contains 79% α-cellulose, 8% hemicellulose, and 6% lignin. The density of the fiber is 1.05 g/cc, which is lower compared to many other known natural fibers. X-ray diffraction analysis reveals its high level of crystallinity (86%), and the microfibrillar angle calculated from the X-ray diffraction data is found to be 29. Thermogravimetric analysis and the derivative thermogravimetric analysis indicate its good thermal stability, and the maximum degradation occurred at 358 °C for the degradation of the α-cellulose [22].

Madival et al. (2022) evaluated the effect of different chemical treatments (sodium hydroxide, acetic acid, and potassium permanganate) on the surface characteristics and the adhesion capabilities of Furcraea foetida fiber. It is reported that the chemical treatments eliminate the O-H functional groups and enhance the hydrophobic characteristics of the fiber. Also, the amorphous organic attachments were removed, and the crystallinity in the fiber was improved by chemical treatments. The microscopic analysis of chemically treated fiber showed the elimination of organic

attachments and a neat, uniform surface structure. The sodium hydroxide-treated fiber exhibited a maximum tensile strength of 242 MPa. Whereas the acetic acid-treated fiber showed a maximum tensile modulus of 7 GPa and an interfacial shear strength of 0.06 MPa compared to treated and untreated Furcraea foetida fibers [23].

Atagür et al. (2020a) demonstrated whether Carpinus betulus particles can be used as a filler for polypropylene. About 5, 10, 15, and 20 wt% Carpinus betulus-filled polypropylene composites were prepared by a high-speed thermokinetic mixer. They reported that the melting temperature of the composites decreased with the increase in Carpinus betulus content. The crystallization temperature of polypropylene increased with the addition of Carpinus betulus into polypropylene. When 10 wt% Carpinus betulus filler was loaded into polypropylene, the tensile strength of polypropylene increased by about 29 wt%. The storage modulus of polypropylene was remarkably enhanced with an increasing Carpinus betulus weight fraction. About 5 wt.% of Carpinus betulus added into polypropylene increased the flexural strength of polypropylene by about 32% [24].

Atagür et al. (2020b) investigated the reinforcing effect of Ceratonia siliqua as a filler for polypropylene. By filling 5% and 10% of Ceratonia siliqua into polypropylene, the tensile strength and flexural strength of polypropylene increased by about 32 and 23%, respectively. Ceratonia siliqua filling into polypropylene led to lower coefficients of thermal expansion, which could help prevent the thermal expansion [25].

Jiang et al. (2019) studied wood fiber-polypropylene composites with strong interfacial compatibility. First, they applied an alkali treatment to the wood fiber. Then they synthesized multi-monomer grafted copolymers of polypropylene and polypropylene wax. They reported that the so-synthesized polypropylene well compatibilized the interfaces of the alkali-treated wood fiber-polypropylene composites. The mechanical properties and water resistance results indicated that synergistically compatible alkali-treated wood fiber-polypropylene composites had better performance than other composites [26].

Kaya et al. (2018) investigated the filling properties of olive pomace powder, an agricultural waste, for polypropylene matrix. They produced composites with

different weight fractions of olive pomace (from 10 to 40 wt.%) using a high-speed thermokinetic mixer. They reported that when 40 wt% olive pomace filler was loaded into polypropylene, Young's modulus and flexural modulus of polypropylene increased by about 62% and 19%, respectively, and the storage modulus and thermal stability of polypropylene were remarkably enhanced with increasing olive pomace weight fraction [27].

Sohn and Cha (2018) used wood chips from furniture-manufacturing byproducts in their study. The wood chips were used for the flouring process and the chemical modification of wood flour. After chemical modification, the wood flour was mixed with polypropylene through extrusion compounding and injection molding to prepare wood-plastic composite injection-molded samples. The researchers reported that the impact strength was improved by up to 56% and the tensile strength by up to 34%. As a result of chemical modification, the measured contact angle of the wood-plastic composite increased, which means that the wettability of the wood-plastic composite sample surface decreased [28].

Maache et al. (2017) investigated the properties of a new lignocellulosic fiber extracted from Juncus effusus. They reported that the study of the surface morphology revealed that the cross-section of the fiber bundle has a cellular shape similar to other fibers reported in the literature. Also, the longitudinal section of the fiber was characterized by the presence of rough surfaces, which should greatly improve the mechanical anchoring in the matrix. The X-ray diffraction analysis showed the semi-crystalline nature of the fiber with a crystallinity index of 33.4%. Thermogravimetric analysis of fiber evidenced a thermal stability up to 220 °C, which confirms the possibility of its use as reinforcement for polymer matrix composites. The mechanical properties resulting from the tensile tests performed on the fiber bundle, i.e., strength of 113 MPa, strain at break of 2.7%, and Young’s modulus of 4.4 GPa, showed that these values are globally similar to other plant fibers reported in the literature [29].

Nukala et al. (2022) developed wood-polymer composites using recycled plastic waste as a matrix and recycled wood waste as reinforcement or filler by melt-blending technique. They reported that the mechanical strength of the wood-polymer composites was found to increase from 26.59 to 34.30 MPa with an increase in the

wood content in the matrix. The thermal stability was higher in the composite with a higher percentage of wood in the matrix. The wettability results indicated that the composite with a higher percentage of wood (20%) had a higher water uptake. The SEM micrograph indicated good interaction between recycled wood waste reinforcement and filler and recycled plastic waste matrix [30].

Atagür et al. (2020c) evaluated the performance of sandalwood as a potential filler material for high-density polyethylene. From DMA analysis, storage and loss moduli values of the high-density polyethylene composites increased with increasing the weight fraction of sandalwood. They reported that sandalwood incorporation into high-density polyethylene at weight fractions of 5% and 20% exhibited improvements in tensile and flexural strengths, and the reinforcement effect of sandalwood on high-density polyethylene is more prominent at high temperatures, too [31].

Murad and Sirahbizu (2022) investigated the effect of waste wood species from the furniture industries on wood-plastic composites. They prepared the samples by varying the wood flours at 30 wt.% mixed with 70 wt.% high-density polyethylene. The composite from the mixture of wood species exhibited the best interfacial bonding between matrix and reinforcement, which resulted in the best water absorption property and the maximum tensile strength of the composite with a 15.5 MPa value. They also observed that with the addition of wood, the impact strength was reduced compared with pure high-density polyethylene [32].

Kılınc et al. (2018) manufactured and characterized vine stem-reinforced high-density polyethylene composites. They produced the samples using a twin screw extruder by adding different amounts of filler (5%, 10%, and 20% wt.) into high-density polyethylene. They reported that HDPE containing 10% waste vine stem exhibited the highest tensile strength and flexural strength. Vine stem powder addition into high-density polyethylene delayed the thermal decomposition of high-density polyethylene. Dynamic mechanical analyses showed that the storage modulus values of reinforced high-density polyethylene are higher than those of neat high-density polyethylene throughout the whole temperature scale [33].

Gairola et al. (2022) studied the potential of novel lignocellulosic crop residue fibers (husk) extracted from finger millet and barnyard millet. They reported that chemical constituent analysis reveals higher cellulosic and lower lignin content in finger millet (38% cellulose and 16.3% lignin) than barnyard millet (cellulose, 34.5%, and lignin, 21.3%). Thermal kinetics shows higher activation energy for barnyard millet (207.2 kJ/mol) than finger millet (129.8 kJ/mol), as per the Flynn-Wall-Ozawa model. Barnyard millet-reinforced composites offer higher thermal stability and flame resistance than finger millet-reinforced composites, while finger millet-reinforced composites show higher mechanical properties than barnyard millet-reinforced composites [34].

Narlıoğlu (2022) studied to determine the effect of modified wood flour on thermoplastic composites. For this purpose, wood flour treated with sodium hydroxide at 3%, 6%, and 12% concentrations was added to polyvinyl chloride polymer. He reported that the tensile strength, flexural strength, and tensile modulus values of the composite samples containing alkali-treated wood flour were higher than those containing untreated ones. The highest tensile and flexural strength values were determined in the composite sample containing 6% sodium hydroxide-treated wood flour. In addition, thermogravimetric analysis results showed that alkali treatment caused an increase in the thermal stability of composites [35].

Erdogan and Huner (2018) studied the production and characterization of different types of lignocellulosic fillers, pinewood sawdust, walnut shell flour, and black rice husk powder-reinforced polypropylene composites. They also investigated the effect of maleic anhydride-grafted polypropylene as a coupling agent (4 wt.%) on the physical and mechanical properties of composites. Composite samples were prepared at different rates of matrix/filler weight percent by using an extrusion and hot compression molding process. Maximum values of tensile and flexural strength were obtained as 26 MPa and 43 MPa, respectively, whereas the elongation at break value was 4% at 10% pine wood sawdust-reinforced polypropylene. The tensile and flexural moduli of composites reached maximum values of 3850 MPa and 3630 MPa with the composite of 30% walnut shell flour-reinforced polypropylene [36].

Hung et al. (2017) selected four kinds of cellulose-based fibers, from Chinese fir (Cunninghamia lanceolata), Taiwan red pine (Pinus taiwanensis), India-charcoal

trema (Trema orientalis), and Makino bamboo (Phyllostachys makinoi), for their research. These fibers were added to high-density polyethylene to manufacture wood-plastic composites as reinforcements and fillers. In addition to comparing the differences in the physicomechanical properties of composites, the researchers evaluate chemical compositions and analyze thermal decomposition kinetics to investigate the effects of the lignocellulosic species on the properties of composites. They reported that the composite made with Chinese fir displayed a typical M-shaped vertical density profile due to the high aspect ratio of its cellulose-based fibers, while a flat vertical density profile was observed for the composites made with other cellulosic fibers. Thus, the composite made with Chinese fir exhibited higher flexural properties and lower internal bond strength than other composites. In addition, the Taiwan red pine contained the lowest holocellulose content and the highest extractives and cellulose contents, which gave the resulting composite lower water absorption and flexural properties. These results indicate that the morphology, chemical composition, and thermal stability of the cellulose-based fibers can have a substantial impact on the physicomechanical properties of the resulting wood-plastic composites [37].

Nnodu et al. (2020) studied the effects of chemical modifications of pineapple leaf fiber, with an average particle size of 75 μm, on the mechanical and physical properties of fiber-filled polypropylene composites. The fiber was alkali-treated using sodium hydroxide and bleached using hydrogen peroxide. Maleic anhydride-grafted polypropylene was used as a compatibilizer. Analysis of the pineapple leaf fiber showed that it contains 65.3% cellulose, has a density of 1.9 g/cm3, and has a moisture content of 6.1%. They reported that the addition of maleic anhydride-grafted polypropylene and the use of treated pineapple leaf fibers improved the tensile strength of the composites. The untreated pineapple leaf fiber-prepared composites exhibited the least tensile strength and had higher elongation at break than the filled composites. The elongation at the break of the polypropylene composites decreased with an increase in fiber content, while the addition of maleic anhydride-graft-polypropylene and treated pineapple leaf fiber improved the elongation at the break of the composites. As a result, the study has shown that the use of maleic anhydride-graft-polypropylene, alkali treatment, and bleached pineapple leaf fibers in compounding polypropylene increased the hardness and

specific gravity of the resulting composites and decreased their water absorption properties [38].

Hamou et al. 2023 investigated polypropylene composites reinforced/filled with alkali-treated hemp fibers at different weight percents. They reported that a value of 2.10 GPa for young's modulus is achieved from 30 wt% of hemp fibers containing biocomposite, which is significantly higher than the 0.85 GPa of polypropylene matrix. Also, flexural modulus increased by 46%, 165%, and 232% compared to neat polypropylene at 10, 30, and 40 wt% fiber content, respectively. Such stiffness increases were followed by flexural strength increases of 52%, 78%, and 92% relative to neat polypropylene in the presence of 20, 30, and 40 wt% hemp fibers, respectively. They also studied the effects of various parameters on the thermo-mechanical properties of the final composites, which were hybrids made of polypropylene reinforced with both hemp fibers and wood fiber. These hybrid biocomposites were prepared with weight ratio of 20% and 40% hemp fibers and wood fiber, and variable ratios of the two reinforcements showed a positive hybridization effect. Nevertheless, the modulus of the hybrid biocomposites reinforced by both fibers, hemp/wood fibers (20/20), is 166% greater than the modulus of neat polypropylene and 34% greater than the hemp/polypropylene composite with 40% fiber content [39].

Vinod et al. (2023) extracted Capsicum annum stem fibers from the agro-waste of Capsicum annum stem as an alternative raw material resource. The extracted fibers were subjected to sodium hydroxide and oxalic acid treatments to study the effect of chemical treatments on the physical, chemical, thermal, and mechanical properties of fibers. They reported that the oxalic acid treatment improved the cellulose weight percent by up to 30%, and the sodium hydroxide treatment decreased the diameter of the fibers by up to 17%. The thermal stability of oxalic acid-treated fibers was 359ºC, and they exhibited the highest activation energy of 49×103 Jmol 1 at the final degradation phase, which was 11% higher than untreated fiber. The half-life period of the oxalic acid-treated fibers was increased from 3.8 min 1 to 5.3 min 1 at the cellulose degradation phase, revealing better thermal stability when compared to the untreated and sodium hydroxide-treated fibers. The scanning microscopic images

and the surface plots revealed an enhancement in the surface roughness and wettability of the oxalic acid-treated fibers [40].

Youbi et al. (2022) aimed to evaluate the influence of chemical treatment on the surface modification of Raphia vinifera fibers. They treated the fibers with different concentrations of alkali solution (1%, 5%, and 10%) for 30 min, 60 min, and 90 min, and silane (1% and 5%) for 30 min and 60 min. Researchers reported that the results reveal a modification of the chemical structure as well as the thermal degradation of the fibers after treatment with alkali and silane. Scaning electron microscopy analyses show that alkali treatment of raffia fibers induces a significant reduction (confidence level 90%) in fiber cross-section compared to untreated fiber, resulting in a change in surface roughness and the appearance of cracks. Furthermore, the use of silane and 1% alkali treatments significantly improves the surface energy of the fibers over time, while 5% and 10% alkali concentrations decrease the surface energy over time. Statistical analysis of the mechanical performance results reveals a significant increase in the Young's modulus of the fibers with the treatment time and the concentration of the treated solutions [41].

In general, considering the previous research in literature, novel lignocellulosic fibers were characterized and their use as fillers in thermoplastics was investigated in this thesis study. Surface modification was applied to the lignocellulosic filler in order to strengthen the interfacial adhesion between polymer and filler and the MAPP coupling agent was reinforced into the PP matrix. Ultimately, the biocomposite was produced and characterized according to the final recipe. As a result, compared with PP and untreated particle-filled biocomposites, the biocomposite with improved thermal and mechanical properties was produced.

Chapter 3

Motivation

In this chapter, the purpose and the aim of this thesis study were explained, and information was given about the planned and obtained achievements within the scope of this research.

Research on composite materials, which started in the second half of the 20th century, has continued rapidly until today. Through the properties that can be imparted to polymer materials, the performance properties of products made from other materials were first achieved and then largely surpassed. This situation has increased interest in the composite industry [42,43]. The low weight-to-strength ratio, low cost compared to other material types, and good abrasion resistance have been important factors in the widespread use of polymer matrix composites. The ability to increase various strength values by reinforcement or filling according to the place of use has allowed it to be used in places where metal or other materials are used. In addition, the ease of processing provides significant advantages to composite materials. Because of their low melting temperatures in terms of manufacturability, they can be easily shaped by heat and pressure methods, providing variety and convenience in product designs [44].

While a wide variety of reinforcement/filling materials are used in the production of composite materials, the use of lignocellulosic fibers instead of synthetic fibers such as glass fiber and aramid has been popularized. The decrease in resources in recent years and the increase in environmental awareness play an important role in this popularization. Therefore, studies on the utilization of waste materials as natural fiber sources in biocomposite production, thus preventing environmental pollution, ensuring recycling, and reducing composite production costs, have accelerated globally [45].

Within the scope of the thesis, the preparation of filling materials from pruning wastes and the examination of filler-matrix interface improvement studies in order to bring the strength and thermal values to a reasonable level were studied. It is provided that the results obtained as a result of extensive studies will supply preliminary information that will facilitate the use of such biocomposites in future application areas. In general, with the study, an environmentally friendly material that is less harmful to nature has been obtained as a result of both reusing agricultural pruning wastes in biocomposite production and reducing the use of plastic as much as possible.

The aim of the thesis carried out is to develop the design and industrial production systematic of biocomposite materials where economic, environmental, and social benefits are expected by evaluating agricultural pruning wastes, having a limited collection and recovery in the current system, together with polymers. It is aimed to transform the material obtained by the wastes added into the matrix in the form of particles into biocomposite products that can provide the expected mechanical and thermal properties in required utilization conditions. In addition, through this study, while contributing to the disposal of pruning wastes the amount of plastic usage will be reduced also. Since the new biocomposite materials to be produced could provide alternative usage areas, and new products, it is thought that the gains to be obtained will increase even more after these researches. With this work, it is also aimed to transform waste materials that have no commercial value into valuable materials for these rapidly developing sectors which have an important site in countrys' industry.

Looking at the objectives of the study in general, a study was carried out on the production and development of polypropylene matrix composite filled with pruning wastes. The use of cherry tree pruning wastes as filling materials in thermoplastics has not been investigated before in academia and industry. Within the scope of the study, firstly, the chemical and physical properties of the filling materials completed with the related tests and analysis. In this way, the most ideal material and particle size were determined and the basis of the doctoral thesis was formed. After determining the ideal material and particle size, limited strength values were achieved as a result of the poor fiber-matrix interface adhesion observed in the biocomposite structure. In order to include the considered particles as an alternative

material in applications, improvement studies were carried out on mechanical strength values and thermal properties. In this context, surface treatment and coupling agent were used to improve the filler-matrix interface adhesion.

In summary, the objectives of this research are reducing the dependence on abroad, especially for thermoplastics, by reducing the use of plastic raw materials; bringing pruning wastes to the economy; to bring different filler materials to the sector by turning an important cost into value added product, to develop systematic research and development study for other agricultural and industrial wastes. In general, in line with the results of the research, it is seen as a priority target to obtain a new biocomposite with a pruning waste-filled polymer matrix. It might be potentially new and alternative material for potential areas such as automotive, construction, housewares, and garden landscape sectors.

Chapter 4

Materials and Methods

4.1 Materials

Polypropylene (PP) co-polymer was used in this research as a matrix material that has the LG M1500 commercial brand. It has a melt flow index of 16 g/10 min (230 ℃, 2.16 kg) and a density of 0.9 g/cm^3 as physical characteristics. In addition, the typical mechanical and thermal properties were given in Table 4.1 [46].

Table 4.1: The typical properties of polypropylene

Characteristics	Value	Unit	Test Method
Tensile Strength at Yield	25	MPa	ASTM D638
Flexural Modulus	1200	MPa	ASTM D790
Elongation at Break	300	%	ASTM D638
Izod Impact Strength (Notched, 23 ℃)	107	J/m	ASTM D256
Hardness (R-scale)	90	-	ASTM D785
Vicat Softening point (1 kgf)	150	°C	ASTM D1525
Heat Deflection Temperature (4.6 kgf/cm^2)	105	°C	ASTM D648

Cherry tree (Prunus avium L.) pruning branches were used as a lignocellulosic fillers in this study. These agricultural wastes were collected from an orchard at an altitude

of about 1600 meters in the Taurus Mountains in the Mediterranean region of Türkiye. The age of the trees in the garden is in the range of 5-10 years.

Sodium hydroxide (NaOH) used for chemical treatment was purchased from Tekkim, Türkiye. It has a density of 2.13 g/cm^3 at 20 ℃ and its molar mass is 40 g/mol. Maleic anhydride-grafted polypropylene (MAPP), which is used as a compatibilizer during the production of biocomposites, was purchased from Grafen, Türkiye. Its melt flow index is 120 g/10 min (190 ℃, 2.16 kg), the density is 0.9 g/cm^3 and the melting temperature is 162 ℃. Sodium chloride ($NaClO_2$; 90.44 g/mol; Sigma-Aldrich), ammonia (NH_3; Merck Corp.), sodium hydroxide (NaOH, 40 g/mol; Merck Corp.), hydrochloric acid (HCl; Merck Corp.) and sulfuric acid solutions (H_2SO_4; Merck Corp.) were used for the analysis of the chemical content of lignocellulosic fibers. These chemicals were get from the laboratories of the Faculty of Engineering and Architecture of İzmir Kâtip Çelebi University.

4.2 Methods

4.2.1 Preparation of Fillers

The wood and bark parts of the pruning waste branches were separated from each other. Then, they are divided into small pieces for homogeneous drying and ease of grinding. The materials were first dried in outdoor for a week and then oven-dried at 80 ℃ for 24 hours before grinding. Wood and bark were grounded in a laboratory-type grinder (Mertest LB160, Türkiye), separately. After the grinding process, 100 micron and 250 micron sieving was performed with a sieve shaker (Retsch RS200, Germany). Finally, wood and bark fillers were categorized into two particle sizes: under 100 micron and between 100 and 250 micron.

4.2.2 Surface Treatment and Coupling Agent Processes

Although alkali surface treatment is one of the most common methods, the efficiency of the application changes according to the NaOH concentration and the treatment duration. For this reason, it is beneficial to optimize the appropriate treatment values for the material. The fillers were optimized by applying different concentration ratios

at a constant time. It can be seen that these concentration ratios are applied in the range of 1% to 40% for lignocellulosic fibers [25,47,48].

Within the scope of the study, alkali treatment of the filler was carried out in order to improve adhesion between filler and matrix. In this method, primarily NaOH solutions with 3%, 5%, and 10% concentration ratios were prepared. After adding filler, the solution was mixed an hour with magnetic stirrer. After treatment, the filler was washed with distilled water until the pH value was about 7 and filtered. Then, the treated filler materials extracted from the distilled water were dried with the help of an oven. Figure 4.1 shows a schematic illustration of the surface modification process flow (modified from Akyüz, 2020 [49]). The functional surface groups of treated fillers were investigated by FTIR analysis. Thus, in the NaOH application, the different solution concentrations at constant treatment time were investigated.

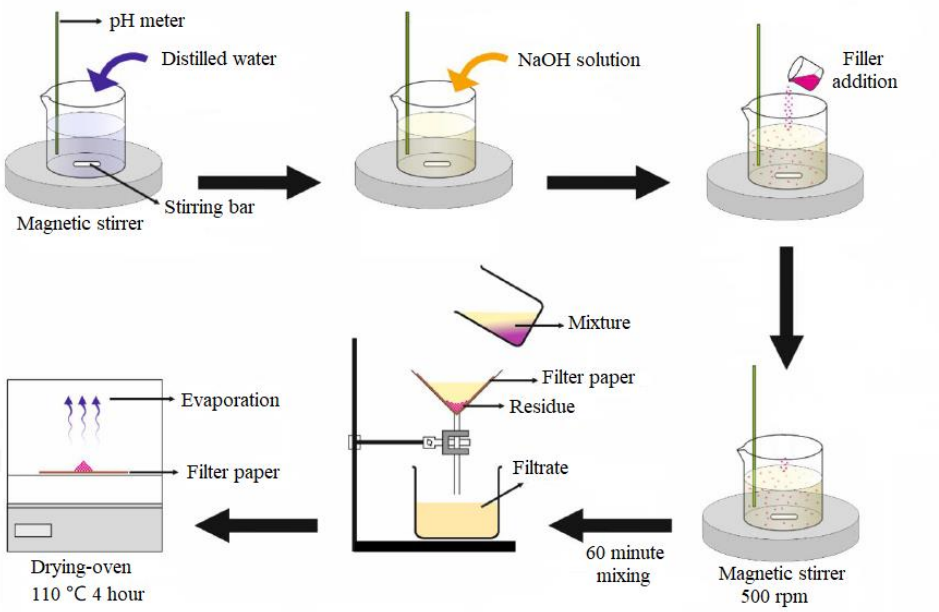

Figure 4.1: Schematic illustration of the filler surface treatment process

In order to optimize the compatibilizer ratio in the matrix material, maleic anhydride-grafted polypropylene (MAPP) was added at the rates of 1%, 3% and 6% by weight into the neat PP and samples were produced by the laboratory type thermokinetic

mixer. These samples were subjected to tensile and three-point bending tests to determine the optimum MAPP ratio.

4.2.3 Manufacturing of Biocomposites

A high-speed thermokinetic mixer and a hydraulic press (Gülnar Machine, Türkiye) were used to produce biocomposites. The high-speed thermokinetic mixer is generally used to prepare composites for thermoplastics with low melting temperatures (PP, HDPE, LDPE etc.). It is widely used in pre-tests in the plastics industry and academia because it provides simple and rapid productions [25,47,48]. The most important advantage of the mixer is that it allows the production of composite materials in a short time. This type of mixer operates at a high speed to create friction with the polymers. In the mixer, which rotates at 2000 rpm, the materials can reach a temperature of about 190 ℃. The power of the motor is transferred directly to the material with the help of blades. The added filling materials and the polymer are thoroughly mixed in the chamber. The resulting polymer-based pastes are molded in a temperature and time-controlled hot-cold hydraulic press to enable the preparation of samples for various tests. All composite plates were cut for mechanical tests and dynamical mechanical analysis according to the related test standards. A schematic representation of all this production flow is given in Figure 4.2 (modified from Akyüz, 2020 [49]).

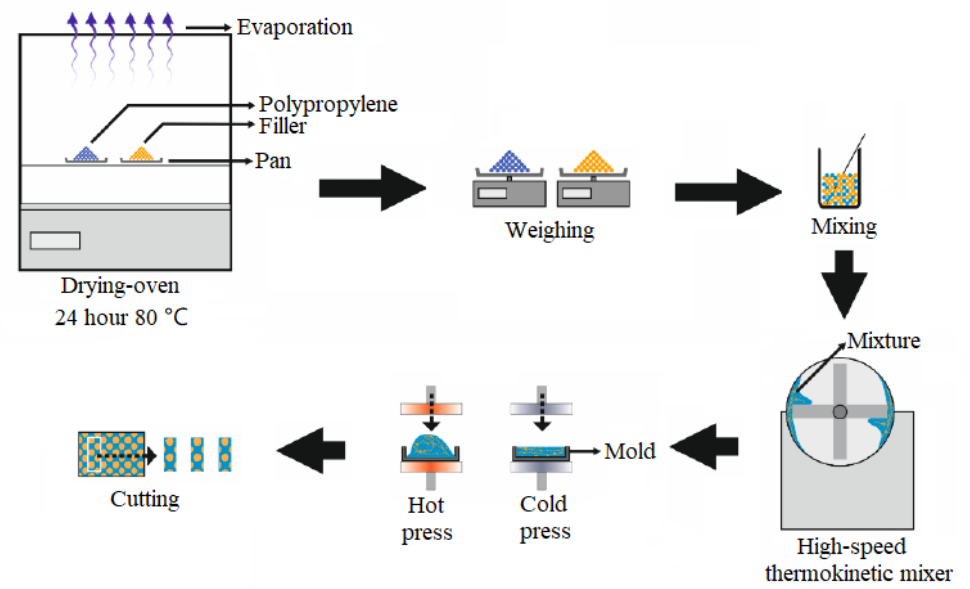

Figure 4.2: Schematic illustration of the biocomposite manufacturing process

The nomenclature of all fillers, matrix materials, and biocomposites prepared and used in this study are presented in the Table 4.2.

Table 4.2: Nomenclature of materials

Abbreviation	Sample
Wood	Wood particles without particle size categorization
Bark	Bark particles without particle size categorization
UTW	Untreated wood with <100µ particle size
UTW2	Untreated wood with 100 – 250µ particle size
UTB	Untreated bark with <100µ particle size
UTB2	Untreated bark with 100 – 250µ particle size
3ATW	3% alkali treated wood filler (<100µ)
5ATW	5% alkali treated wood filler (<100µ)
10ATW	10% alkali treated wood filler (<100µ)
PP	Neat polypropylene
5UTW	5 wt. % untreated wood (<100µ) filled polypropylene
10UTW	10 wt. % untreated wood (<100µ) filled polypropylene

15UTW	15 wt. % untreated wood (<100μ) filled polypropylene
20UTW	20 wt. % untreated wood (<100μ) filled polypropylene
5UTW2	5 wt. % untreated wood (100 – 250μ) filled polypropylene
10UTW2	10 wt. % untreated wood (100 – 250μ) filled polypropylene
15UTW2	15 wt. % untreated wood (100 – 250μ) filled polypropylene
20UTW2	20 wt. % untreated wood (100 – 250μ) filled polypropylene
5UTB	5 wt. % untreated bark (<100μ) filled polypropylene
10UTB	10 wt. % untreated bark (<100μ) filled polypropylene
15UTB	10 wt. % untreated bark (<100μ) filled polypropylene
20UTB	10 wt. % untreated bark (<100μ) filled polypropylene
5UTB2	5 wt. % untreated bark (100 – 250μ) filled polypropylene
10UTB2	5 wt. % untreated bark (100 – 250μ) filled polypropylene
15UTB2	5 wt. % untreated bark (100 – 250μ) filled polypropylene
20UTB2	5 wt. % untreated bark (100 – 250μ) filled polypropylene
1MAPP	1 wt. % maleic anhydride-grafted polypropylene added polypropylene
3MAPP	3 wt. % maleic anhydride-grafted polypropylene added polypropylene
6MAPP	6 wt. % maleic anhydride-grafted polypropylene added polypropylene
5AT10W	5% alkali-treated, 10 wt. % wood particle (<100μ) filled polypropylene
5AT10W-3MAPP	5% alkali-treated, 10 wt. % wood particle (<100μ) and 3 wt. % maleic anhydride-grafted polypropylene filled polypropylene

4.3 Characterization of Fillers and Biocomposites

In this thesis study, a series of test and analysis techniques are employed to characterize the untreated fillers, treated fillers, biocomposites and other related materials. These techniques are explained in detail.

4.3.1 Untreated and Treated Fillers

In this section, the tests and analyses performed for the characterization of untreated and treated fillers are described. The completed tests and analyses for these fillers are summarized in Table 4.3.

4.3.1.1 Determination of Chemical Composition

Wise's chloride method [50] was used to determine the chemical composition of the fiber including cellulose, hemicellulose, lignin, and extractive contents. The chemical content of lignocellulosic fibers was determinated in three steps; extraction process, determination of holocellulose, and alpha-cellulose, respectively.

Table 4.3: Completed analysis and tests for untreated and treated fillers

Sample / Test & Analysis	Chemical Content	Density	XRD	TGA	FTIR	PSD	SEM
Wood	+	+	+	+	+		
Bark	+	+	+	+	+		
UTW						+	+
UTB						+	+
UTW2						+	+
UTB2						+	+
3ATW					+		
5ATW			+	+	+	+	+
10ATW					+		

First, in order to remove the extractive substances in the lignocellulosic fibers, the fibers were extracted for 6 hours in a soxlet with a solvent containing a toluene/acetone/ethanol mixture at a ratio of 4/1/1 by volume.

Second, chloride method was applied to determine the holocellulose amounts of lignocellulosic fibers. This process is as follows; 2.5 grams of fiber, which was extracted, was taken into a 250 ml flask. Then, 80 ml of distilled water, 1 gram of Sodium chlorite ($NaClO_2$) and 0.5 ml of acetic acid (CH_3COOOH) were added into the flask and put into a water bath at 70-80°C. $NaClO_2$ and CH_3COOOH in 6 portions were added to the flask at 1 hour intervals and the system was stirred occasionally. After the process, the hot mixture was left to cool. Then, filtration with distilled water and acetone was applied on the crucible, which had been weighed completely dry before. After filtration, the sample was dried at a temperature of 103±2°C until it reached a constant weight, and the percentage of holocellulose was determined.

Third, TAPPI-T203 standards were applied to determine the alpha-cellulose amounts of lignocellulosic fibers prepared within the scope of the study. 2 grams of dry samples were taken from the samples obtained after the holocellulose determination. Afterward these samples were transferred into a 200 ml beaker and 10 ml of 17.5% sodium hydroxide (NaOH) was added to it, and they were mixed with a glass baguette and waited for 5 minutes. Next, 15 ml of NaOH solution was continued to be added to the samples in portions. After this process, 33 ml of distilled water was added to the samples and left for an hour. Then, the mixture was filtered and the washing process was terminated by pouring 100 ml of 8.3% NaOH solution, 10% CH_3COOOH, and 250 ml of distilled water. The filtrate after washing was kept in the oven at a temperature of 103±2°C until it reached a constant weight. Then, the weights of the samples were taken and the alpha-cellulose ratio was determined.

4.3.1.2 Density Measurement

Actual density measurements of fillers were performed using a helium pycnometer (Micromeritics AccuPyc II 1340). The helium pycnometer uses Archimedes' fluid overflow principle and Boyle's Law to determine the true volume and true density in powder and solid materials based on the gas displacement method.

4.3.1.3 Fourier Transformed Infrared Spectroscopy (FTIR)

Fourier transform infrared spectroscopy (FTIR) is an analysis method used for identifying the chemical bonds or functional groups existing in a material. Middle range infrared spectrum (400 – 4000 cm-1) is generally used for the characterization of samples. The absorption and transmission of infrared lights on the molecular level make it possible to obtain information about the chemical composition of unknown materials [51]. In this work, potassium bromide (KBr)/sample pellets were obtained after mixing the samples with KBr in agate mortar. FTIR analyzes of the samples were performed using the Thermo Scientific Nicolet iS50 spectrophotometer. IR spectra were obtained by making 25 scans at a resolution of 2 cm-1 in the range of 400-4000 cm-1.

4.3.1.4 X-Ray Diffraction (XRD) Analysis

XRD analyzes of the fillers were carried out with a Panalytical Empyrean Diffractometer with LynxEye detector in 2θ scanning mode (45 kV and 40 mA) with CuKα radiation to determine the characteristic peaks. The scanning detector collected data between 2θ=5° and 80°.

4.3.1.5 Thermogravimetric Analysis (TGA)

Thermogravimetric analysis is a technique used to measure materials' resistance to heat. In this technique, a sample is continuously weighed as its temperature is increased with a constant heating rate. The analysis can be performed under a nitrogen (inert) or air atmosphere. As the temperature of the sample increases, the sample starts to degrade or evaporate, which results in a decrease in the initial weight of the sample.

TGA analyzes were performed on the STA analyzer (TA Instruments, SDT Q600) to determine the thermal degradation temperatures. These analyzes were performed by heating the samples from 30°C to 600°C in a nitrogen gas atmosphere at a heating rate of 10°C/min.

4.3.1.6 Particle Size Distribution (PSD) Analysis

Malvern Mastersizer 3000 particle size analyzer was used to determine the average size of particles. Dry dispersion method was used to disperse the particles. The analysis process is based on the determination of particle sizes by looking at the scattering angle and intensity of the light obtained as a result of the reflection and refraction of the laser light sent to the sample from the particles.

4.3.1.7 Scanning Electron Microscopy (SEM) Observation

SEM is a microscopic analysis technique, which is widely used in the characterization of materials' surface morphology. In this technique, an electron beam sent from an electron gun scans the surface of the sample. The interaction of the electron beam with the surface atoms of the sample produces signals that are detected by a detector. The variations in the intensity of signals are processed and transformed into visible images. The surface of the sample should be electrically conductive. If the sample is electrically isolating, it should be made conductive by coating it with an electrically conductive material such as carbon or gold.

The morphological properties of the wood and bark particles were examined with a scanning electron microscope (SEM) (Carl Zeiss 300VP). Before SEM observation, the surfaces of the samples were homogeneously coated with gold with a plasma coating device (Quorum Q150 Res).

4.3.2 Biocomposites

In this section, detailed information about the tests and analyses performed on manufactured biocomposites and other related materials is explained. The completed tests and analyses for these materials are summarized in Table 4.4.

4.3.2.1 Fourier Transformed Infrared Spectroscopy (FTIR)

In this work, potassium bromide (KBr)/sample pellets were obtained after mixing the samples with KBr in agate mortar. FTIR analyzes of the samples were performed using the Thermo Scientific Nicolet iS50 spectrophotometer. IR spectra were

obtained by making 25 scans at a resolution of 2 cm-1 in the range of 400-4000 cm-1.

4.3.2.2 Thermogravimetric Analysis (TGA)

TGA analyzes were performed on the STA analyzer (TA Instruments, SDT Q600) to determine the thermal degradation temperatures of the PP and its composites. These analyzes were carried out by heating the samples from 30 °C to 600 °C in a nitrogen gas atmosphere at a heating rate of 10 °C/min.

4.3.2.3 Differential Scanning Calorimetry (DSC) Analysis

In differential scanning calorimetry (DSC) analysis, the sample is placed inside a miniature pan, with another empty pan –reference pan- next to it. Both pans are heated by applying thermal energy. The heat is conveyed to the pans in a manner that the temperature of both pans increases at the same rate. The difference between the rate of heat transferred to the sample pan and the empty pan is recorded with respect to temperature. The difference in the heat flow is basically the energy absorbed by the sample to increase its own temperature. When the sample undergoes physical changes such as melting, crystallization, or glass transition, the plot starts to disorder from its

Table 4.4: Completed analysis and tests for PP and its biocomposites

Sample / Test & Analysis	Tensile	Flexural	DMA	FTIR	TGA	DSC	SEM
PP	+	+	+	+	+	+	+
5UTW	+	+	+				
10UTW	+	+	+	+	+	+	+
15UTW	+	+	+				
20UTW	+	+	+				
5UTW2	+	+	+				
10UTW2	+	+	+				

15UTW2	+	+	+				
20UTW2	+	+	+				
5UTB	+	+					
10UTB	+	+					
15UTB	+	+					
20UTB	+	+					
5UTB2	+	+					
10UTB2	+	+					
15UTB2	+	+					
20UTB2	+	+					
1MAPP	+	+					
3MAPP	+	+					
6MAPP	+	+					
5AT10W	+	+	+	+	+	+	+
5AT10W-3MAPP	+	+	+	+	+	+	+

normal trend since more or less heat is needed for the sample to undergo physical changes. In addition, the heat capacity and transition enthalpies of the analyzed sample can be easily determined from this plot [52].

DSC analyzer (TA Instruments, DSC Q2000) was used in nitrogen gas atmosphere to determine thermal properties of composites such as melting temperature, crystallization temperature, melting enthalpy, and crystallization enthalpy. To erase the thermal history of the samples, the samples were heated from 20 °C to 200 °C at a heating rate of 10 °C/min and held at this temperature for 3 minutes. The samples were then cooled to 20 °C at a cooling rate of 10 °C/min and heated again from 20 °C to 200 °C at a heating rate of 10 °C/min.

4.3.2.4 Dynamic Mechanical Analysis (DMA)

In the dynamic mechanical analysis (DMA), the storage modulus is the variable used to calculate the stored energy, which represents the elastic region of the plastics and the loss modulus is the measure of the heat energy loss along the viscous region of the plastics. Storage and loss modules of PP and its composites were determined by Dynamic mechanical analyzer (DMA Q800, TA instruments). Analyzes were performed with a single cantilever clamp at a temperature range of 40-140°C and heating rate of 3°C/min.

4.3.2.5 Tensile Test

A universal testing machine (Shimadzu AG-IC, Japan) with a 5 kN load cell was used to determine the mechanical properties of the PP and its composites. Tensile tests were carried out according to ASTM D638 standard. Crosshead speed is 50 mm/minute. As a result of tensile tests, the tensile modulus and tensile strength of the samples were determined. The tests were repeated at least five times for each samples. The mean and standard deviations of the values obtained as a result of the tests were calculated with precision.

4.3.2.6 Flexural Test

The universal testing machine (Shimadzu AG-IC, Japan) with a 5 kN load cell was used to determine the flexural properties of the PP and its composites. Flexural tests were carried out according to ASTM D790 standard. Crosshead speed is 1 mm/minute. As a result of this test, the flexural modulus and flexural strength values of the samples were determined. The tests were repeated at least three times for each samples. The mean and standard deviations of the values obtained as a result of the tests were calculated with precision.

4.3.2.7 Scanning Electron Microscopy (SEM) Observation

The morphological properties of the fracture surfaces of the samples obtained as a result of the tensile tests were observed with a scanning electron microscope (SEM)

(Carl Zeiss 300VP). Before SEM observation, the surfaces of the samples were homogeneously coated with gold with a plasma coating device (Quorum Q150 Res).

Chapter 5

Results and Discussions

This chapter consist of five main parts. First, the results of the characterization studies of untreated fillers were examined. In the second part, characterization results of biocomposites produced with untreated fillers were presented. In the third and fourth parts, the results of the optimization study of alkali treatment and MAPP compatibilizer were given, respectively. In the fifth part, the test and analysis results of the ultimate biocomposite materials were observed and interpreted in comparison with the literature.

5.1 Untreated Fillers

The possibility of using cherry tree pruning branches as a filler in thermoplastics was investigated in order to convert the agricultural wastes into added value bio-based products and to reduce the use of plastic. In the first stage of the study, the wood and bark parts of branches were separated from each other, and these parts were grinded and sieved into two different particle sizes, under 100 microns and 100 - 250 microns. Then, the characterization studies were completed as follows: the determination of chemical composition, density measurements, particle size distributions (PSD), Fourier transform infrared spectroscopy (FTIR) analysis, X-Ray diffraction (XRD) analysis, thermogravimetric analysis (TGA), and scanning electron microscopy (SEM) observation, respectively.

5.1.1 Chemical Composition

The chemical content of wood could not be defined precisely for a tree because the chemical content varies with stem, branch, or root type (i.e., normal, tension, or

compression), geographic location, climate, and soil conditions. There are two major chemical components in wood; carbohydrate (65 - 75%) and lignin (18 - 35%) [53]. Minor amounts of external materials, mostly in the form of organic extractives and inorganic minerals, are also present in wood (usually 4 - 10%). Overall, wood has an elemental composition of about 50% carbon, 6% hydrogen, 44% oxygen, and trace amounts of several metal ions [53]. Reaction wood is seen on the stem and branch of the tree, grown on one side wind effect or on sloping land. These woods differ from normal wood in both chemical composition and physical properties. The cellulose ratio of the reaction wood group is higher than other species and stem woods [54]. The cherry orchard where the pruning branches were obtained is located on the slopes of the Taurus Mountains at an altitude of 1600 in the Mediterranean Region. Therefore, the tree branches used in this study are in the reaction wood group. Wise's Cloride Method [50] was applied to determine the chemical composition of the wood and bark particles of the cherry tree branches.

Table 5.1: Chemical contents of wood and bark (wt. %)

Material/Content (%)	Cellulose	Hemicellulose	Lignin	Extractives
Wood	70.65 ±1.35	17.47 ±0.22	7.27 ±1.15	4.61 ±0.55
Bark	63.85 ±0.78	22.28 ±0.48	9.46 ±0.36	4.42 ± 0.81

The chemical composition analysis results were summarized in Table 5.1. When the wood and bark particles were compared, the cellulose content of the wood was 10% higher, and the hemicellulose and lignin contents were 27% and 30% lower than the bark, respectively. Extractive substances were found as 4.31 wt. % and 4.42 wt. % for wood and bark, respectively. It has been also reported, compared to the typical chemical composition of wood, bark has lower cellulose content and higher lignin content [55]. Also, it has higher inorganic content, mainly due to the presence of silicon oxide (SiO_2).

5.1.2 Density

Density is one of the most crucial property affecting the quality of lignocellulosic filler and composites [56]. It is related to other physical properties of the filler such as strength and stiffness [57]. It has been reported that density is one of the best predictors to predict the mechanical properties of wood fiber [58]. For several softwood tree species, research has demonstrated that the density of the branches is higher than the density of the stem wood, but studies on hardwoods are uncommon [59].

Density measurement values of wood and bark particles are given in Table 5.2. The density of the wood was 1.4551 ± 0.0024 g/cm^3, while the density of the bark was 1.4013 ± 0.0037 g/cm^3. The density of the wood was approximately 4% higher than the bark. The environmental impact on bark density can be important because bark structure and chemistry can be changed significantly in response to environmental changes [60]. The environmental effects can result into density differences between bark and wood.

Table 5.2: Density of wood and bark

Material/Content	Density (g/cm^3)
Wood	1,4551 ± 0,0024
Bark	1,4013 ± 0,0037

Though the density of the wood particles is about 1.35–1.55 g/cm^3 [61,62], the porous anatomy of solid wood densities is about 0.32–0.72 g/cm^3 [63]. This difference is due to the compressibility of wood filler [3].

5.1.3 Fourier Transformed Infrared Spectroscopy (FTIR)

FTIR and the functional groups of the wood and bark particles were presented in Figure 5.1 and Table 5.3. The first wide peak was observed in the ranges 3338 cm 1

and 3335 cm 1 for wood and bark, respectively. This was attributed to the presence of Cellulose Iβ due to the stretching and vibration of O-H groups [64,65]. The next two peaks were found at 2884 cm 1 and 2918 cm 1 for the wood and bark. These peaks represented the existence of cellulose and hemicellulose, attributed to the stretching and vibration of C-H from CH and CH2 [66,67].

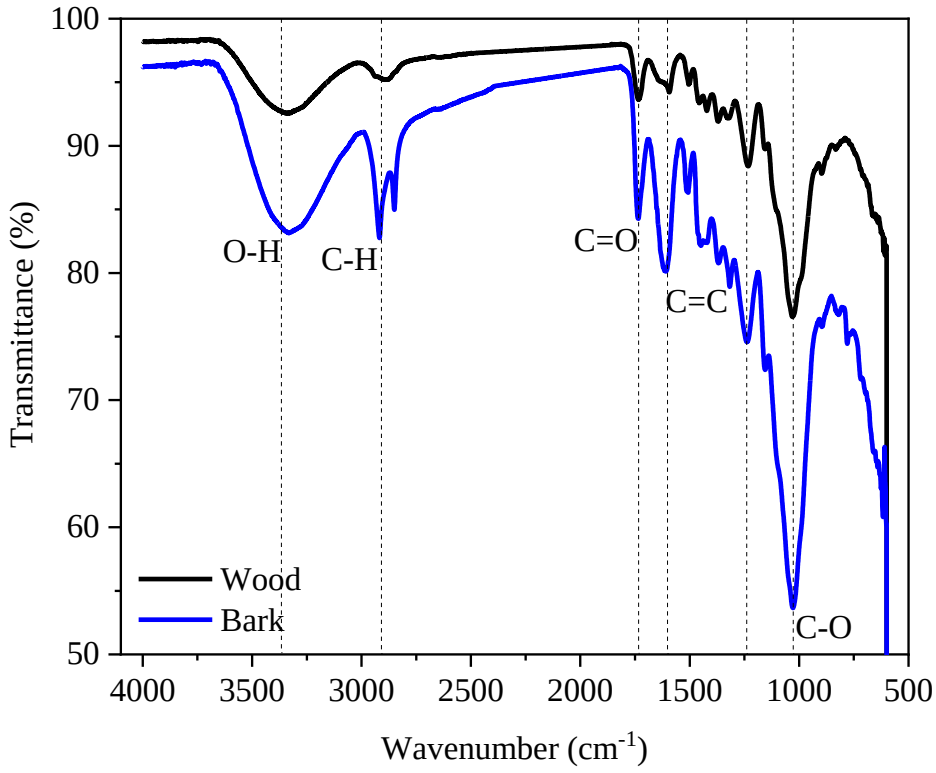

Figure 5.1: FTIR results for wood and bark

The next following transmittance peak found rougly at 1734 cm 1 represented the presence of hemicellulose due to the bending vibrations of C=O. The next peaks at 1505 and 1513 cm 1, was due to the bending and vibrations of C=C, and it confirmed the existence of lignin and hemicellulose [68,69]. Next subsequent transmittance peaks which were detected around at 1371 cm 1 was due to the vibrations in CH and it was attributed to the presence of cellulose and lignin [70]. The transmittance peaks were observed at 1232 cm 1 and 1031 cm 1, which were attributed to the bending

vibrations of C-O, caused by the presence of acetyl groups in lignin and hemicellulose structures [71,72].

Table 5.3: FTIR peaks and bond types for wood and bark

Bond Type	Wavenumber (cm^{-1})	
	Wood	Bark
O-H stretching and hydrogen bonds	3344	3332
C-H stretching of hemicellulose	2891	2918
C=O stretching of acetyl or carboxylic acid	1730	1735
Absorbed H_2O	1593	1610
C=C stretching of aromatic ring of lignin	1505	1513
CH bending	1373	1368
C–O–C asymmetric stretching	1156	1155
C–O stretching vibration of acetyl group in hemicellulose	1232	1239
Cyclic alcohol groups	1030	1024

5.1.4 X-Ray Diffraction (XRD) Analysis

The X-ray diffractograms and the analytical data of the wood and bark particles are presented in Figure 5.2 (a-b). From the diffractograms of the particles, the distinctive intensity peaks that were observed at 2θ in the 21.9º for wood and 21.4º for bark were indicative of the presence of cellulose-1β [73,74].

When compared to the wood, the peaks in the bark are more distinct and noticeable between 30 and 50 degrees as seen in Figure 5 (b). These peaks indicate the presence of inorganic whewellite (Calcium Oxalate) minerals. It can be said that the bark is affected by environmental effects much more than wood because of the direct contact with the external environment like wind and soil. This is also supported by

the fact that no calcium oxalate was detected in the wood.Another factor for this may be the use of pesticides for various reasons [75,76].

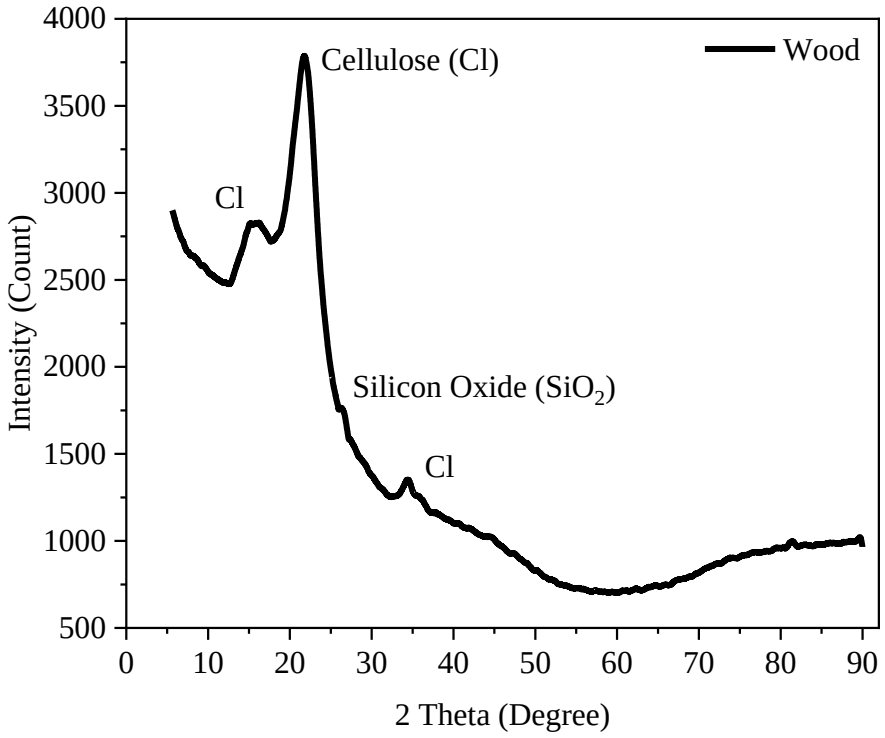

(a)

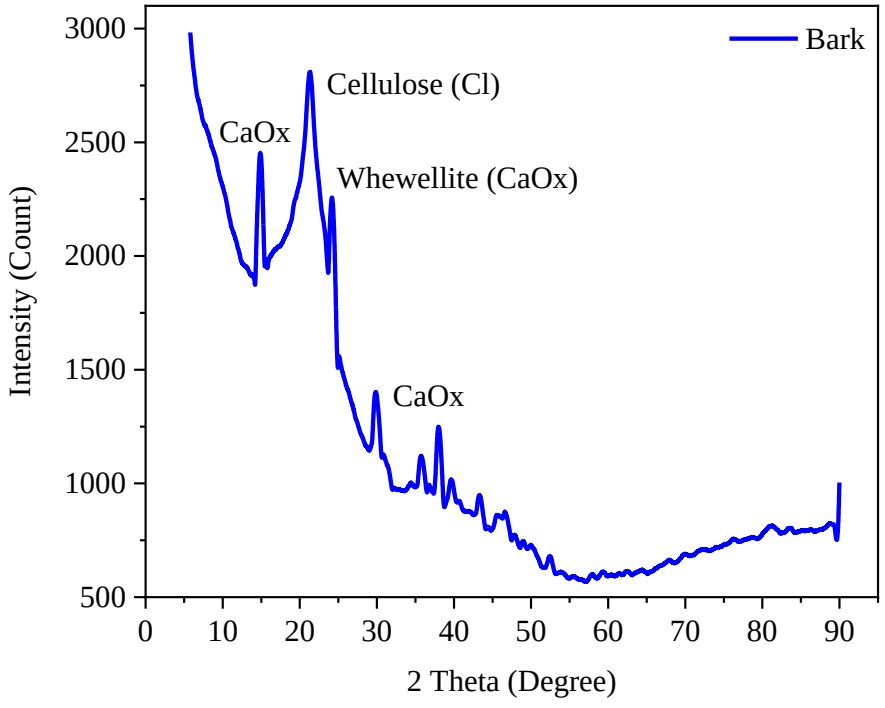

(b)

Figure 5.2: XRD results; a) wood and b) bark

5.1.5 Thermogravimetric Analysis (TGA)

The thermogravimetric and % derivative curves along with weight loss percent at each degradation phase of wood and bark were presented in Figure 5.3 (a – b). The onset temperature (T_{onset}), maximum degradation temperature (T_{max}) and degraded weight (DW) values are shown in Table 5.4. The onset temperatures were observed at 202.7 ºC and 161.1 ºC for wood and bark, respectively. This is due to the degradation of moisture content and some wax present in the lignocellulosic filler [77]. Also, this may due to the existence of fewer structurally integrated water molecules and a lower percent of hemicellulose as confirmed in chemical composition analysis result (Table 5.1).

Table 5.4: TGA results for wood and bark

Material	T_{onset} (°C)	T_{max} (°C)	DW (wt. %)
Wood	202.7	357.3	18.4
Bark	161.1	355.4	18.1

The maximum degradation occurred at the temperature range of 357ºC to 355ºC for wood and bark, and this was attributed to the thermal degradation of cellulose [78,79]. This phenomenon represents that the cellulose content plays a significant role in influencing the thermal stability of the lignocellulosic fillers. Wood and bark exhibited a weight loss of 40% and 50.7%, respectively, at the maximum degradation temperature. These degradation ranges were similar to the degradation temperatures of other lignocellulosic fibers reported in literature [25,43,80].

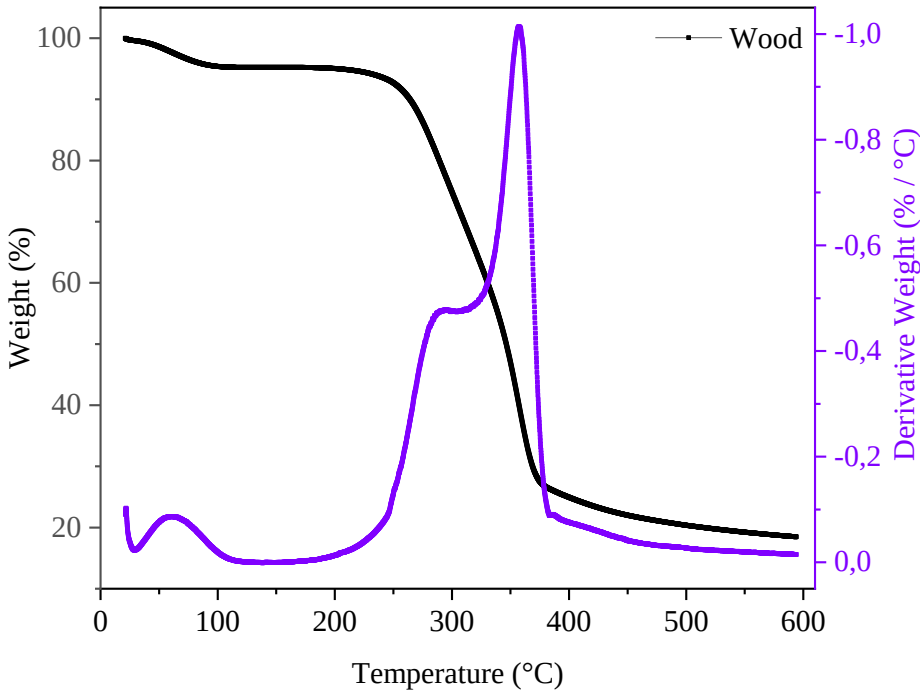

(a)

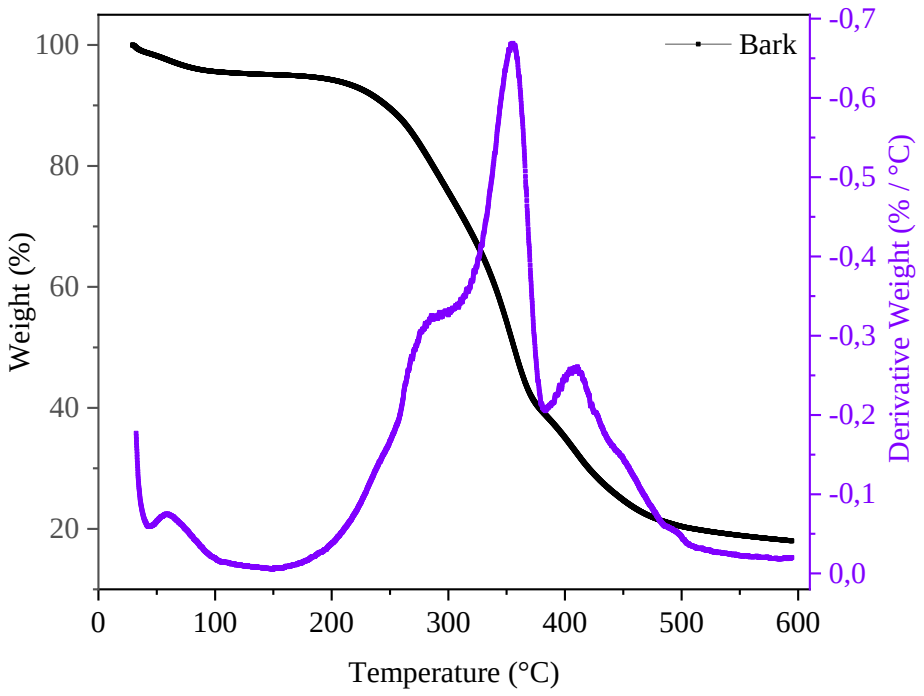

(b)

Figure 5.3: TGA results; a) wood and b) bark

As inferred from the thermogravimetry and the % derivative curves in Figures 5.4 and Figure 5.5, the wood revealed the slightly high thermal stability of 357.3 ℃ which was 0.5% higher than the bark (355.4 ℃). The cellulose was more thermally stable when compared to the hemicellulose and other amorphous constituents. It is possible to say that wood has greater thermal stability than bark because it has a lower amount of amorphous components. The thermal stability of the lignocellulosic fibers can be further confirmed by the presence of char residue at the final degradation temperature [81]. At the highest temperature of 600 ℃, the char residue of wood and bark fillers was found at 18.4% and 18.2%, respectively. This residue is mostly made up of carbonaceous elements that cannot be reduced further into smaller volatile pieces and will stay until the process is completed. It might also be attributed to the presence of inorganic material that produces chars and could serve as the basis for quantitative measurement [29,82].

5.1.6 Particle Size Distribution (PSD) Analysis

Particle size distribution (PSD) analysis is important for the determination of the size distribution of the fillers before the manufacturing of biocomposites. The PSD analysis results and distribution graphs for the lignocellulosic fillers are given in Table 5.5 and Figure 5.4 (a - d). D50 is the value that gives the size of 50% of the particle size.

Table 5.5: Particle size distribution results

Material/D	D10	D50	D90
UTW	13,1	57,7	161
UTW2	127	271	555
UTB	9,8	40,8	128
UTB2	91,5	216	382

For wood and bark particle sizes, under 100 microns, the D50 values are 57 and 40, respectively, while the D50 values are 271 and 216 for particle sizes of 100-250 microns. The effect of particle size on the mechanical properties of PP-based biocomposites was investigated in Section 5.2.

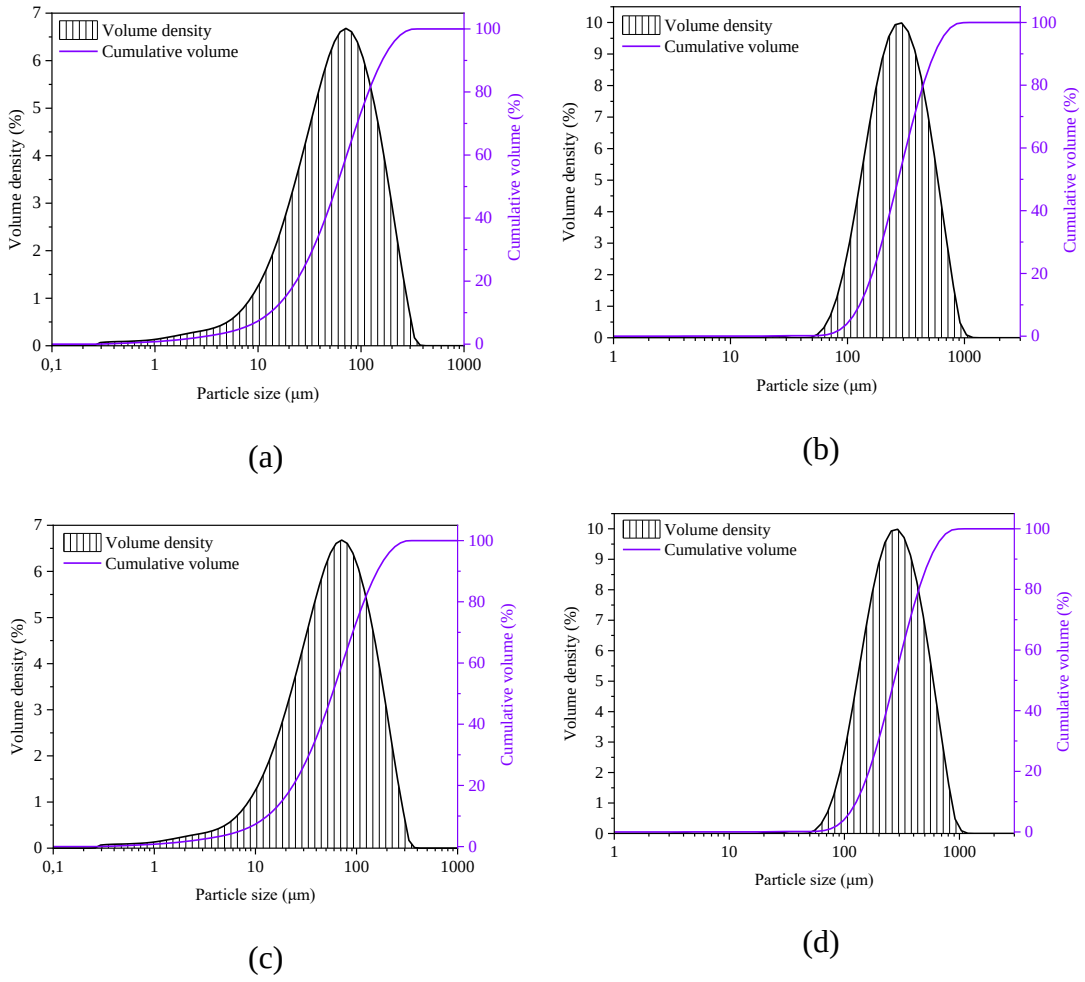

Figure 5.4: Particle size distributions; a) UTW, b) UTW2, c) UTB, and d) UTB2

5.1.7 Scanning Electron Microscopy (SEM) Observation

The morphological characteristics of the UTW, UTW2, UTB, and UTB2 were presented in Figure 5.5 (a - d). From the SEM images, it was observed that there was the presence of impurities like wax, and other non-polar materials that were

responsible for restraining the wettability [83]. There were voids and microcracks over the particle surface, which would decrease the performance of the biocomposites when used as filler or reinforcements [70]. SEM analysis represented that the both wood and bark particles have irregular shapes and sizes. The sharp corner points of these irregularly shaped particles may cause stress concentration areas in the polymer matrix [25].

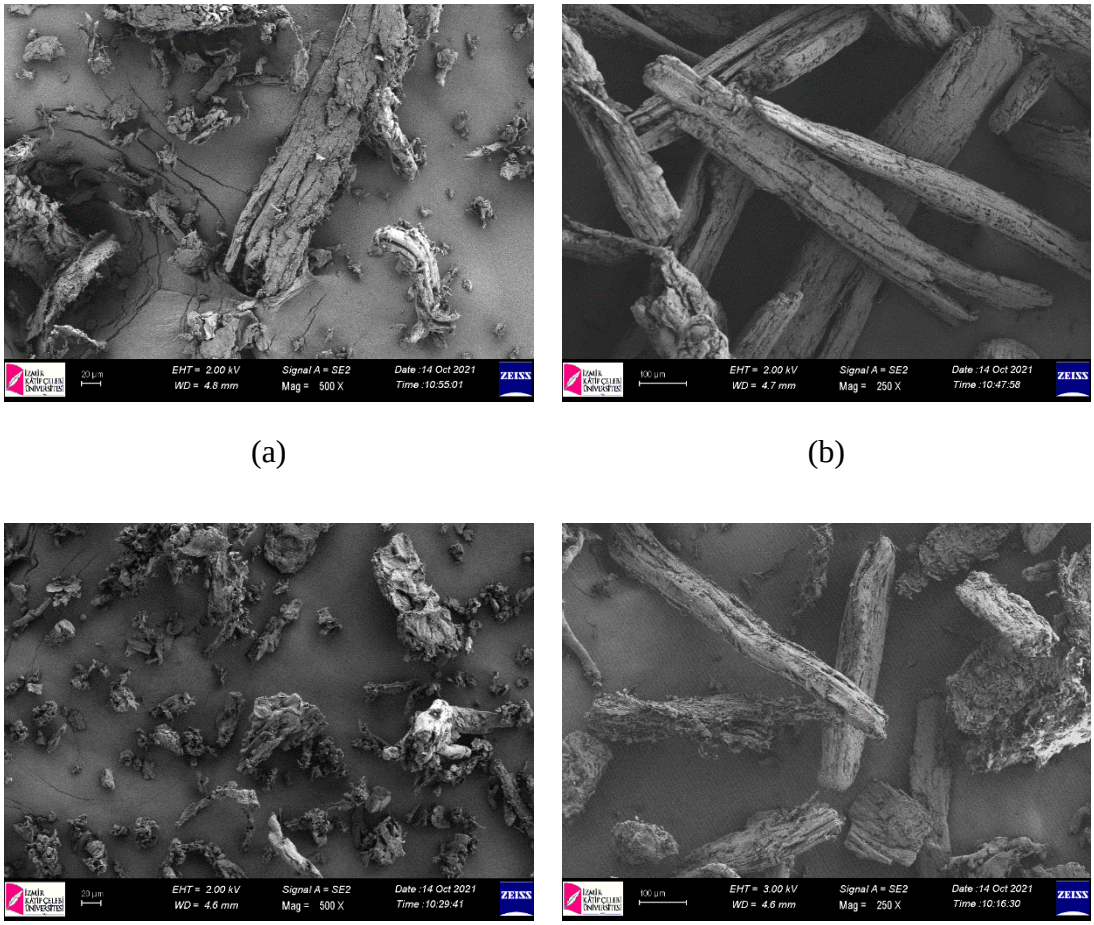

(a) (b)

(c) (d)

Figure 5.5: SEM images of the particles; a) UTW, b) UTW2, c) UTB, and d) UTB2

5.2 Biocomposites Filled with Untreated Fillers

Tensile tests, flexural tests and dynamic mechanical analyzes were performed to observe the mechanical properties and viscoelastic behaviors of biocomposites. Tensile strength, tensile modulus, flexural strength, and flexural modulus were determined by tensile and flexural tests, and storage and loss moduli were found by dynamic mechanical analyzes and presented comparatively.

5.2.1 Tensile Test

Tensile strength and tensile modulus values of PP and its biocomposites were given in Table 5.5. For all samples, tensile strength and tensile modulus results, compared with PP, were illustrated in detail in Figure 5.6 (a-c) and in Figure 5.7 (a-c), respectively.

Table 5.5: Summary of the tensile test results

Sample	Tensile Strength (MPa)	Tensile Modulus (MPa)
PP	22.2 ± 0.1	704.4 ± 16.2
5UTW	21.9 ± 0.4	1047.8 ± 17.8
10UTW	21.2 ± 0.5	1148.6 ± 6.6
15UTW	20.6 ± 0.3	1195.3 ± 15.9
20UTW	20.4 ± 0.1	1230.2 ± 14.7
5UTW2	20.8 ± 0.6	813.7 ± 65.7
10UTW2	19.9 ± 0.8	942.5 ± 59.2
15UTW2	19.7 ± 0.8	1007.3 ± 63.9
20UTW2	19.1 ± 0.5	1058 ± 59.4
5UTB	21.7 ± 0.4	971 ± 48.6
10UTB	20.2 ± 0.4	1052.4 ± 33.7
15UTB	19.5 ± 0.6	1065.6 ± 55.4

20UTB	17.5 ± 0.5	955.8 ± 57.3
5UTB2	21.5± 0.5	944.5 ± 28
10UTB2	20.1 ± 0.5	950.4 ± 3.3
15UTB2	18.4 ± 0.4	942.9 ± 14.8
20UTB2	16.2 ± 0.3	910.3± 12.3

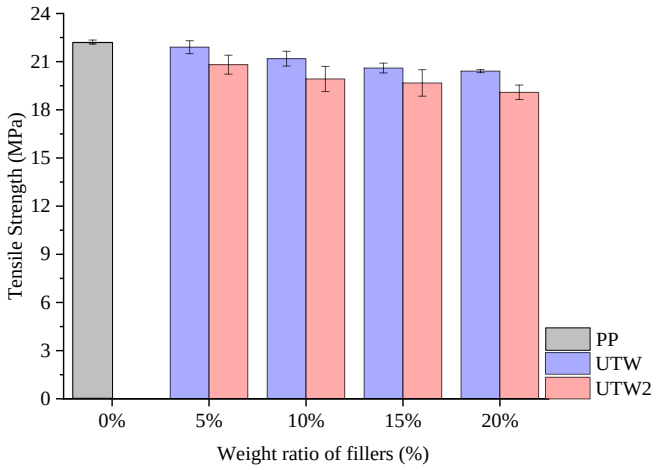

(a)

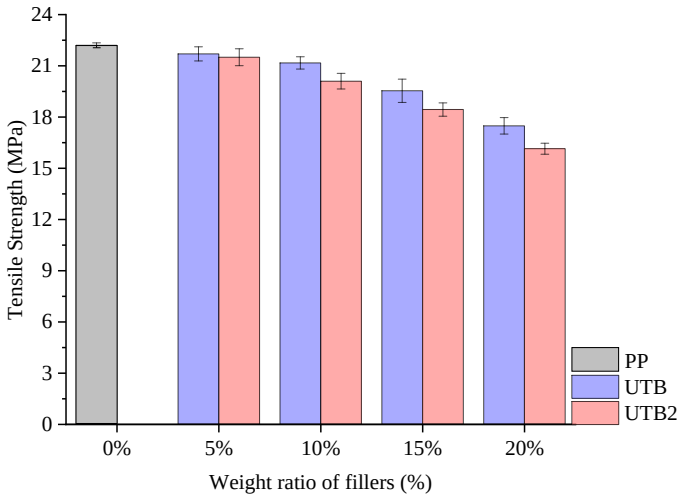

(b)

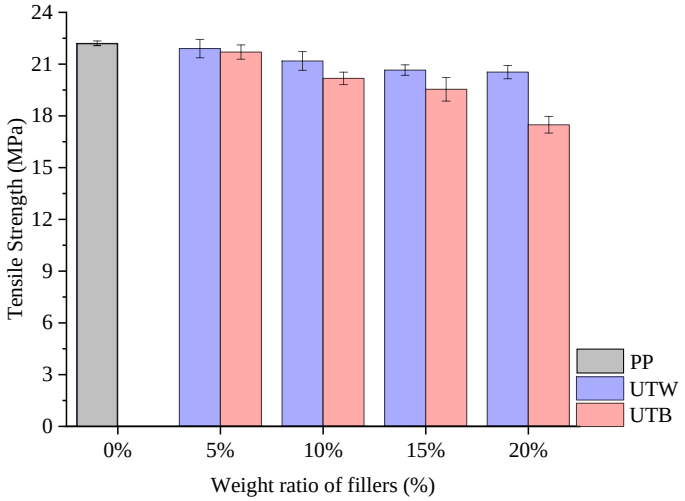

(c)

Figure 5.6: (a –c) Tensile strength graphs

As shown in Figure 5.6 (a-c), the tensile strength of PP begins to decrease with the addition of particles into PP. It was determined that the tensile strength of PP decreased from 22.2 MPa to 16.2 MPa (20UTB2) after adding 20% particle into the PP.

Related to the tensile strength of the biocomposites; it can be said that the wood and bark particles are not sufficiently wetted by the PP matrix, the fillers are not homogeneously dispersed in the matrix, and the interfacial adhesion between fillers and the PP is reduced. In addition, the decrease in tensile strength can be associated with particle weight ratio and an increase in interfacial surface area [84]. Since the fillers are very small, the interfacial area between the polar lignocellulosic particles and the non-polar PP matrix rises with the increase of the filler ratio in the PP, which may cause the interfacial bond to aggravate [25,85].

The changes in the tensile modulus of PP and its biocomposites are shown in the Figure 5.7 (a-c). The tensile modulus of PP is found 704 MPa where the tensile modulus was increased with the addition of 5% filler into the PP. The increment in the tensile modulus of PP continued regularly up to 20% weight ratio. Among all the biocomposites, the highest tensile modulus was determined for the 20UTW sample with a value of 1230 MPa, which means the tensile modulus was increased by 75% compared to the PP. This increase could be attributed to the fact that the tensile

modulus of lignocellulosic fillers is substantially higher than that of the polymer matrix [86].

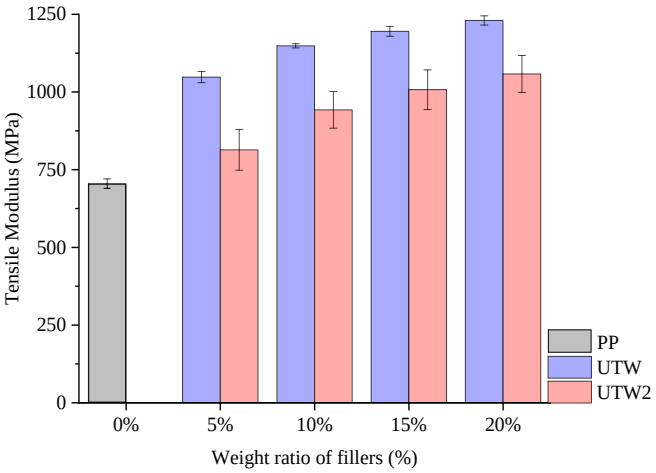

(a)

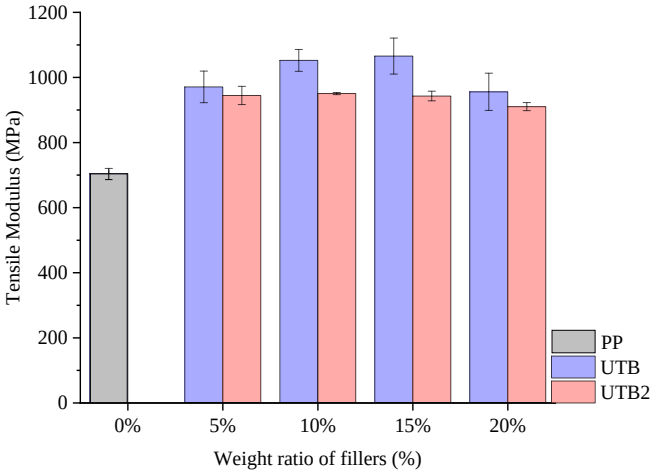

(b)

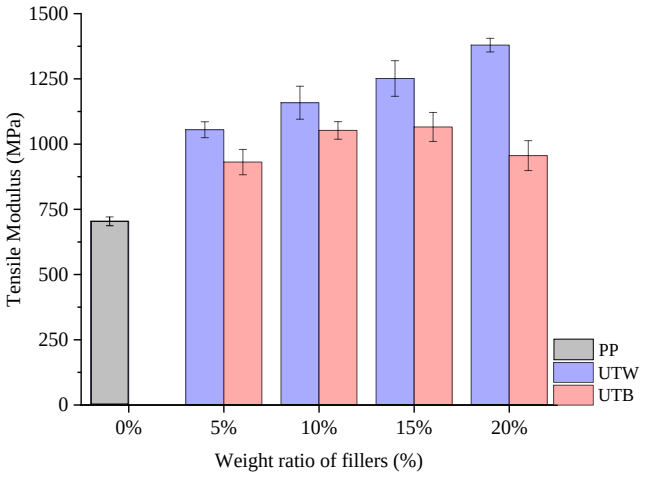

(c)

Figure 5.7: (a –c) Tensile modulus graphs

5.2.2 Flexural Test

Flexural strength and flexural modulus values of PP and its biocomposites were summarized in Table 5.6. For all samples, flexural strength and flexural modulus results, compared with PP, were illustrated in detail in Figure 5.8 (a-c) and in Figure 5.9 (a-c), respectively.

Table 5.6: Summary of the flexural test results

Sample	Flexural Strength (MPa)	Flexural Modulus (MPa)
PP	38.3 ± 2.7	1170.3 ± 164.2
5UTW	34.5 ± 1.2	1310.7 ± 79
10UTW	33.8 ± 2.2	1333.7 ± 67.8
15UTW	33.7 ± 1.8	1333.3 ± 172.9
20UTW	31.4 ± 0.3	1412.5 ± 24.3
5UTW2	34.5 ± 1.6	1181.6 ± 37.4
10UTW2	33.7 ± 1.2	1320.8 ± 99.5
15UTW2	32.6 ± 1.8	1335.2 ± 92.1

20UTW2	31.1 ± 1.8	1449.8 ± 72.3
5UTB	28.4 ± 1	945.2 ± 58.9
10UTB	26 ± 0.4	960.1 ± 24.2
15UTB	26.5 ± 1.2	1014.7 ± 35.1
20UTB	25.1 ± 1.7	1109.5 ± 22.7
5UTB2	28.9 ± 1.6	855.5 ± 58
10UTB2	27.5 ± 1.5	976.7 ± 28.7
15UTB2	25.8 ± 1.7	998.9 ± 3.7
20UTB2	24.2 ± 0.5	1065.9 ± 27.3

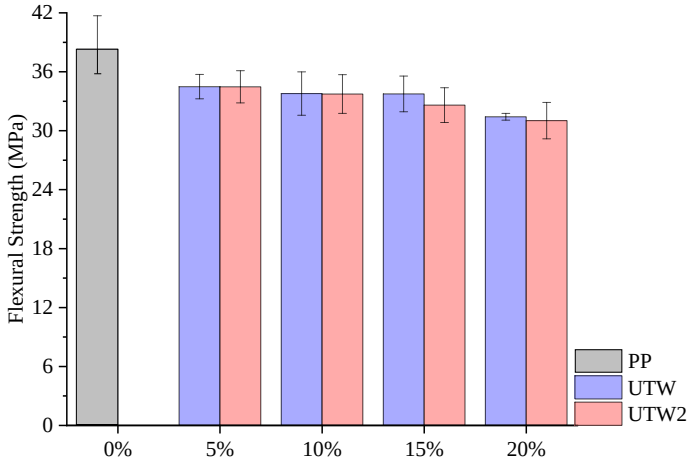

(a)

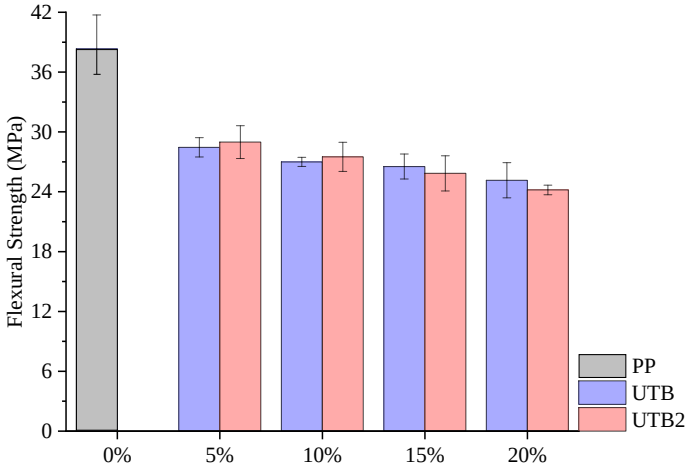

(b)

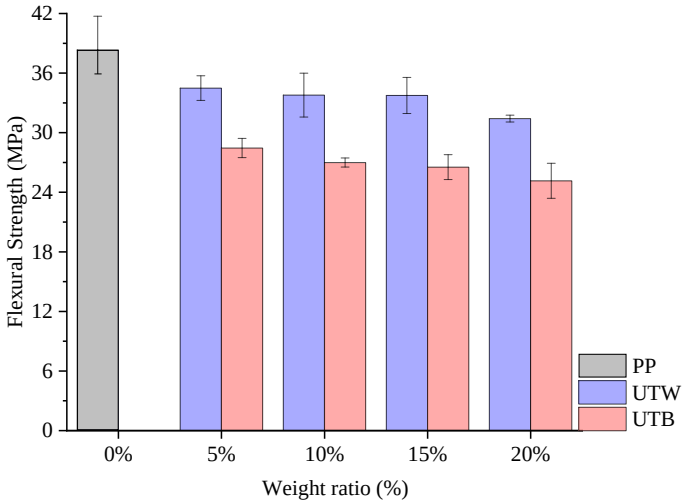

(c)

Figure 5.8: (a-c) Flexural strength graphs

As seen in Figures 5.8 (a-c), the flexural strength of PP is higher than all biocomposites with a value of 38.3 MPa. It has been observed that the flexural strength of PP begins to decrease when 5% filler is added to the PP. As the ratio of fillers in the matrix increased, the overall decrease in flexural strength continued. Among all biocomposites, the lowest flexural strength was found in the 20UTB2 sample with 24.2 MPa, decreasing by 30.5% compared to PP. The reasons for this reduction with the increasing filling rate can be listed as follows: Inadequate wetting of the particles and the matrix, poor dispersion of particles in the matrix, poor interfacial adhesion between the particles and the matrix, and the presence of agglomerations can be considered as the reasons for the decrease in flexural strength [24,27,86,87]. Furthermore, poor interfacial bonding can cause micro gaps between the lignocellulosic fillers and the matrix, which inhibit stress propagation when force is loaded. Thereby, these micro-voids may act as stress concentration points to initiate cracks during loading [88]. This leads to stress concentration in the filler/matrix boundary region, resulting in the weakness of the filler/matrix interface. In addition, the filler materials effectively inhibits chain movement during deformation [83].

The changes in the flexural modulus of PP and its biocomposites are shown in the Figure 5.9 (a-c). The flexural modulus of PP is found 1170 MPa where the modulus was increased with the addition of 5% filler into the PP. The increment in the flexural modulus of PP-based biocomposites continued regularly up to 20% weight ratio of UTW and UTW2. Among all the biocomposites, the highest flexural modulus was determined for the 20UTW2 sample with a value of 1450 MPa, which means the flexural modulus was increased by 34% compared to the PP. The reason for this increase is the fact that the wood particles are more rigid than the PP. It is reported that the modulus of the lignocellulosic particles is much higher than that of the polymer matrix [86]. Although, it is an expected result that the flexural modulus increases with the incorporation of relatively rigid materials into thermoplastics [25].

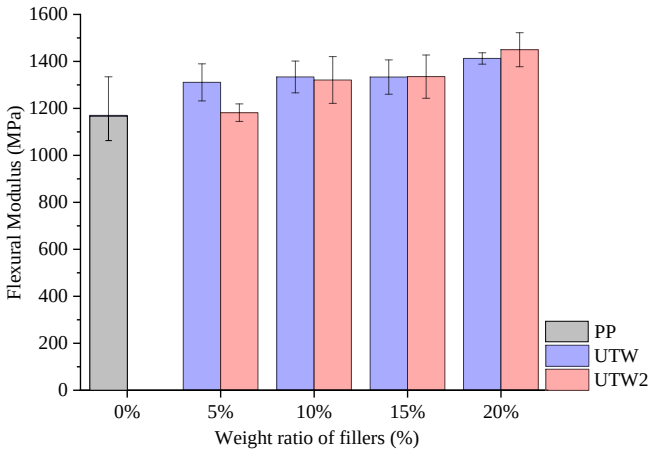

(a)

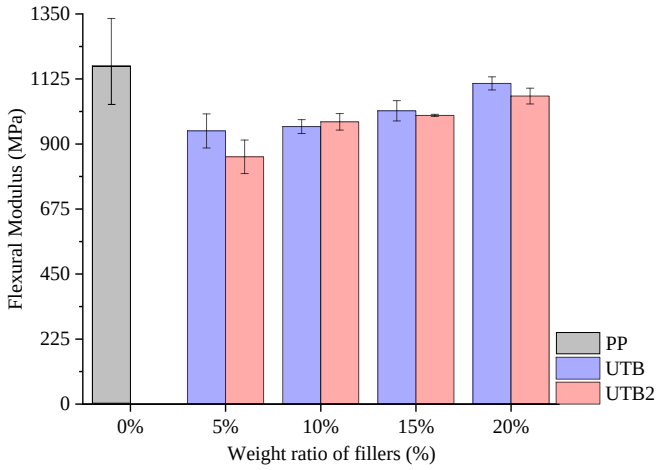

(b)

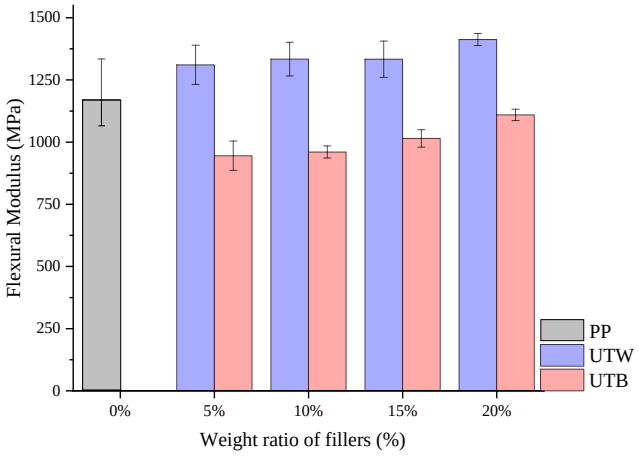

(c)

Figure 5.9: (a-c) Flexural modulus graphs

5.2.3 Dynamic Mechanical Analysis (DMA)

Dynamic mechanical analyzes (DMA) were performed to understand the viscoelastic behavior of PP and its biocomposite samples. The changes in the storage modulus values of the samples as a function of temperature are shown in Figure 5.10 (a – b). As seen in the Figure, the storage modulus values of biocomposites are higher than that of PP at the whole temperature range. This shows that the stiffness of biocomposites is increased with the addition of lignocellulosic fillers. The initiation of the relaxation process and softening of the matrix may cause this decrease [89]. Also, the increase in storage modulus was due to mechanical limitation posed by increasing particle embedded in the viscoelastic polymer matrix.

The changes in the loss modulus values of PP and its biocomposites as a function of temperature are shown in Figure 5.11 (a–b). As seen, the loss modulus of biocomposites are higher than PP. The highest loss modulus was investigated in 20 wt. % filled samples for both particle sizes. The increase in the loss modulus can be attributed to the decrease in energy absorption [90,91].

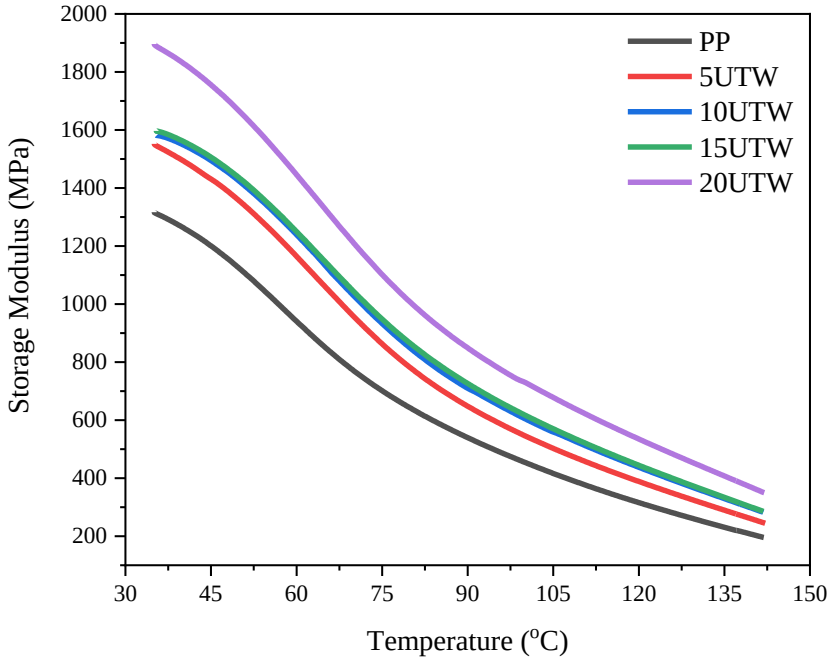

(a)

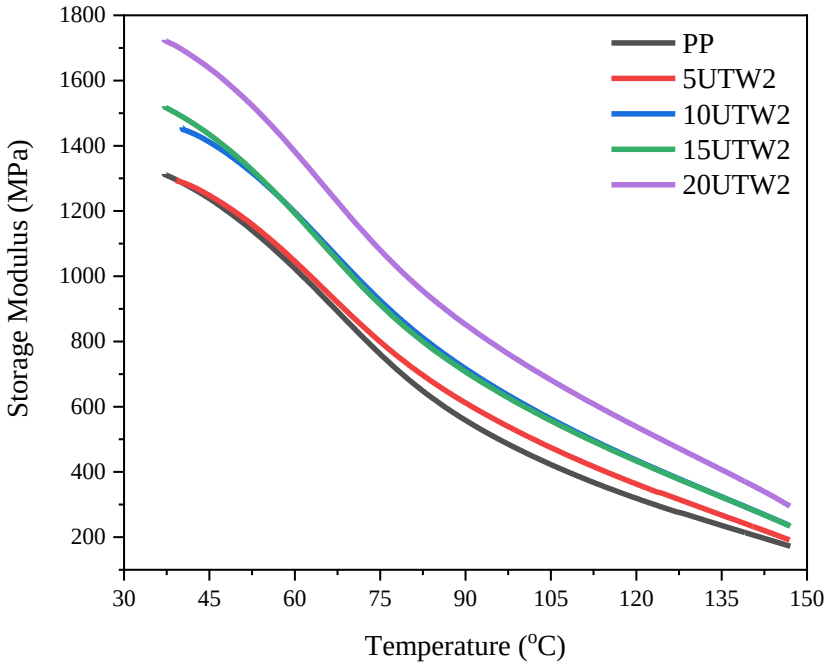

(b)

Figure 5.10: (a-b) Storage modulus results

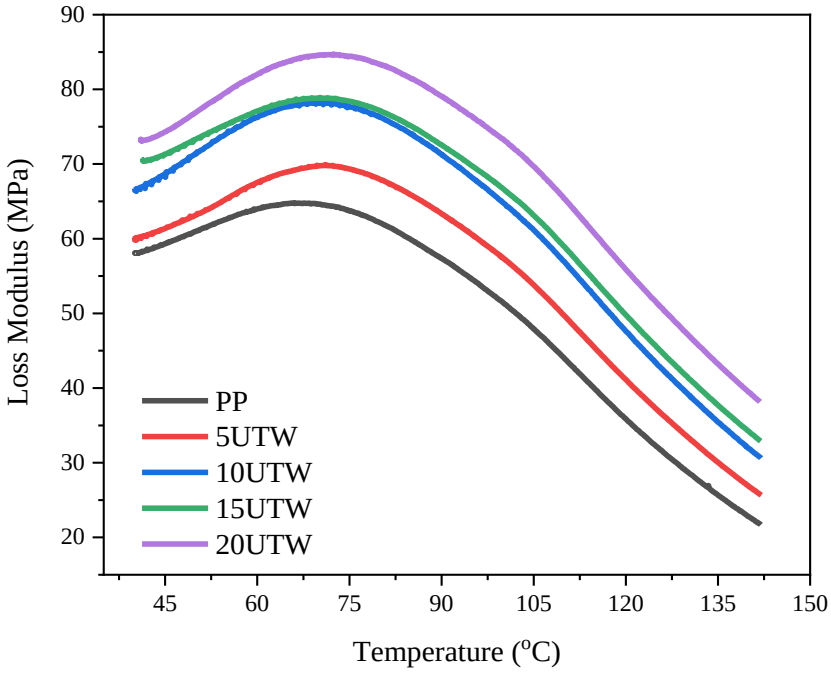

(a)

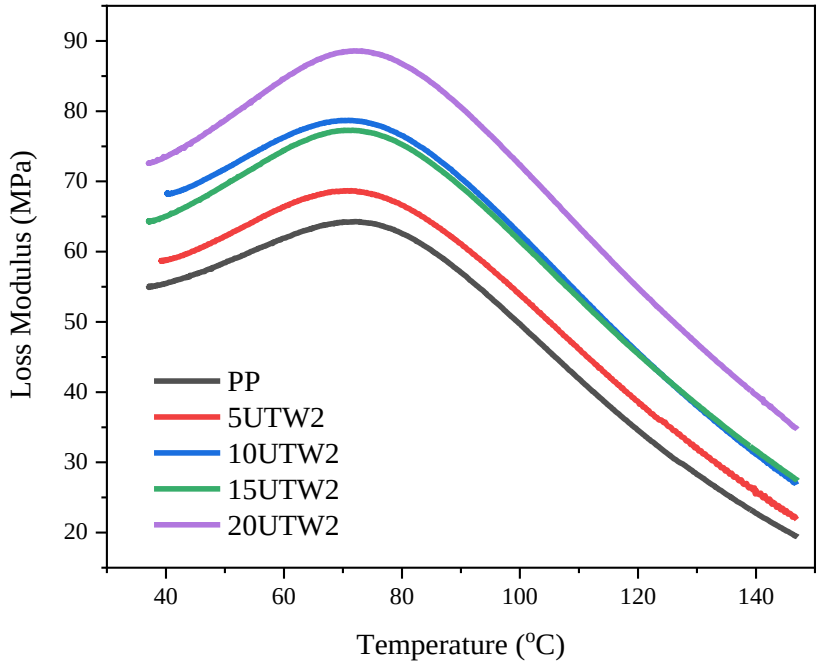

(b)

Figure 5.11: (a-b) Loss modulus results

5.2.4 Scanning Electron Microscopy (SEM) Observation

Lignocellulosic fillers are observed in the PP matrix when the fracture surfaces obtained after the tensile test of biocomposites given in Figure 5.12 (a–d) are examined. As seen in the Figure 5.12, there are many small pores around the filling material and it means that the matrix/filling material interface compatibility is weak. When the rate of additives increases, the homogeneous dispersion decreases. As the amount of filler increases, the compatibility of the matrix-filler interface weakens. As seen in Figure 5.12, the formation of larger sizes of particles on the fracture surface was observed with the addition of a high amount of particles into the PP matrix. As a result, the tensile strength of the composite decreased dramatically at high addition filler rates as summarized in Table 5.5.

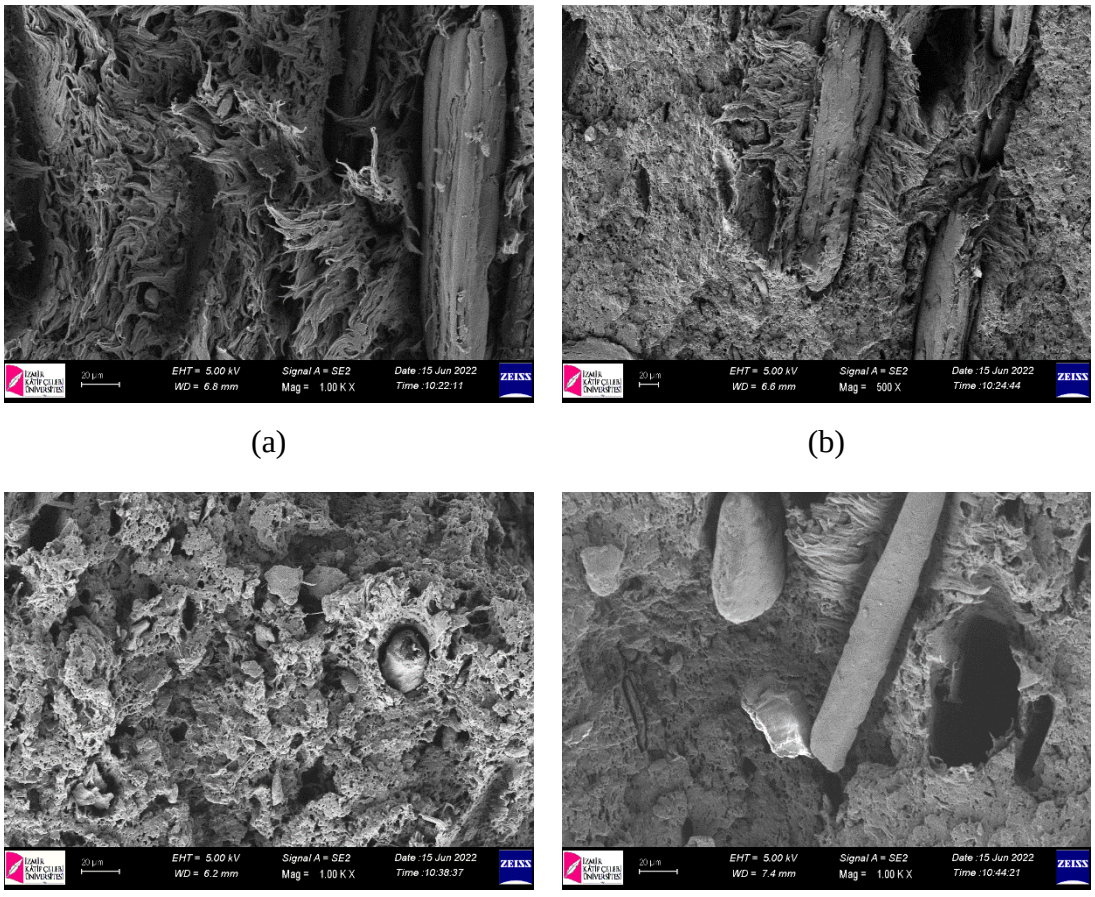

(a) (b)

(c) (d)

Figure 5.12: SEM images of the fracture surfaces of biocomposites; a) 10UTW, b) 10UTW2, c) 10UTB, and d) 10UTB2

5.3 Optimization of Alkali Treated Fillers

In order to examine the effect of the modification process, the characterization analyses and performance tests detailed below were applied to the filling materials, and the modification rate that gave the most suitable properties for the purpose was determined.

5.3.1 Fourier Transformed Infrared Spectroscopy (FTIR) Analysis

The Fourier transform infrared spectrograms and their corresponding functional groups with the components of the untreated and alkali treated fillers were presented in Figure 5.13. The first wide peak was observed in the range 3400 cm^{-1}. It has been reported that it was attributed to the presence of Cellulose Iβ due to the stretching and vibration of O-H groups [65]. The next peaks were found roughly at 2900 cm^{-1} for all fillers. This represented the existence of cellulose and hemicellulose, attributed to the stretching and vibration of C-H from CH and CH_2 [66]. The next following peaks found at 1700 cm^{-1} represented the presence of hemicellulose due to the bending vibrations of C=O. The 5ATW filler had a greater transmittance at this region when compared to the untreated and other alkali treated fillers. This may be because of a decrement in hemicellulose content due to alkali treatment [92]. The subsequent transmittance peaks which were detected at 1431 cm^{-1} and 1030 cm^{-1} were due to the vibrations in CH2 and C-OH and it was attributed to the presence of cellulose and lignin [70]. The peak was observed at wave number 1270 cm^{-1}, which was attributed to the bending vibrations of C=C, caused by the presence of acetyl groups in lignin and hemicellulose [71].

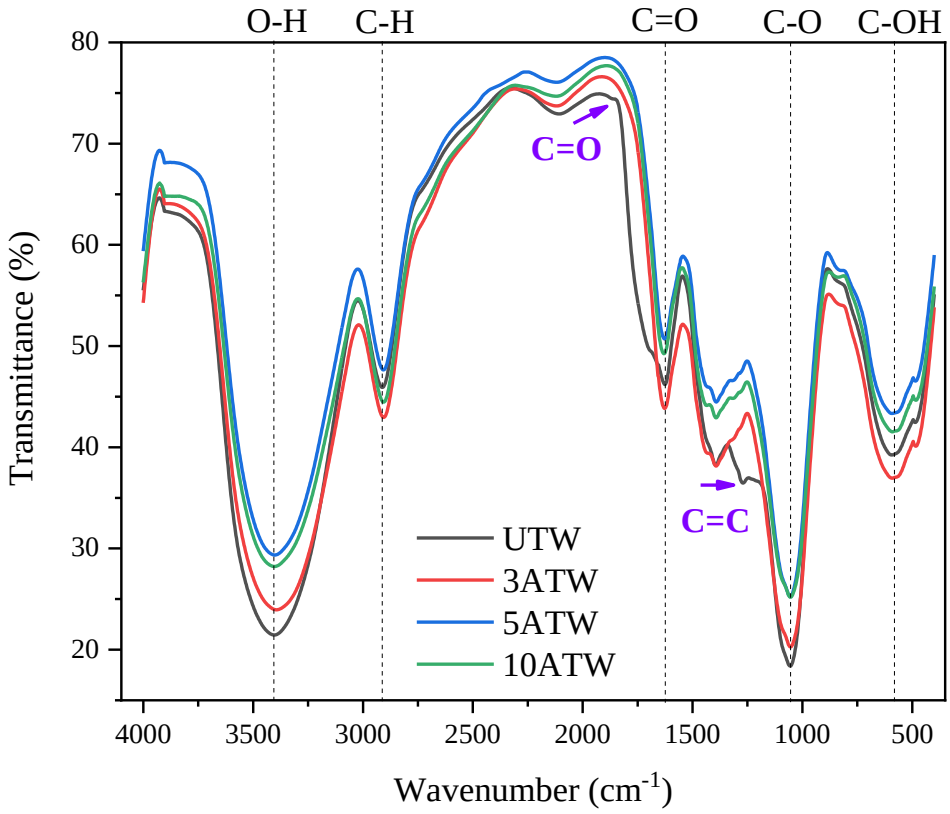

Figure 5.13: FTIR results of alkali treated particles

The 5ATW filler had a greater transmittance at this region when compared to the other alkali treated fillers. This is because of a decrement in hemicellulose content due to alkali treatment [68]. Furthermore, the transmittance percent in treated filler was higher compared to the untreated filler as noticed in Figure 5.13. This phenomenon was due to the elimination of excessive amorphous components such as hemicellulose, lignin, pectin, wax, and impurities from the lignocellulosic fiber through alkali treatment which allowed infrared rays to easily penetrate the fibers.

5.3.2 X-Ray Diffraction (XRD) Analysis

The XRD analysis results of untreated wood and alkali-treated wood particles are given in Figure 5.14 comparatively. While the cellulose intensity value was 3786 at untreated wood, this ratio increased approximately 80% after alkali treatment to 6760. This can be associated with the successful complete or partial removal of hemicellulose, lignin, and extractive substances in the fiber structure after alkali

surface treatment. It is reported that the higher cellulose weight percentage improves the thermal stability, crystallinity, and tensile strength of the lignocellulosic fibers and its biocomposites [93].

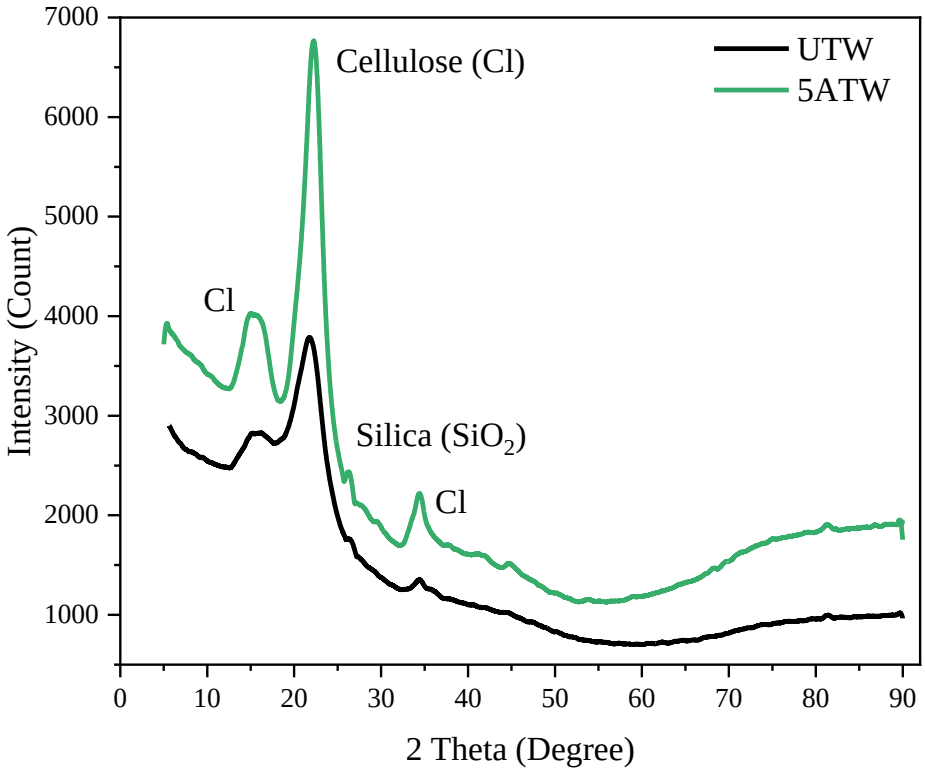

Figure 5.14: XRD results

From the diffractograms of untreated and alkali treated fillers, presented in Figure 5.12, the distinctive intensity peaks which were observed at 2θ approximately in ranges 15.3º, 22.2º, and 34.4º was attributed to the presence of cellulose-1β [73,74]. It was observed that there was no phase transition of cellulose during the alkali treatment, which was confirmed by the presence of cellulose-1β through the FTIR spectrograms in Figure 5.13.

5.3.3 Thermogravimetric Analysis (TGA)

The thermogravimetric curves along with weight loss percent of 5ATW and the comparison with wood were presented in Figure 5.15 and Figure 5.16. The onset

temperature (T_{onset}), maximum degradation temperature (T_{max}) and degraded weight (DW) values are given in Table 5.7. The onset temperatures were observed at 202.7 ºC and 84.1 ºC for wood and 5ATW, respectively. When compared to untreated wood, the onset temperature of 5ATW was very much lower. This was due to the degradation of moisture content and some wax present in the lignocellulosic filler [77]. Also, this may due to the existence of fewer structurally integrated water molecules and a lower percent of hemicellulose due to alkali treatment as confirmed in FTIR analysis results presented in Figure 5.13.

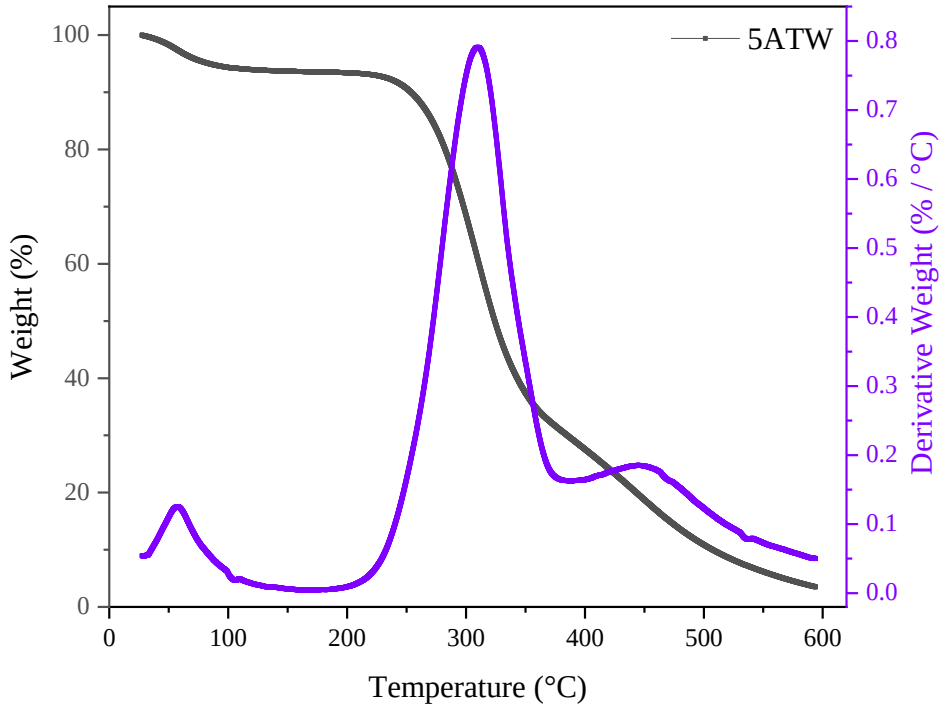

Figure 5.15: TGA for 5ATW particles

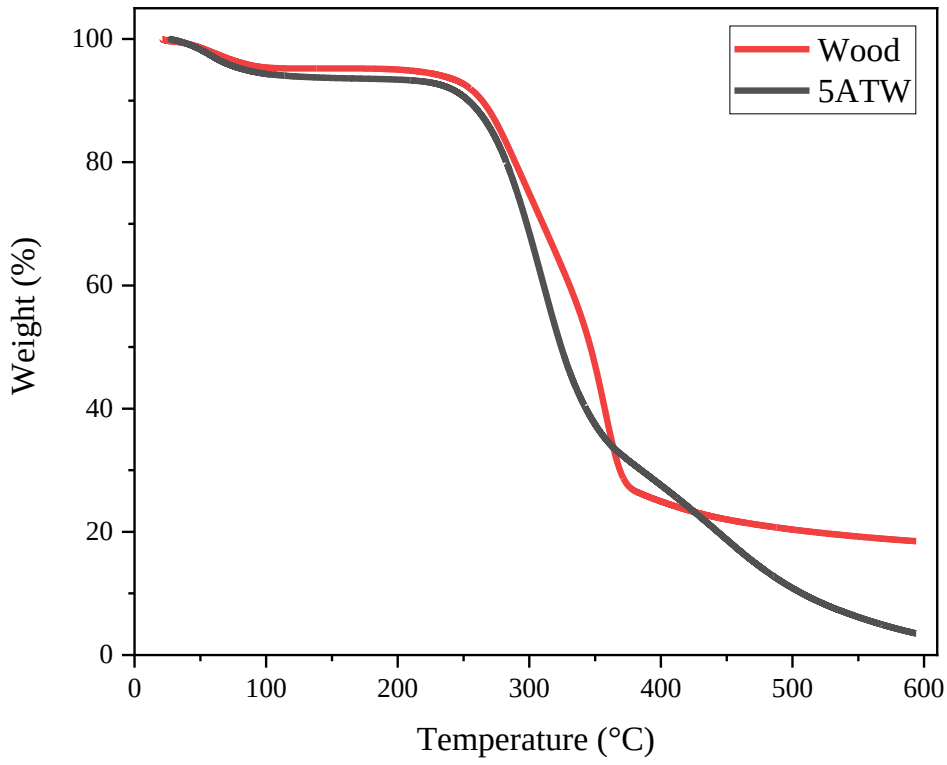

Figure 5.16: Comparison of wood and 5ATW

During the T_{onset} degradation stage, the 5ATW depicted the lowest weight loss of 1.65%. This was because the NaOH treatment was able to disintegrate hemicellulose during the treatment by breaking hydroxyl groups. Owing to the presence of higher amorphous elements, the wood showed the highest thermal weight loss of 7.13% during the T_{onset}, resulting in a sharp decline in weight until reaching the temperature 239ºC. The maximum degradation temperature, T_{max}, occurred at the temperatures of 357.3 ºC and 309 ºC for the wood and 5ATW fillers, respectively. It has been reported that this reduce was attributed to the thermal degradation of cellulose [78,79]. This phenomenon shows that the amount of cellulose in lignocellulosic fillers significantly affects their thermal stability. Wood and 5ATW exhibited a weight loss of 40% and 61.5%, respectively, at the maximum degradation temperature. These degradation ranges were similar to the degradation temperatures of other lignocellulosic fibers reported in literature [25,27,31,33].

Table 5.7 Comparison of TGA results

Material	T_{onset} (°C)	T_{max} (°C)	DW (wt. %)
Wood	202.7	357.3	18.4
5ATW	184.1	309	3.5

As inferred from the Table 5.7, the wood revealed the highest thermal stability of 357.3 ◦C which was 15.6% higher than the 5ATW (309 ◦C). The wood had the maximum thermal stability due to the existence of a lower percent of less thermally stable amorphous elements, which resulted in the enhanced weight ratio of more thermally stable crystalline cellulose. The cellulose was more thermally stable when compared to the hemicellulose and other amorphous constituents [40]. As a result, it was determined that the alkali treatment played a crucial role in influencing the thermal degradation phases of the lignocellulosic filler.

5.3.4 Particle Size Distribution (PSD) Analysis

The PSD analysis results and distribution graphs for 5ATW and UTW are given in Table 5.8 and Figure 5.17. According to the measurement results, it was determined that 50% of the 5ATW was less than 123 μm in diameter, while UTW was 57.7. Furthermore, D50 value increased by more than 200% after alkali treatment. The reason for that may be an aggregation of the particles during the treatment process [94,95].

Table 5.8: Comparison of PSD results

Material/D	D10	D50	D90
UTW	13.1	57.7	161
5ATW	44.5	123	290

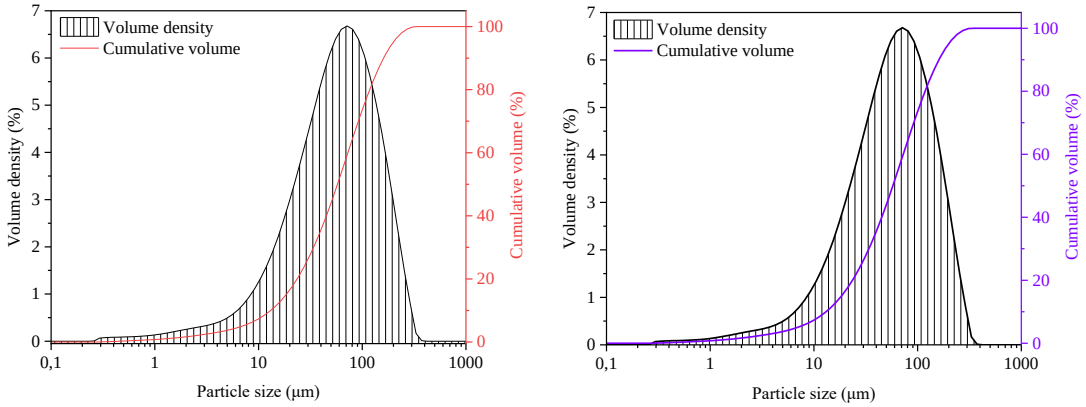

(a) (b)

Figure 5.17: Particle size distributions: a) 5ATW and b) UTW

5.3.5 Scanning Electron Microscopy (SEM) Observation

The morphological characteristics of the 5ATW and UTW were given in Figure 5.16 (a - d). It was observed that the morphology of lignocellulosic fillers was significantly influenced by the alkali treatment. From the SEM observation of wood particles seen in Figure 5.16 (a - b), significant changes were observed over the particle surface as a result of the alkali treatment. Even, it was noticed that the alkali treatment had removed impurities and non-polar materials improving wettability [96].

As a result of the alkali treatment studies, it has been determined that the most effective ratio is the 5%. Furthermore, it is shown that the alkali treatment with its roughness-increasing effect on the particles which has the effect of increasing the fiber-matrix compatibility and providing adhesion, yields good results.

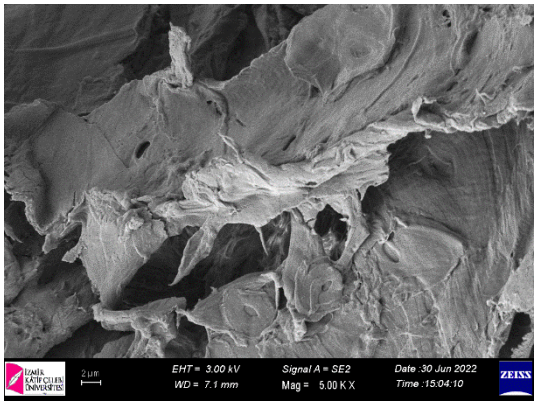

(a) 5ATW

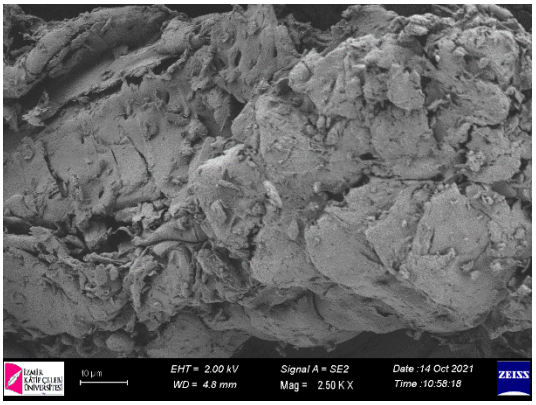

(b) UTW

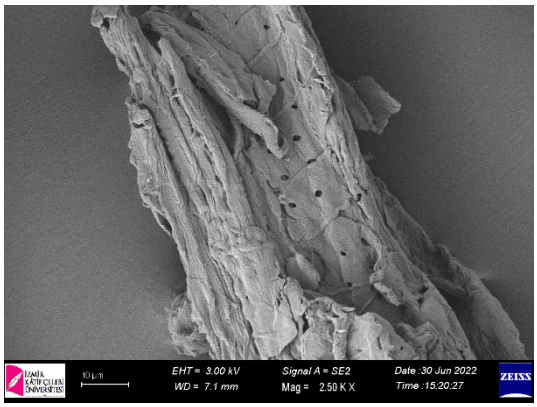

(c) 5ATW

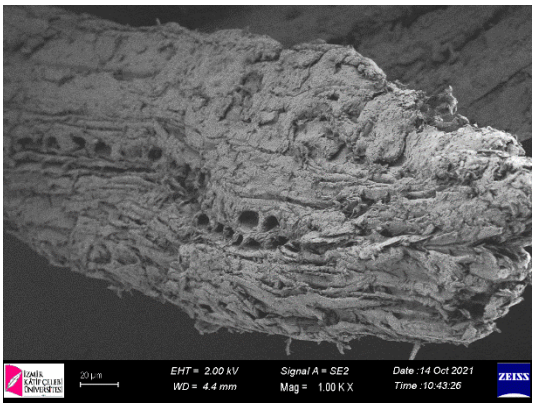

(d) UTW

Figure 5.18: (a-d) SEM images of the particles before and after alkali treatment

5.4 Optimization of MAPP Treated Polypropylene

In order to determine the appropriate ratio of the MAPP coupling agent, it was added to PP in three different weight ratios, as given in Table 4.2, and samples were produced. Tensile and three-point bending tests were applied to the samples in accordance with ASTM D638 and ASTM D790 standards. The obtained results were given in Table 5.9.

5.4.1 Tensile Test

Figure 5.17 represents the tensile strength and tensile modulus values of PP and MAPP-added PP samples. The tensile strength values were obtained as 22.2 ± 0.1,

23.6 ± 0.2, 28.8 ± 0.6, and 19.2 ± 0.4, for PP, 1MAPP, 3MAPP, and 6MAPP, respectively. The best tensile strength was obtained with a 30% increase in the 3MAPP sample when compared to PP. However, there was a dramatic decrease with a 33% value in 6MAPP against 3MAPP. Tensile modulus values also showed a similar trend with tensile strength. It reached the maximum value in 3MAPP with a 1075 MPa which is more than 50% high of PP. There was a sudden decrease in the 6MAPP sample where the value of it almost 60% lower than 3MAPP. The tensile properties reduction observed with 6% MAPP loading was caused by the interaction between the coupling agent (MAPP) and the matrix (PP). Coupled with MAPP's low average molecular weight, the interaction between the PP matrix and MAPP becomes dominated principally by Van der Waals forces; since chain entanglement of PP and MAPP is virtually impossible. MAPP is not utilized for fiber-matrix adhesion and therefore mechanically has a negative effect on the biocomposites, which leads the significant performance variation except the optimum loading value [97,98].

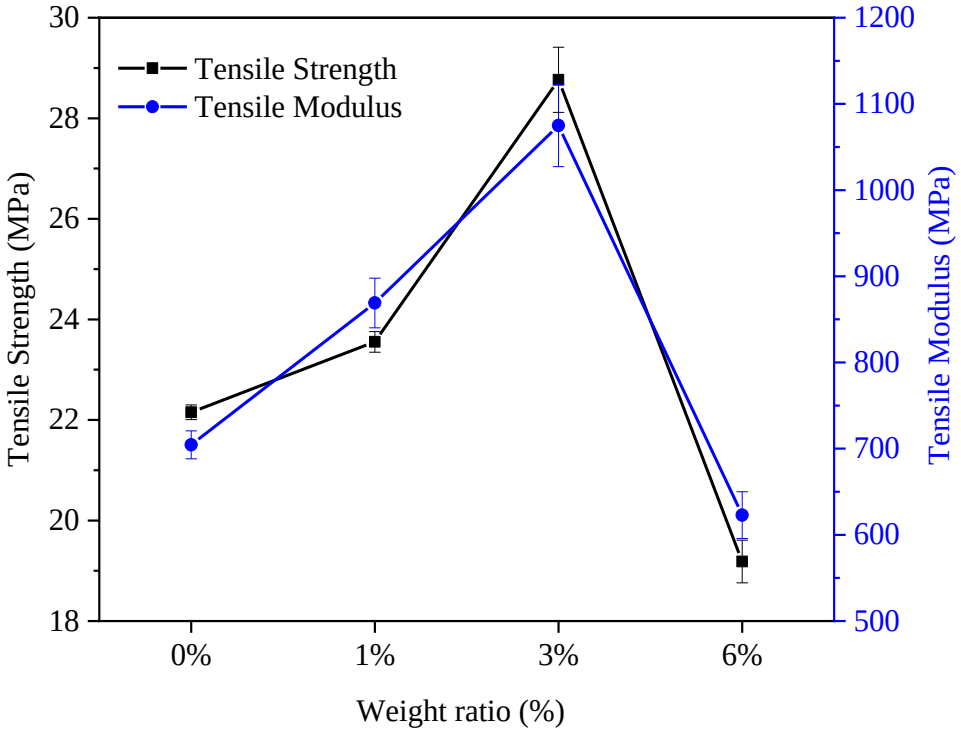

Figure 5.19: Tensile test results

Table 5.9: Mechanical test results

Sample	Tensile Strength (MPa)	Tensile Modulus (MPa)	Flexural Strength (MPa)	Flexural Modulus (MPa)
PP	22.2 ± 0.1	704.4 ± 16.2	38.3 ± 0.6	1429 ± 16.4
1MAPP	23.6 ± 0.2	869 ± 28.8	31.4 ± 1	860 ± 19.4
3MAPP	28.8 ± 0.6	1074.9 ± 47.7	47.2 ± 2.2	1863.2 ± 19
6MAPP	19.2 ± 0.4	622.9 ± 27.1	42.1 ± 2.3	1602.3 ± 28.7

5.4.2 Flexural Test

Figure 5.18 shows the flexural strength and flexural modulus values of PP and MAPP-added PP samples. The flexural strength values were obtained as 38.3 ± 0.6, 31.4 ± 1, 47.2 ± 2.2, and 42.1 ± 2.3, for PP, 1MAPP, 3MAPP, and 6MAPP, respectively. The best flexural strength was obtained with a 23% percent increase in the 3MAPP sample when compared to PP. On the contrary, there was a decrease in 6MAPP sample with 11% value contrary to 3MAPP. Flexural modulus values also showed a similar tendency with flexural strength. It has the maximum value in 3MAPP with 1863 MPa which is more than almost 30% high of PP. The flexural properties reduction observed with 1% and 6% MAPP loading was caused by the interaction between the compatibilizer and the polyolefin matrix. Coupled with MAPP's low average molecular weight, the interaction between the PP matrix and MAPP becomes dominated principally by Van der Waals forces; since chain entanglement of PP and MAPP is virtually impossible. As reported, MAPP is not utilized for fiber-matrix adhesion and therefore mechanically has a negative effect on the biocomposites, which leads the significant performance variation except the optimum loading value [97,98].

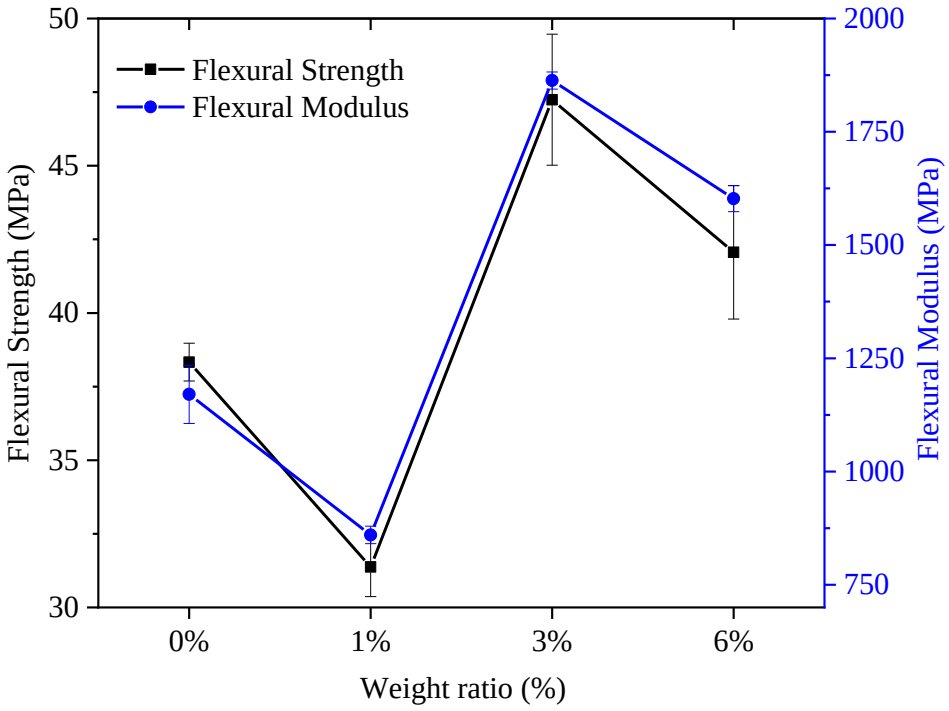

Figure 5.20: Flexural test results

In light of the data obtained from the mechanical tests, the 3 wt. % MAPP added PP (3MAPP) sample provided the best tensile and mechanical properties within the scope of this study.

5.5 Evaluation of Analyses and Test of Biocomposites

As a result of the studies completed in Chapters 3 and 4, it was determined that the most effective ratio among the surface treatment is 5% alkali treatment of filler, and among the coupling agent is the 3% addition of maleic anhydride grafted to polypropylene. Eventually, considering the alkali treatment in its roughness-increasing effect on the particles, and the combination of the coupling agent, which has the effect of increasing the compatibility of filler-matrix, yields better results.

5.5.1 Fourier Transformed Infrared Spectroscopy (FTIR) Analysis

The Fourier transform infrared spectrograms and their corresponding functional groups with the components of the PP and its biocomposites were presented in Figure 5.21. The absorption peak observed at 2962 cm−1 is related to –CH3 asymmetric stretching vibration. Symmetric bending vibration mode of –CH3 group is detected at 1381 cm−1. Absorption peaks displayed at 1020 and 1168 cm1 are assigned to –CH3 rocking vibration. Absorption peak located at 802 cm−1 is assigned to C–CH3 stretching vibration. All the previous referred absorption peaks are related to methyl group presence in the PP. In addition, the peaks at 2916, 2877 and 1458 cm−1 are attributed to –CH2– asymmetric stretching, –CH2– symmetric stretching and –CH2– symmetric bending, respectively [99,100].

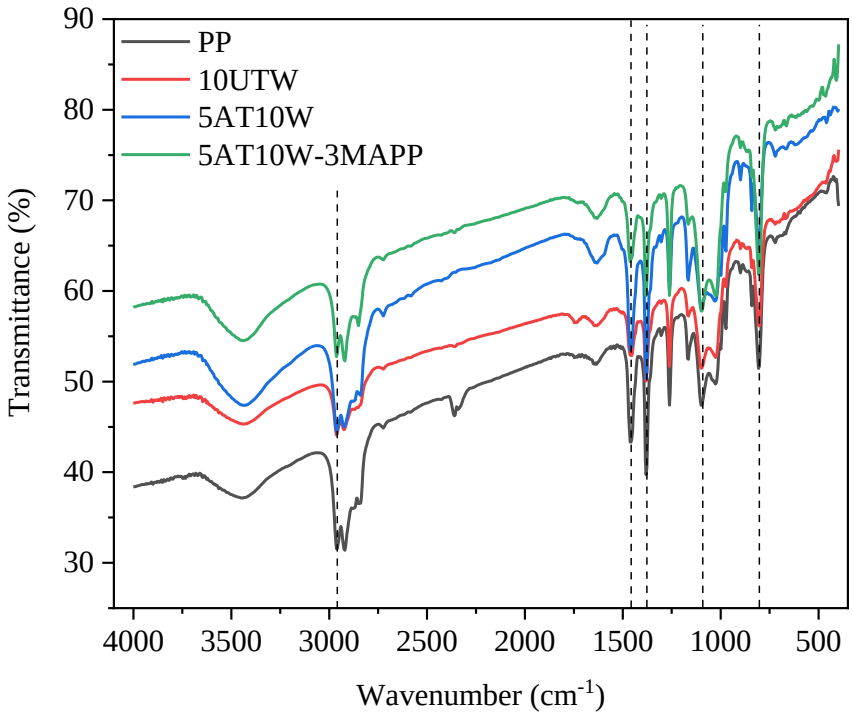

Figure 5.21: FTIR results

5.5.2 Tensile Test

The tensile strength and tensile modulus values of PP and its biocomposites are presented in Figure 5.22. The tensile strength values were obtained as 22.2 ± 0.1, 21.2 ± 0.5, 21.15 ± 0.2, and 23.9 ± 0.5, for PP, 10UTW, 5AT10W, and 5AT10W-3MAPP, respectively. As seen, the tensile strength of PP decreased about 4.5% with the addition of untreated wood particles. As mentioned in Section 5.2.1, the reason for this reduction in tensile strength may include inadequate wetting of the particles and the matrix, poor dispersion of the particles in the matrix, poor interfacial adhesion between the particles and the matrix, and the presence of agglomerations [79]. The tensile strength of 5AT10W sample is 21.15 MPa. There is a slightly decrease in tensile strength of biocomposite after alkali treatment. The reason for this low rate of decrease may be the aggregation that occurs after alkali treatment, as represent in the particle size distribution analysis in Section 5.3.4. Among all the biocomposites and PP, the highest tensile strength was determined for the 5AT10W-3MAPP sample with a value of 23.9 MPa.

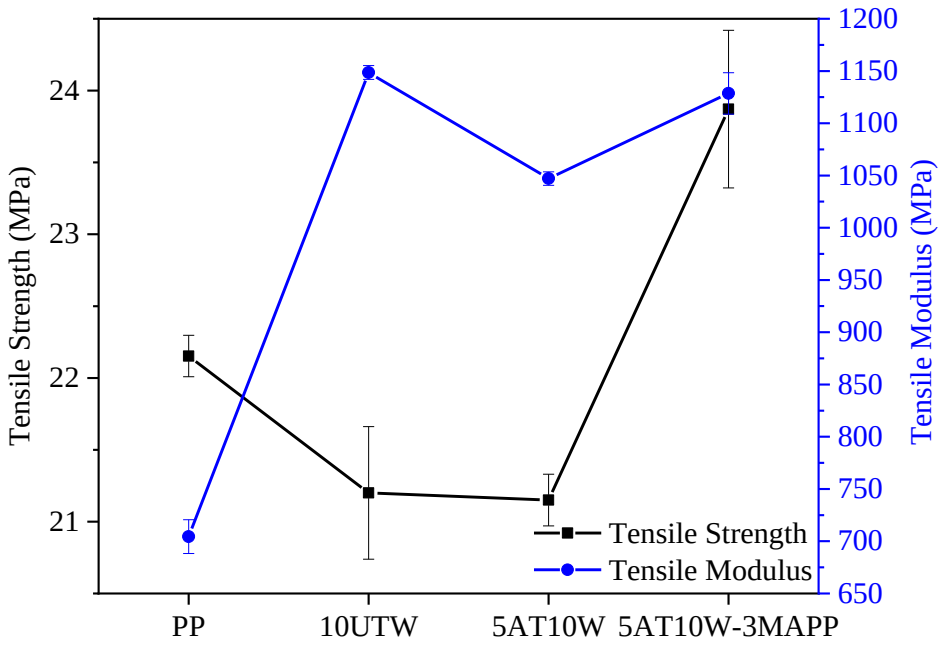

Figure 5.22: Tensile test results

The changes in the tensile modulus of PP and its biocomposites are shown in the Figure 5.22. The tensile modulus of PP is found 704 MPa where the tensile modulus was increased with the addition of filler into the PP. Among all the biocomposites, the highest tensile modulus was determined for the 10UTW sample with a value of 1148 MPa, which means the tensile modulus was increased by 60% compared to the PP. This increase could be attributed to the fact that the tensile modulus of lignocellulosic fillers is substantially higher than that of the polymer matrix [86].

5.5.3 Flexural Test

The flexural strength and flexural modulus values of PP and its biocomposites are presented in Figure 5.23. The flexural strength values were obtained as 38.32 ± 0.7, 33.8 ± 0.9, 39.5 ± 0.8, and 37.3 ± 1, for PP, 10UTW, 5AT10W, and 5AT10W-3MAPP, respectively. As seen in Figure 5.23, the flexural strength of PP decreased by 12% with the addition of untreated wood particles. The reasons for this reduction might inadequate wetting of the lignocellulosic particles and the matrix, poor dispersion of particles in the matrix, poor interfacial adhesion between the particles and the matrix, and the presence of agglomerations can be considered as the reasons for the decrease in flexural strength [24,27,80,81]. Among all the biocomposites and PP, the highest tensile strength was determined for the 5AT10W sample with a value of 39.5 MPa, which means the flexural strength was increased by 3% compared to the PP. The increase can be attributed to the improvement of the interface after surface treatment [35,42] . 5AT10W-3MAPP sample has lower flexural strength compared to PP and 5AT10W. The reason for that decrease may be that coupled with MAPP's low average molecular weight, the interaction between the PP matrix and MAPP becomes dominated principally by Van der Waals forces; since chain implication of PP and MAPP is virtually impossible [97].

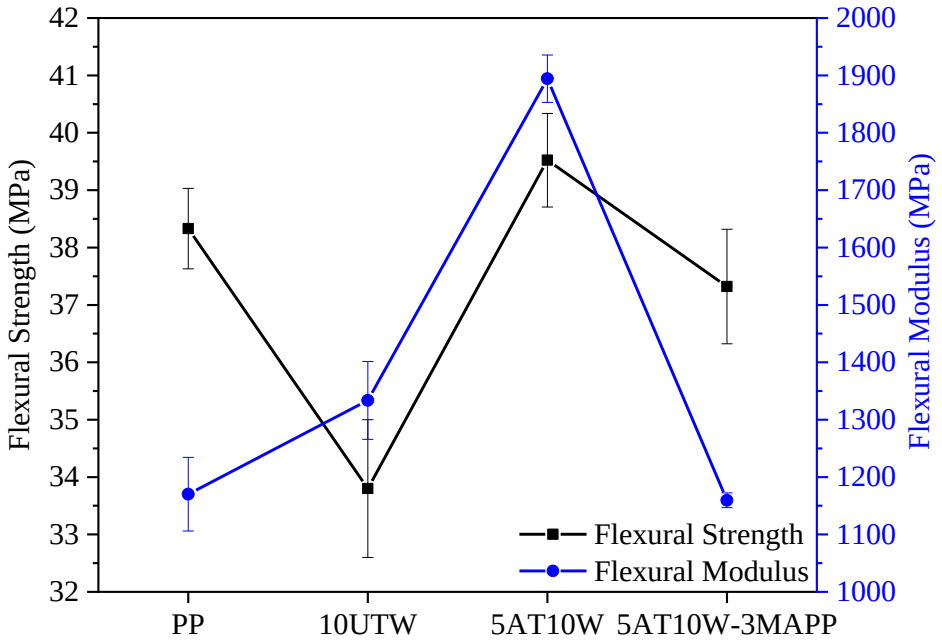

Figure 5.23: Flexural test results

The changes in the flexural modulus of PP and its biocomposites are shown in the Figure 5.21. The flexural modulus of PP is found 1170 MPa where the modulus was increased with the addition of untreated and treated fillers into the PP as 1333 MPa and 1894 MPa, respectively. Among all the biocomposites, the lowest flexural modulus was determined for the 5AT10W-3MAPP sample with a value of 1160 MPa, which means the flexural modulus was decreased by 19% compared to the PP. One of the the reason for this decrease, when compared to 10UTW and 5AT10W samples, may be the fact that the wood particles are more rigid than the PP. It is reported that the modulus of the lignocellulosic particles is much higher than that of the polymer matrix [80]. The effect of MAPP compatibilizer to enhance the interaction between the hydrophilic lignocellulosic fibers and hydrophobic PP matrix has been assessed. As a result, MAPP managed to the decrease of hydrophilicity and the increase of surface energy of lignocellulosic fiber, and improved the chemical affinity of the matrix, thereby resulted in enhanced wettability of the fiber by the matrix and interfacial adhesion [101,102].

5.5.4 Dynamic Mechanical Analysis (DMA)

Viscoelastic properties of PP and its biocomposites were investigated by DMA analysis. Variations of storage and loss moduli of PP and biocomposites as a function of temperature are shown in Figure 24 and Figure 25, separately. As seen in Figure 24, the storage modulus values of biocomposites are higher than that of PP at the whole temperature range. This shows that the stiffness of biocomposites is increased with the addition of untreated and treated particles. The increase in storage modulus was due to mechanical limitation posed by increasing filler embedded in the viscoelastic polymer matrix. It is reported that with increasing temperature, the storage modulus values of biocomposites decreased due to the softening of the matrix and initiation of the relaxation process [27,103].

The variation of the loss modulus of the PP and biocomposites as a function of temperature are presented in Figure 25. Loss modulus represents energy loss as heat or molecular rearrangements during the loading cycle, which indicates the viscous nature of the polymer [104,105]. As shown in Figure 25, the loss modulus of biocomposite was much higher than that of PP at all temperature ranges. The relaxation transition peak represents the transition region from the glassy state to the rubbery state [105]. The relaxation peaks of PP, UTW, 5AT10W, and 5AT10W-3MAPP were obtained to be at 67.2, 70.3, 71.2, and 72.2 ℃, respectively. It can be noted a relaxation peak of PP was increased with increasing the weight fraction of untreated and treated fillers into PP.

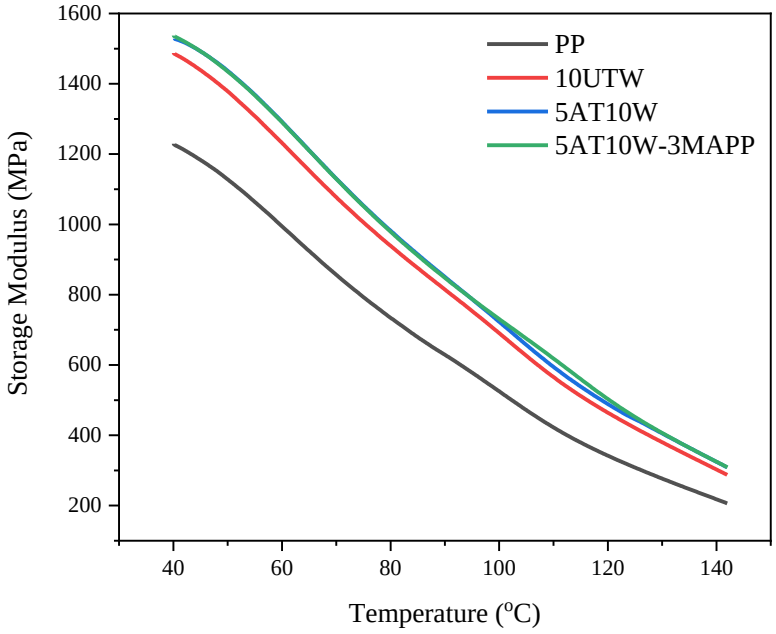

Figure 5.24: Storage modulus

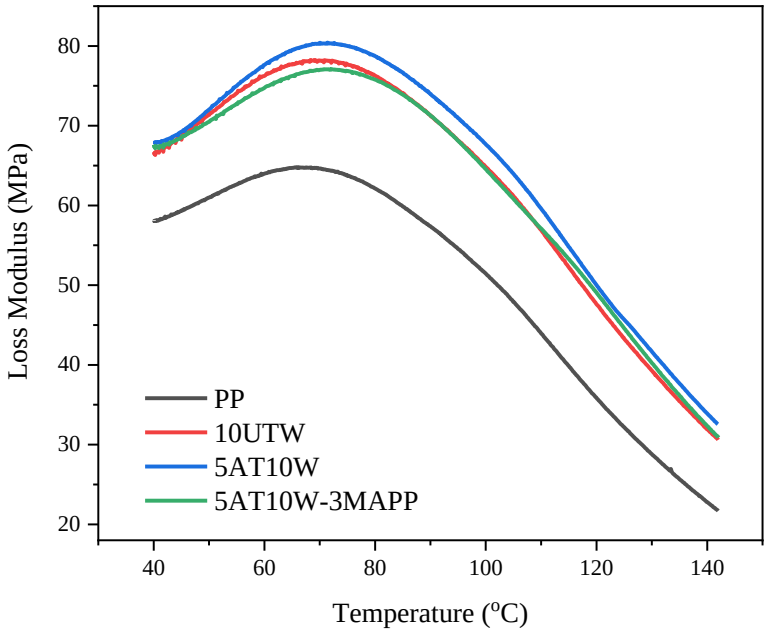

Figure 5.25: Loss modulus

5.5.5 Thermogravimetric Analysis (TGA)

TGA curves of PP and its biocomposites are presented in Figure 5.26 and onset temperature, maximum degradation temperature, and degraded weight values of all samples are given in Table 5.10. While PP exhibited a one-stage degradation process, biocomposites shows two-stage degradation process. It is reported that, the first step is due to the thermal depolymerization of hemicellulose and the glycosidic linkages of cellulose, whereas the second step is due to the cellulose decomposition [106].

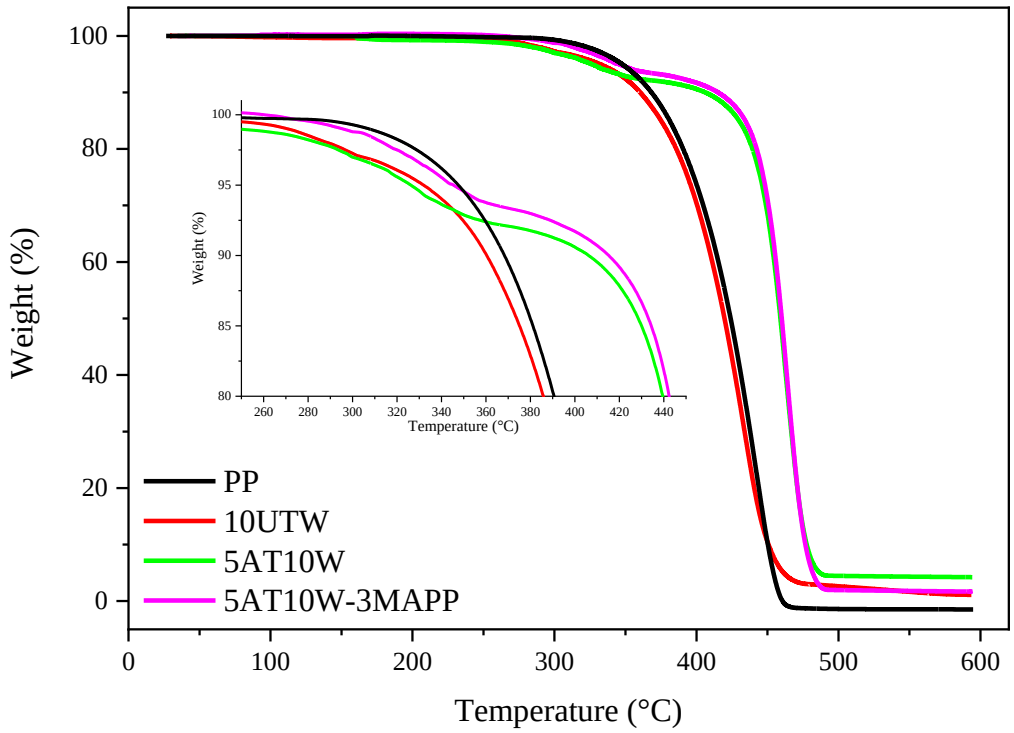

Figure 5.26: TGA results

When TGA is examined, onset temperatures of PP, 10UTW, 5AT10W and 5AT10W-3MAPP samples were obtained as 395.07, 387.86, 440.06 and 441.95℃, respectively. As applied surface treatment and MAPP coupling agent at optimum values, it was observed that the onset temperature of the biocomposites increases. Maximum degradation temperatures of PP, 10UTW, 5AT10W and 5AT10W-3MAPP samples were measured as 442.7, 433.56, 463.05, and 464.05℃,

respectively. When the results are examined, it is indicated that 10UTW have a negative effect on the maximum degradation temperature of the PP, but it is observed that the maximum degradation temperatures increase by applying surface treatment and MAPP coupling agent at optimum ratios. Degraded weight values of PP, 10UTW, 5AT10W and 5AT10W-3MAPP samples were obtained as 100, 98.89, 95.78 and 98.34%, respectively. When the results are evaluated, the degraded weight value of PP decreased with adding filler. These degradation ranges were similar to the degradation temperatures of other PP-based biocomposites reported in literature [107,108].

Table 5.10: TGA data for PP and biocomposites

Sample	T_{onset} (°C)	T_{max} (°C)	Weight loss (%)
PP	395.07	442.7	100
10UTW	387.86	433.56	98.89
5AT10W	440.06	463.05	95.78
5AT10W-3MAPP	441.95	464.05	98.34

5.5.6 Differential Scanning Calorimetry (DSC) Analysis

Figure 5.27 displays the calorimetric curves obtained from the DSC runs which corresponds the cooling step and the second heating step. These were used to calculate crystallization peak temperature (T_c), melting peak temperature (T_m), crystallization enthalpy (ΔH_c), melting enthalpy (ΔH_m), and degree of crystallinity (X_c). In addition, DSC melting and crystallization parameters are presented in Table 5.11.

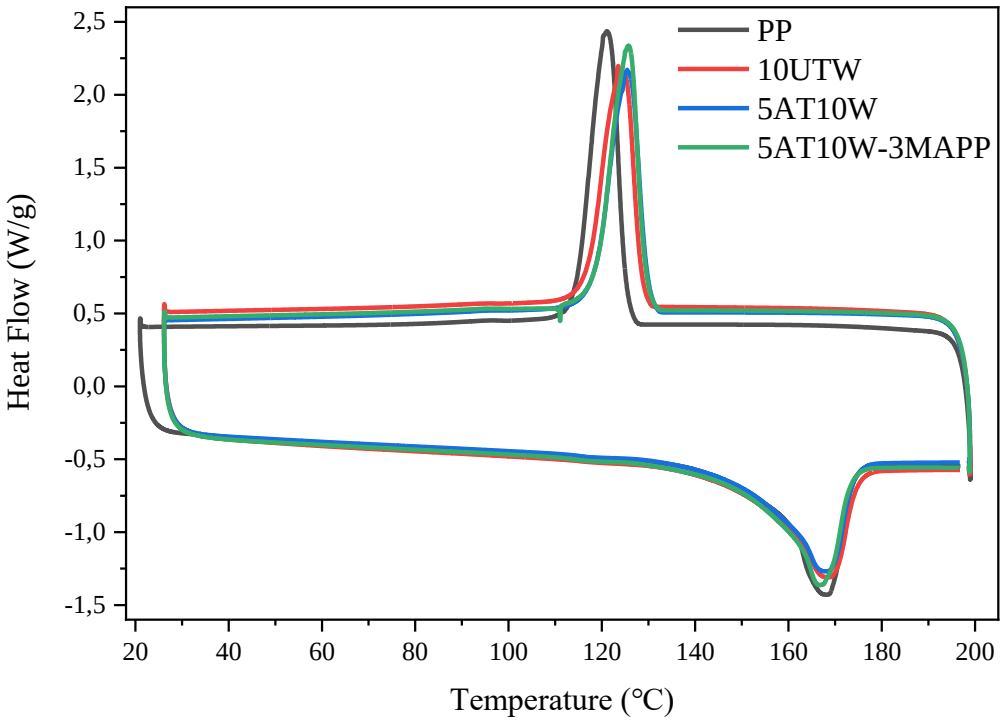

Figure 5.27: DSC results

As can be seen in Figure 5.27, the melting temperatures of PP slightly increased after the untreated and treated filler added, which indicates that the crystal size of PP did not change considerably. In the 5AT10W-3MAPP sample, although the melting temperature value decreased to 166.6 with the addition of MAPP coupling agent, it still has a value of approximately 1% more than PP. Besides, lignocellulosic fillers into PP improved the crystallization of PP because of the fact that the crystallization temperature enhanced by 4 ℃. Crystallization temperature of PP was found 122.4. It increased with adding untreated filler, treated filler and coupling agent by 123.5, 125.4 and 125.8, respectively. Crystallization enthalpy of PP decreased almost 18% when compared to its biocomposites. Melting enthalpy of PP decreased with adding untreated and treated filler. Adding MAPP increased the melting entalhpy when compared to 10UTW and 5AT10W where it still 6% below the PP. Crystallinity degree of PP was found 43.5%. For 10UTW and 5AT10W samples the crystallinity degree found almost same with 36.9% and 36.8% values. It exhibit that the surface treatment did not affect the crystallinity degree of PP. Moreover, adding 3% MAPP into the 5AT10W sample increased the crystallinity degree almost 10%.

In summary, some factors must be considered to understand the crystallization and melting behavior of PP and its biocomposites. First, the presence of a low molecular weight MAPP, and its lubricating effect on the higher molecular weight PP. Second, the presence of MAPP results in interactions, covalent and acid-base, between the anhydride and the hydroxyl groups on the lignocellulosic particle surface. The third one is the interaction between the anhydride groups among themselves, within the same molecule, or between neighboring coupling agent molecules. As reported, good interaction between the MAPP and the lignocellulosic particle surface restricts the mobility of the molecules [107,109].

Table 5.11: Summary of thermal parameters obtained by DSC curves of PP and biocomposites

Sample	Tm (°C)	Tc (°C)	Hc (J/g)	Hm (J/g)	Xc (%)
PP	165.6	122.4	97.6	90.9	43.5
10UTW	169.5	123.5	80.2	77	36.9
5AT10W	169.4	125.4	79	76.9	36.8
5AT10W-3MAPP	166.6	125.8	80.1	85.1	40.7

T_m(°C): melting peak temperature, T_c(°C): crystallization peak temperature, ΔH_c(J/g): crystallization enthalpy, ΔH_m(J/g): melting enthalpy, X_c(%): degree of crystallinity ($X_c = (\Delta H_m / \Delta H^0_m) * 100$ [melting enthalpy of PP (ΔH^0_m) is 209 [110]])

5.5.7 Scanning Electron Microscopy (SEM) Observation

The scanning electron microscopy (SEM) images are presented in Figure 5.28 (a-c) to evaluate the microstructure of fractured surfaces of biocomposites. As stated before, efficient homogenization is always a challenge in particulate-filled polymers. The tendency for aggregation depends on the size of the particles and on their surface energy; small particle size and high surface energy favor aggregation [111,112]. A

better fiber-matrix interface was obtained after alkali treatment where fiber-matrix weak bonds and voids did not occur in Figure 5.28 (b) as compared to Figure 5.28 (a). It was reported in flexural test results that the stiffness of biocomposite decreased with the addition of MAPP coupling agent. The reason for this reduction may be the plasticizer effect of MAPP [109] as seen obviously in Figure 5.28 (c).

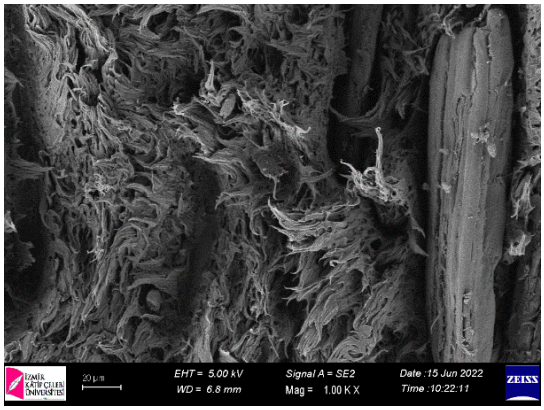

(a) 10UTW

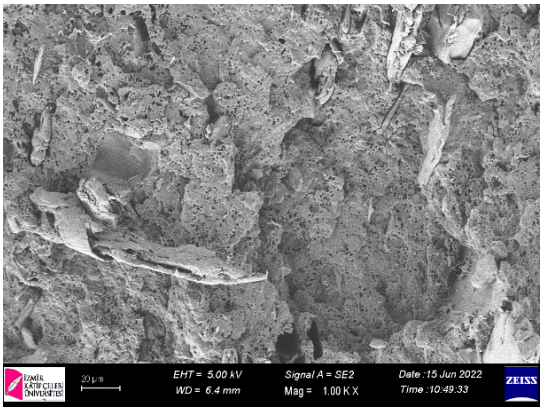

(b) 5AT10W

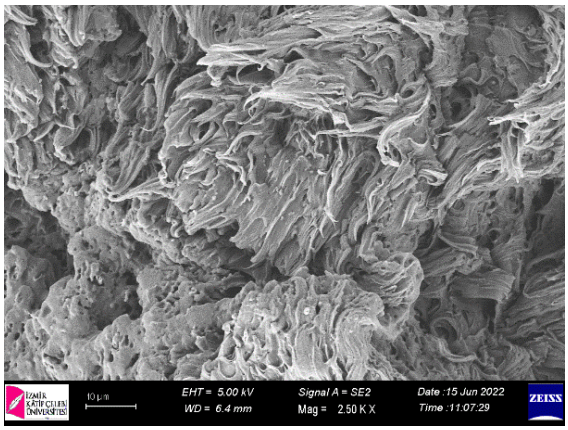

(c) 5AT10W-3MAPP

Figure 5.28: SEM images of the fracture surfaces; a) 10UTW, b) 5AT10W and c) 5AT10W-3MAPP

Chapter 6

Conclusion

In the context of this thesis, cherry tree (Prunus avium L.) pruning wastes were characterized and the usability of these materials, classified as agricultural waste, as a filling material in thermoplastics was investigated.

At first, the characterization of the lignocellulosic fillers obtained from the wood and bark parts of the branches was completed. The fillers' cellulose, hemicellulose, and lignin contents were determined by chemical composition analysis. The cellulose ratios of wood and bark are 70.65 ±1.35 and 63.85 ±0.78 and densities are 1.4551 ± 0.0024 and 1.4013 ± 0.0037 g/cm^3, respectively. Fillers functional groups were analyzed by using Fourier transform infrared spectroscopy (FTIR) and X-ray diffraction analysis (XRD) confirming the presence of cellulose and amorphous substances in the fillers. The thermogravimetric analysis (TGA) justified the thermal stability of fillers up to 200 ℃, which is within polymerization process temperature conditions. The morphology of fillers was observed using a scanning electron microscope (SEM).

Second, biocomposite production was performed by adding untreated fillers to polypropylene (PP) with particle sizes under 100 microns and 100-250 microns at the rates of 5%, 10%, 15%, and 20% by weight. The effects of the particle size of fillers and filler types on the mechanical and viscoelastic properties of biocomposites were investigated by performing tensile tests, three-point bending tests, and dynamic mechanical analyses (DMA). When the mechanical properties of biocomposites were compared with the neat PP; it was determined that the biocomposite, which contains 10% of wood filler with under 100 microns particle size, provided the optimum values among all other fillers with a tensile strength of 21.2 MPa, a tensile modulus of 1150 MPa, a flexural strength of 34 MPa, and a flexural modulus of 1334 MPa.

In the third step, wood filler under 100 microns was treated with sodium hydroxide (NaOH) at 3%, 5%, and 10% ratios in order to determine the ideal ratio for surface modification. According to the results of the FTIR analysis, 5% NaOH was determined as the most effective modification parameter. In the fourth part of the study, maleic anhydride-grafted polypropylene (MAPP) was added to the neat PP at 1%, 3%, and 5% by weight. Tensile and three-point bending tests were applied to the samples to determine the ideal additive ratio. As a result of these tests, with 29 MPa tensile strength, 1075 MPa tensile modulus, 47 MPa flexural strength, and 1864 MPa flexural modulus values, the best results were obtained in the 3 wt.% MAPP added sample.

Lastly, the final biocomposite with improved thermal and mechanical properties was produced by using the most ideal ratios obtained until this stage of the thesis study. The content of this biocomposite consists of 5% alkali-treated wood (<100μ) 10 wt.%, and 3 wt.% MAPP-filled polypropylene. According to the mechanical analysis results, this biocomposite provided an increase of 10% in tensile strength and 60% in tensile modulus when compared to neat PP. Nevertheless, when the thermal properties of the 5AT10W-3MAPP biocomposite were compared with pure PP, the thermal stability and crystallization rates of the biocomposites improved by 21.5 °C and 5.6%, respectively.

Appendices

Appendix A

A1. Stress-Strain curves of PP and biocomposites

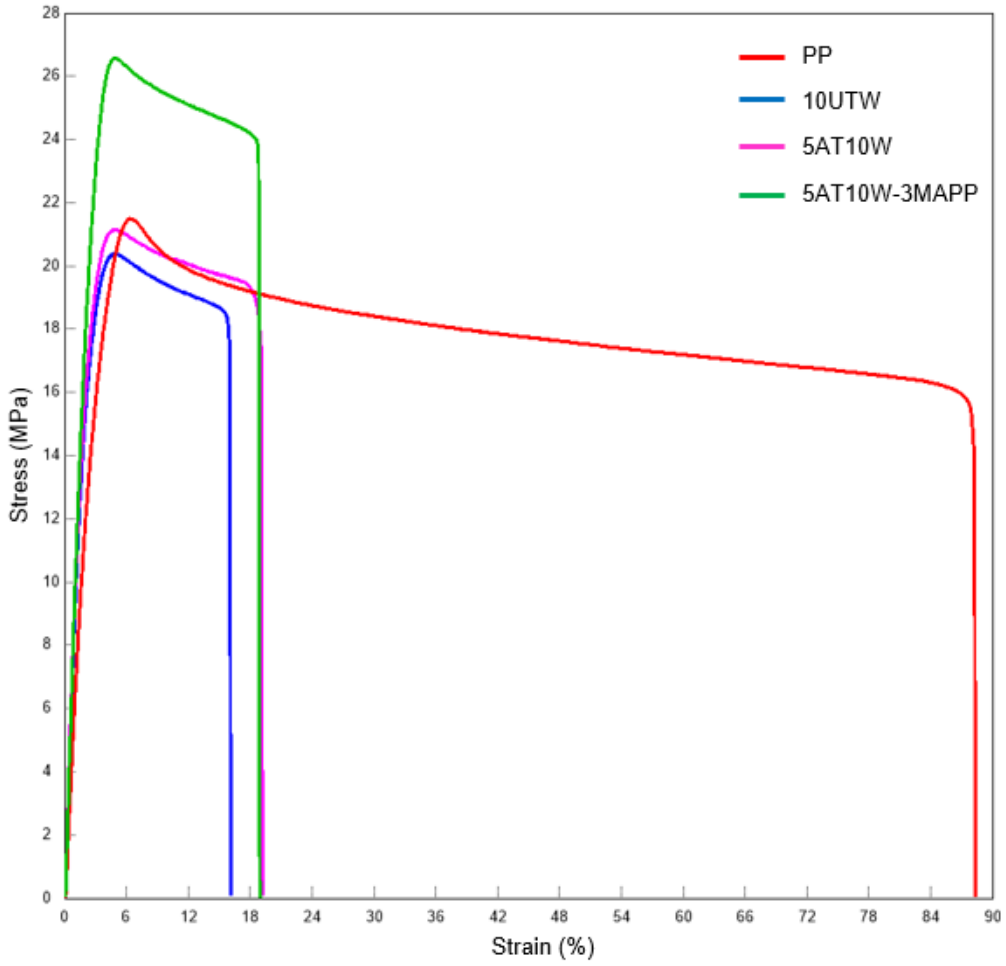

A2. SEM images of biocomposites

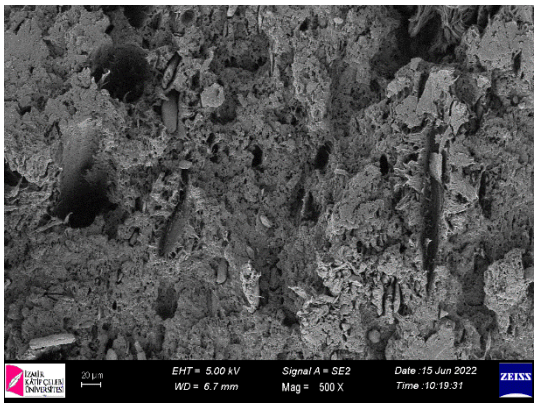

10UTW

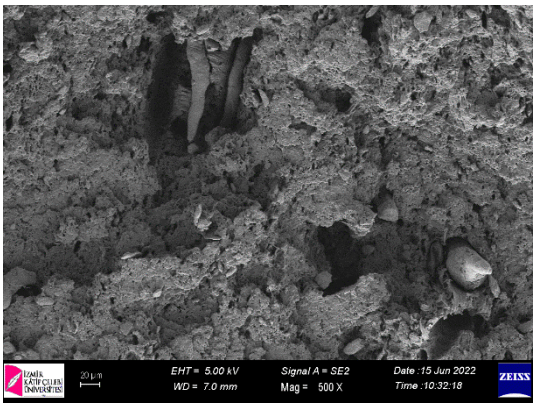

10UTB

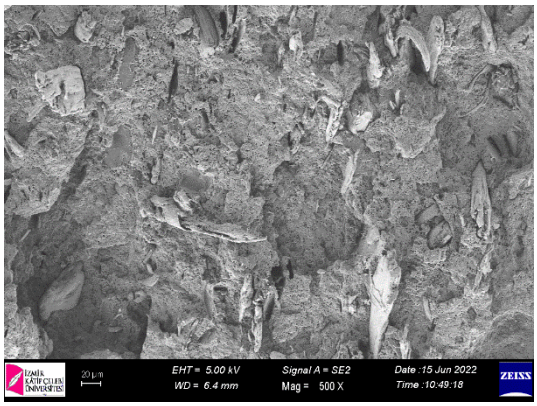

5AT10W

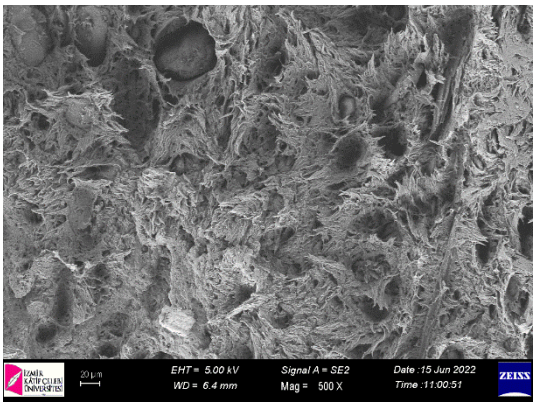

5AT10W-3MAPP

References

1. Kaw K. Mechanics of Composite Materials. 2nd Ed. CRC Press; 2005.
2. Jones RM. Mechanics of Composite Materials. 2nd Ed. CRC Press; 1999.
3. Xanthos M. Functional Fillers for Plastics. John Wiley & Sons; 2010. 538 p.
4. Ebewele RO. Polymer Science and Technology. 1st Ed. CRC Press; 2000.
5. Jordan J, Jacob KI, Tannenbaum R, Sharaf MA, Jasiuk I. Experimental trends in polymer nanocomposites—a review. Mater Sci Eng A. 2005;393(1–2):1–11.
6. Mitra B. Environment Friendly composite materials: Biocomposites and Green composites. Def Sci J. 2014;64(3).
7. Mohanty AK, Misra M, Drzal LT. Natural fibers, biopolymers, and biocomposites. CRC press; 2005.
8. Rothon R. Particulate-filled Polymer Composites. iSmithers Rapra Publishing; 2003. 564 p.
9. Moon RJ, Martini A, Nairn J, Simonsen J, Youngblood J. Cellulose nanomaterials review: structure, properties and nanocomposites. Chem Soc Rev. 2011 Jun 20;40(7):3941–94.
10. TÜİK - Veri Portalı [Internet]. [cited 2023 May 10]. Available from: https://data.tuik.gov.tr/Kategori/GetKategori?p=tarim-111&dil=1
11. Araştırma Kuruluşları [Internet]. [cited 2023 May 10]. Available from: https://arastirma.tarimorman.gov.tr/
12. Mohanty A, Misra M, Drzal LT. Surface modifications of natural fibers and performance of the resulting biocomposites: An overview. Compos Interfaces. 2001;8(5):313–43.
13. Herrmann A, Nickel J, Riedel U. Construction materials based upon biologically renewable resources—from components to finished parts. Polym Degrad Stab. 1998;59(1–3):251–61.
14. Pickering KL, Efendy MGA, Le TM. A review of recent developments in natural fibre composites and their mechanical performance. Spec Issue Biocomposites. 2016 Apr 1;83:98–112.
15. Ngo TD. Natural Fibers for Sustainable Bio-Composites. In: Günay E, editor. Natural and Artificial Fiber-Reinforced Composites as Renewable Sources

[Internet]. InTech; 2018 [cited 2021 Jan 7]. Available from: http://www.intechopen.com/books/natural-and-artificial-fiber-reinforced-composites-as-renewable-sources/natural-fibers-for-sustainable-bio-composites

16. Zhou Y, Fan M, Chen L. Interface and bonding mechanisms of plant fibre composites: An overview. Compos Part B Eng. 2016 Sep;101:31–45.

17. Beckermann G. Performance of Hemp-Fibre Reinforced Polypropylene Composite Materials [Internet] [Thesis]. The University of Waikato; 2007 [cited 2023 May 10]. Available from: https://researchcommons.waikato.ac.nz/handle/10289/2543

18. Cao Y, Sakamoto S, Goda K. EFFECTS OF HEAT AND ALKALI TREATMENTS ON MECHANICAL PROPERTIES OF KENAF FIBERS.

19. Bismarck A, Mishra S, Lampke T. Plant fibers as reinforcement for green composites. In: Natural fibers, biopolymers, and biocomposites. CRC Press; 2005. p. 52–128.

20. Chand N, Fahim M. Tribology of natural fiber polymer composites. Woodhead publishing; 2020.

21. Sivaraj Vijaya G, Gounder RI, Natarajan SS. Characterization of Natural Cellulose Fibers from the Barks of *Ziziphus nummularia* as a Reinforcement for Lightweight Composite Applications. J Nat Fibers. 2022 Dec 2;19(17):15663–79.

22. Hossain S, Jalil MA, Islam T, Rahman MM. A low-density cellulose rich new natural fiber extracted from the bark of jack tree branches and its characterizations. Heliyon. 2022 Nov;8(11):e11667.

23. Madival AS, Maddasani S, Shetty R, Doreswamy D. Influence of Chemical Treatments on the Physical and Mechanical Properties of *Furcraea Foetida* Fiber for Polymer Reinforcement Applications. J Nat Fibers. 2023 Dec 31;20(1):2136816.

24. Atagur M, Seki Y, Pasaoglu Y, Sever K, Seki Y, Sarikanat M, et al. Mechanical and thermal properties of *Carpinas betulus* fiber filled polypropylene composites. Polym Compos. 2020 May;41(5):1925–35.

25. Atagur M, Seki Y, Oncu O, Sever K, Seki Y, Sarikanat M, et al. Evaluating of reinforcing effect of Ceratonia Siliqua for polypropylene: Tensile, flexural and other properties. Polym Test. 2020 Sep;89:106607.

26. Jiang X, Wang J, Wu G, Peng X, Ma X. Significant reinforcement of polypropylene/wood flour composites by high extent of interfacial interaction. J Thermoplast Compos Mater. 2019 May;32(5):577–92.

27. Kaya N, Atagur M, Akyuz O, Seki Y, Sarikanat M, Sutcu M, et al. Fabrication and characterization of olive pomace filled PP composites. Compos Part B Eng. 2018 Oct 1;150:277–83.

28. Sohn J, Cha S. Effect of Chemical Modification on Mechanical Properties of Wood-Plastic Composite Injection-Molded Parts. Polymers. 2018 Dec 15;10(12):1391.

29. Maache M, Bezazi A, Amroune S, Scarpa F, Dufresne A. Characterization of a novel natural cellulosic fiber from Juncus effusus L. Carbohydr Polym. 2017 Sep;171:163–72.

30. Nukala SG, Kong I, Kakarla AB, Kong W, Kong W. Development of Wood Polymer Composites from Recycled Wood and Plastic Waste: Thermal and Mechanical Properties. J Compos Sci. 2022 Jul 1;6(7):194.

31. Atagür M, Kaya N, Uysalman T, Durmuşkahya C, Sarikanat M, Sever K, et al. A detailed characterization of sandalwood-filled high-density polyethylene composites. J Thermoplast Compos Mater. 2020 Jul 31;089270572093915.

32. Murad A, Sirahbizu B. Experimental study on the effect of Cordia africana's and Austria pine's wood species on the performance of wood plastic composite. Compos Adv Mater. 2022 Jan;31:263498332211055.

33. Kılınc AC, Atagur M, Ozdemir O, Sen I, Kucukdogan N, Sever K, et al. Manufacturing and characterization of vine stem reinforced high density polyethylene composites. Compos Part B Eng. 2016 Apr 15;91:267–74.

34. Gairola S, Sinha S, Singh I. Novel millet husk crop-residue based thermoplastic composites: Waste to value creation. Ind Crops Prod. 2022 Aug;182:114891.

35. Narlioğlu N. Alkali Konsantrasyonunun Odun Unu Takviyeli PVC Kompozitlerin Mekanik Özelliklerine Etkisi. Bartın Orman Fakültesi Derg [İnternet]. 2022 Mar 23 [cited 2023 May 5]; Available from: https://dergipark.org.tr/tr/doi/10.24011/barofd.1065643

36. Erdogan S, Huner U. Physical and Mechanical Properties of PP Composites based on Different Types of Lignocellulosic Fillers. J Wuhan Univ Technol-Mater Sci Ed. 2018 Dec;33(6):1298–307.

37. Hung KC, Yeh H, Yang TC, Wu TL, Xu JW, Wu JH. Characterization of Wood-Plastic Composites Made with Different Lignocellulosic Materials that Vary in Their Morphology, Chemical Composition and Thermal Stability. Polymers. 2017 Dec 17;9(12):726.

38. Nnodu OG, Igwe IO, Ojingwa A, Nwapa C, Oragwu PI, Okonkwo SN. EFFECTS OF CHEMICAL MODIFICATIONS OF PINEAPPLE LEAF FIBRE ON THE PROPERTIES OF POLYPROPYLENE COMPOSITES.

39. Ben Hamou K, Kaddami H, Elisabete F, Erchiqui F. Synergistic association of wood /hemp fibers reinforcements on mechanical, physical and thermal properties of polypropylene-based hybrid composites. Ind Crops Prod. 2023 Feb;192:116052.

40. A V, Rangappa SM, Srisuk R, Tengsuthiwat J, R AR, Siengchin S. Agro-waste Capsicum Annum stem: An alternative raw material for lightweight composites. Ind Crops Prod. 2023 Mar;193:116141.

41. Youbi SBT, Tagne NRS, Harzallah O, Huisken PWM, Stanislas TT, Njeugna E, et al. Effect of alkali and silane treatments on the surface energy and mechanical performances of Raphia vinifera fibres. Ind Crops Prod. 2022 Dec;190:115854.

42. Gholampour A, Ozbakkaloglu T. A review of natural fiber composites: properties, modification and processing techniques, characterization, applications. J Mater Sci. 2020 Jan;55(3):829–92.

43. Seki Y, Selli F, Erdoğan ÜH, Atagür M, Seydibeyoğlu MÖ. A review on alternative raw materials for sustainable production: novel plant fibers. Cellulose. 2022 Jun;29(9):4877–918.

44. Mazumdar S. Composites Manufacturing: Materials, Product, and Process Engineering. CRC Press; 2001. 417 p.

45. Biocomposites Market Size, Trends, Growth, Report 2030 [Internet]. [cited 2023 May 5]. Available from: https://www.precedenceresearch.com/biocomposites-market

46. Grade : M1500 | LG Chem On PO [Internet]. [cited 2023 May 5]. Available from: https://www.lgchemon.com/s/po/grade/a552x000000XvWEAA0/m1500?language=en_US

47. Gopakumar TG, Pagé DJYS. Compounding of nanocomposites by thermokinetic mixing: Compounding of Nanocomposites. J Appl Polym Sci. 2005 Jun 5;96(5):1557–63.

48. Savran M, Yılmaz M, Öncül M, Sever K. Manufacturing and Modeling of Polypropylene-based Hybrid Composites by Using Multiple-Nonlinear Regression Analysis. Sci Res Commun. 2022 Jan 30;2(1):1–15.

49. Akyüz O. Surface Modification of Micronized Quartz Powders and Investigation of additives as Filling Material in Polymer Matrix Composite Materials [PhD Thesis]. [İzmir]: İzmir Katip Çelebi University; 2020.

50. Wise LE, Karl HL. Cellulose and hemicellulose in pulp and paper science and technology. Earl LC. 1962;(1).

51. Stuart B. Polymer crystallinity studied using Raman spectroscopy. Vib Spectrosc. 1996;10(2):79–87.

52. Bhattacharya S, Kamal M, Gupta R. Rheology of nanocomposites. Polym Nanocomposites Theory Pract Hanser Gardner Publ Cincinnati OH. 2008;145–232.

53. Rowell R, editor. The Chemistry of Solid Wood [Internet]. Washington, DC: American Chemical Society; 1984 [cited 2023 May 5]. (Advances in Chemistry; vol. 207). Available from: https://pubs.acs.org/doi/book/10.1021/ba-1984-0207

54. Bozkurt Y, Erdin N. Odunsu Lifler ve Tanımı. İstanbul Üniversitesi Orman Fakültesi Derg. 1989;39(4):1–16.

55. Yemele MCN, Koubaa A, Cloutier A, Soulounganga P, Wolcott M. Effect of bark fiber content and size on the mechanical properties of bark/HDPE composites. Compos Part Appl Sci Manuf. 2010;41(1):131–7.

56. Zobel BJ, Jett JB, Zobel BJ, Jett JB. The importance of wood density (specific gravity) and its component parts. Genet Wood Prod. 1995;78–97.

57. Saranpää P. Wood density and growth. Wood Qual Its Biol Basis. 2003;87–117.

58. Zink-Sharp A. The mechanical properties of wood. Wood Qual Its Biol Basis Blackwell Publ-CRC Press Biol Sci Ser Boca Raton Fla EUA. 2003;187–210.

59. Liepiņš K, Liepiņš J, Ivanovs J, Bārdule A, Jansone L, Jansons Ā. Variation in the Basic Density of the Tree Components of Gray Alder and Common Alder. Forests. 2023 Jan 11;14(1):135.

60. Wang S, Littell RC, Rockwood DL. Variation in density and moisture content of wood and bark among twenty Eucalyptus grandis progenies. Wood Sci Technol. 1984 Jun;18(2):97–100.

61. Kellog RM. Physical properties of wood. J Educ Modul Mater Sci Eng. 1980;2(2):449–86.

62. Asyraf MRM, Syamsir A, Ishak MR, Sapuan SM, Nurazzi NM, Norrrahim MNF, et al. Mechanical Properties of Hybrid Lignocellulosic Fiber-Reinforced Biopolymer Green Composites: A Review. Fibers Polym. 2023 Feb;24(2):337–53.

63. Simpson W, TenWolde A. Physical properties and moisture relations of wood. Chapter. 1999;3:2–1.

64. Ramadevi P, Sampathkumar D, Srinivasa CV, Bennehalli B. Effect of alkali treatment on water absorption of single cellulosic abaca fiber. BioResources. 2012;7(3).

65. Kamaruddin ZH, Jumaidin R, Ilyas RA, Selamat MZ, Alamjuri RH, Yusof FAM. Biocomposite of Cassava Starch-Cymbopogan Citratus Fibre: Mechanical, Thermal and Biodegradation Properties. Polymers. 2022 Jan;14(3):514.

66. Narayanasamy P, Balasundar P, Senthil S, Sanjay MR, Siengchin S, Khan A, et al. Characterization of a novel natural cellulosic fiber from Calotropis gigantea fruit bunch for ecofriendly polymer composites. Int J Biol Macromol. 2020 May 1;150:793–801.

67. Sudha S, Thilagavathi G. Effect of alkali treatment on mechanical properties of woven jute composites. J Text Inst. 2016;107(6):691–701.

68. Madhu P, Sanjay MR, Jawaid M, Siengchin S, Khan A, Pruncu CI. A new study on effect of various chemical treatments on Agave Americana fiber for composite reinforcement: Physico-chemical, thermal, mechanical and morphological properties. Polym Test. 2020 May 1;85:106437.

69. Seki Y, Seki Y, Sarikanat M, Sever K, Durmuşkahya C, Bozacı E. Evaluation of linden fibre as a potential reinforcement material for polymer composites. J Ind Text. 2016 May;45(6):1221–38.

70. Senthamaraikannan P, Kathiresan M. Characterization of raw and alkali treated new natural cellulosic fiber from Coccinia grandis.L. Carbohydr Polym. 2018 Apr 15;186:332–43.

71. Vijay R, Vinod A, Lenin Singaravelu D, Sanjay MR, Siengchin S. Characterization of chemical treated and untreated natural fibers from Pennisetum orientale grass- A potential reinforcement for lightweight polymeric applications. Int J Lightweight Mater Manuf. 2021 Mar 1;4(1):43–9.

72. Ghavidel A, Bak M, Hofmann T, Hosseinpourpia R, Vasilache V, Sandu I. Comparison of chemical compositions in wood and bark of Persian silk tree (Albizia julibrissin Durazz.). Wood Mater Sci Eng. 2022;17(6):759–70.

73. An Empirical Method for Estimating the Degree of Crystallinity of Native Cellulose Using the X-Ray Diffractometer - L. Segal, J.J. Creely, A.E. Martin, C.M. Conrad, 1959 [Internet]. [cited 2023 May 10]. Available from: https://journals.sagepub.com/doi/abs/10.1177/004051755902901003?journalCode=trjc

74. French AD. Increment in evolution of cellulose crystallinity analysis. Cellulose. 2020 Jul 1;27(10):5445–8.

75. Doege SJ. The Role of Natural Calcium Oxalate Crystals in Plant Defense Against Chewing Insects. Inq Univ Ark Undergrad Res J. 2003;1(4).

76. Nakata PA. An assessment of engineered calcium oxalate crystal formation on plant growth and development as a step toward evaluating its use to enhance plant defense. PloS One. 2015;10(10):e0141982.

77. Palai BK, Sarangi SK, Mohapatra SS. Investigation of Physiochemical and Thermal Properties of Eichhornia Crassipes Fibers. J Nat Fibers. 2021 Sep 2;18(9):1320–31.

78. Herlina Sari N, Wardana ING, Irawan YS, Siswanto E. Characterization of the Chemical, Physical, and Mechanical Properties of NaOH-treated Natural Cellulosic Fibers from Corn Husks. J Nat Fibers. 2018 Jul 4;15(4):545–58.

79. Umashankaran M, Gopalakrishnan S. Effect of Sodium Hydroxide Treatment on Physico-chemical, Thermal, Tensile and Surface Morphological Properties of Pongamia Pinnata L. Bark Fiber. J Nat Fibers. 2021 Dec 2;18(12):2063–76.

80. Alshammari BA, Alotaibi MD, Alothman OY, Sanjay MR, Kian LK, Almutairi Z, et al. A New Study on Characterization and Properties of Natural Fibers Obtained from Olive Tree (Olea europaea L.) Residues. J Polym Environ. 2019 Nov 1;27(11):2334–40.

81. Vinod A, Yashas Gowda TG, Vijay R, Sanjay MR, Gupta MK, Jamil M, et al. Novel Muntingia Calabura bark fiber reinforced green-epoxy composite: A sustainable and green material for cleaner production. J Clean Prod. 2021 Apr 20;294:126337.

82. Diyana Z, Jumaidin R, Selamat M, Alamjuri R, Md Yusof FA. Extraction and characterization of natural cellulosic fiber from pandanus amaryllifolius leaves. Polymers. 2021;13(23):4171.

83. Manimaran P, Senthamaraikannan P, Sanjay MR, Marichelvam MK, Jawaid M. Study on characterization of Furcraea foetida new natural fiber as composite reinforcement for lightweight applications. Carbohydr Polym. 2018 Feb 1;181:650–8.

84. Rosa SML, Santos EF, Ferreira CA, Nachtigall SMB. Studies on the properties of rice-husk-filled-PP composites: effect of maleated PP. Mater Res. 2009;12:333–8.

85. Kılınç AÇ, Köktaş S, Seki Y, Atagür M, Dalmış R, Erdoğan ÜH, et al. Extraction and investigation of lightweight and porous natural fiber from Conium maculatum as a potential reinforcement for composite materials in transportation. Compos Part B Eng. 2018 May;140:1–8.

86. Shumigin D, Tarasova E, Krumme A, Meier P. Rheological and mechanical properties of poly (lactic) acid/cellulose and LDPE/cellulose composites. Mater Sci. 2011;17(1):32–7.

87. Reyes JEP. Effect of surface treatment and particle loading on the mechanical properties of CFB fly ash reinforced thermoset composite. Int J Chem Eng Appl. 2015;6(1):6–11.

88. Thomas S, Pothan LA. Natural fibre reinforced polymer composites: from macro to nanoscale. Archives contemporaines; 2009.

89. Sarikanat M, Seki Y, Sever K, Durmuşkahya C. Determination of properties of Althaea officinalis L.(Marshmallow) fibres as a potential plant fibre in polymeric composite materials. Compos Part B Eng. 2014;57:180–6.

90. Nagarajan T, Babu AS, Palanivelu K, Nayak S. Mechanical and thermal properties of PALF reinforced epoxy composites. In Wiley Online Library; 2016. p. 57–63.

91. Seki Y, Sarikanat M, Sever K, Durmuşkahya C. Extraction and properties of Ferula communis (chakshir) fibers as novel reinforcement for composites materials. Compos Part B Eng. 2013 Jan;44(1):517–23.

92. Boudjellal A, Trache D, Bekhouche S, Khimeche K, Razali MS, Guettiche D. Preparation and characterization of Alfa fibers/graphene nanoplatelets hybrid for advanced applications. Mater Lett. 2021 Apr 15;289:129379.

93. Kathirselvam M, Kumaravel A, Arthanarieswaran VP, Saravanakumar SS. Characterization of cellulose fibers in Thespesia populnea barks: Influence of alkali treatment. Carbohydr Polym. 2019 Aug 1;217:178–89.

94. Duchemin BJC. Mercerisation of cellulose in aqueous NaOH at low concentrations. Green Chem. 2015;17(7):3941–7.

95. Ferro M, Mannu A, Panzeri W, Theeuwen CH, Mele A. An integrated approach to optimizing cellulose mercerization. Polymers. 2020;12(7):1559.

96. Sever K, Sarikanat M, Seki Y, Erkan G, Erdoğan ÜH, Erden S. Surface treatments of jute fabric: The influence of surface characteristics on jute fabrics and mechanical properties of jute/polyester composites. Ind Crops Prod. 2012 Jan;35(1):22–30.

97. Ku H, Wang H, Pattarachaiyakoop N, Trada M. A review on the tensile properties of natural fiber reinforced polymer composites. Compos Part B Eng. 2011;42(4):856–73.

98. Fuqua MA, Ulven CA. Preparation and characterization of polypropylene composites reinforced with modified lignocellulosic corn fiber. In American Society of Agricultural and Biological Engineers; 2008. p. 1.

99. Gopanna A, Mandapati RN, Thomas SP, Rajan K, Chavali M. Fourier transform infrared spectroscopy (FTIR), Raman spectroscopy and wide-angle X-ray scattering (WAXS) of polypropylene (PP)/cyclic olefin copolymer (COC) blends for qualitative and quantitative analysis. Polym Bull. 2019 Aug 1;76(8):4259–74.

100. Cran MJ, Bigger SW. Quantitative analysis of polyethylene blends by Fourier transform infrared spectroscopy. Appl Spectrosc. 2003;57(8):928–32.

101. Liu L, Yu J, Cheng L, Qu W. Mechanical properties of poly (butylene succinate)(PBS) biocomposites reinforced with surface modified jute fibre. Compos Part Appl Sci Manuf. 2009;40(5):669–74.

102. Herrera-Franco PJ, Valadez-Gonzalez A. Mechanical properties of continuous natural fibre-reinforced polymer composites. Compos Part Appl Sci Manuf. 2004;35(3):339–45.

103. Huang R, Xu X, Lee S, Zhang Y, Kim BJ, Wu Q. High Density Polyethylene Composites Reinforced with Hybrid Inorganic Fillers: Morphology, Mechanical and Thermal Expansion Performance. Materials. 2013 Sep;6(9):4122–38.

104. Greene JP, Wilkes JO. Steady-State and dynamic properties of concentrated fiber-filled thermoplastics. Polym Eng Sci. 1995;35(21):1670–81.

105. Wang C, Ying S. Thermal, tensile and dynamic mechanical properties of short carbon fibre reinforced polypropylene composites. Polym Polym Compos. 2013;21(2):65–72.

106. Mofokeng JP, Luyt A, Tábi T, Kovács J. Comparison of injection moulded, natural fibre-reinforced composites with PP and PLA as matrices. J Thermoplast Compos Mater. 2012;25(8):927–48.

107. Feng D, Caulfield D, Sanadi A. Effect of compatibilizer on the structure-property relationships of kenaf-fiber/polypropylene composites. Polym Compos. 2001;22(4):506–17.

108. Joseph P, Joseph K, Thomas S, Pillai C, Prasad V, Groeninckx G, et al. The thermal and crystallisation studies of short sisal fibre reinforced polypropylene composites. Compos Part Appl Sci Manuf. 2003;34(3):253–66.

109. Järvelä P, Shucai L, Järvelä P. Dynamic mechanical properties and morphology of polypropylene/maleated polypropylene blends. J Appl Polym Sci. 1996;62(5):813–26.

110. Brandrup J. EH; Grulke, EA; Abe, A.; Bloch, DR, Polymer Handbook. 2005;

111. Dányádi L, Móczó J, Pukánszky B. Effect of various surface modifications of wood flour on the properties of PP/wood composites. Compos Part Appl Sci Manuf. 2010;41(2):199–206.

112. Móczó J, Pukanszky B. Polymer micro and nanocomposites: Structure, interactions, properties. J Ind Eng Chem. 2008;14(5):535–63.

Curriculum Vitae

Name Surname: Mustafa Öncül

Education:

2008–2013 Karabuk University, Dept. of Mechanical Eng., B.Sc.

2015–2017 Drexel University, Dept. of Mechanical Eng. and Mechanics, M.Sc.

2018–2023 İzmir Kâtip Çelebi University, Dept. of Mechanical Eng., Ph.D.

Work Experience:

2018 – İzmir Kâtip Çelebi University, Faculty of Engineering and Architecture, Department of Mechanical Engineering, Lecturer.